

**A Study on Differential Growth-Arrest of 3T3 Fibroblasts used  
as Feeders for Epidermal Stem Cell Propagation**

**THESIS**

Submitted in the partial fulfillment of  
the requirements for the degree of

**DOCTOR OF PHILOSOPHY**

By

**RISHI MAN CHUGH**

Under the supervision of

**Dr. Lakshmana Kumar Yerneni**



**BIRLA INSTITUTE OF TECHNOLOGY AND SCIENCE**

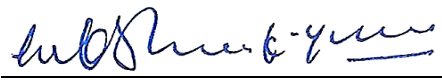
**PILANI (RAJASTHAN) INDIA**

**2015**

**BIRLA INSTITUTE OF TECHNOLOGY AND SCIENCE  
PILANI (RAJASTHAN)**

**CERTIFICATE**

This is to certify that the thesis entitled “**A Study on Differential Growth-Arrest of 3T3 Fibroblasts used as Feeders for Epidermal Stem Cell Propagation**” and submitted by Rishi Man Chugh, ID No. 2010PHXF036P for award of Ph.D. Degree of the Institute, embodies original work done by him under my supervision.

**Signature in full of the Supervisor:** 

**Name in capital block letters:** **LAKSHMANA KUMAR YERNENI**

**Designation:** **Scientist ‘E’**

**Date:** **12<sup>th</sup> October 2015**

## **Acknowledgement**

---

It is with immense respect and gratitude that I acknowledge my supervisor Dr. Lakshmana Kumar Yerneni, Scientist 'E' National Institute of Pathology (ICMR) for his straightforward and down-to-earth attitude in all matters and the liberty he gave me to carry out this research work at my own pace. His realistic technical tips were invaluable and I will always appreciate his analytical and critical scientific temperament.

I acknowledge Dr. Sunita Saxena, Director, National Institute of Pathology (ICMR) for providing me the opportunity to avail the research facilities of the institute and for her constant encouragement.

I am immensely thankful to Prof. B. N. Jain, Vice-Chancellor, BITS, Pilani, for providing me this opportunity to pursue the off-campus Ph.D. of the Institute. I express my gratitude to Prof. S. K. Verma, Dean, Research and Consultancy Division (RCD), BITS, Pilani for your constant official support, encouragement and making the organization of my research work through the past few years easy.

I am thankful to Prof. Hemant R. Jhadav, Associate Dean, Academic Research Division, other nucleus members Dr. Naveen Singh, Dr. Sharad Shrivastava, Ms. Sunita Bansal and other staff of BITS, Pilani, because without their cooperation and guidance it would not have been possible for me to pursue such goal-oriented research during each of the past semesters.

I would like to thank my Doctoral Advisory Committee (DAC) members, Prof. Uma Dubey and Dr. Rajdeep Choudhury, Department of Biological Sciences, Pilani for their

encouragement, insightful comments, and hard questions which strengthened my thesis methodologically.

I would like to acknowledge Dr. Aruna Singh, Dr. Sangeeta Rastogi, Dr. Poonam Salotra, Dr. A. K. Jain, Dr. Usha Agrawal, Dr. Nasreen Z. Ehtesham, Dr. Anju Bansal, Dr. Saurabh Verma, Dr. Avninder Singh, Dr. B.S.A. Raju, Dr. L. C. Singh and Dr. Poonam Gautam for their help in various ways during this study.

I could always rely on Mrs. R. Saratha, Administrative Officer, National Institute of Pathology (ICMR), for her administrative help in countless instances and express my deep felt thanks to her.

A special note of thank to Dr. Usha Agrawal, Incharge of Histopathology Department of our Institute for giving me permission to utilize the histopathology facility for my work. I thank to Mr. Shiv Bahadur for providing me the poly-l-lysine slides, Mrs. Krishna, Mrs. Karuna, Mr. Satyapal, Mr. Anil Verma for sectioning the paraffin embedded cultured epidermal sheet samples and other technical staffs of histopathology department for helping me to optimize my samples for microscopic investigation.

My thanks are due to Mr. Ravi Kapoor, Mr. Jagdish Kain, Mrs. Sunita Ahuja, Mrs. Seema, Mr. S. P. Vashist, Mr. Rajesh, Mrs. Anita Sharma, Mr. Raja Ram, Mr. Subhash Babu, Mr. Mange Ram, Mr. Ajay Joshi, Mr. Jagdish Ram, Mr. Rajat and other technical & non-technical staff of the Institute who have helped me in various ways.

My Sincere thanks, to my lab Senior Dr. Ashok Kumar (Assistant Professor in King Saud University, Saudi Arabia) who have taught me, the culture of Human Epidermal

Keratinocyte cells with feeders and other cell culture related techniques, without their initial help; I could not have started my research work on this topic.

I also thank my seniors and friends Dr. Shantilata, Dr. Sandeep, Dr. Pradeep, Praveen, Vasundhra, Vanila, Avishek, Deepak, Himanshu, Shashi and Pooja for their kind help and cheerful support.

My special thanks to my lab mates Madhusudan and Hemlata, not only for their ready help and cooperation but also for providing a loving and friendly atmosphere in the lab, which made the work enjoyable.

I also thank Mr. Bijendra Kumar, Mrs. Charanjeet Kaur and Mr. Dharmendra for their ready help and cooperation during every need, providing a good-natured atmosphere in the lab made my endeavor much more convenient in the hour of need.

I acknowledge the financial support provided by Indian Council of Medical Research (ICMR), New Delhi in the form of Fellowship which supported me to perform my work comfortably.

Finally, and most importantly, I would like to thank my wife Tanu. Her support, encouragement, quiet patience and unwavering love were undeniably the foundation upon which the past three years of my life have been built. Her tolerance of my occasional bad-mannered moods is a testament in itself of her unyielding devotion and love. I thank my Parents, Brother, Sister In-law, Sister and Brother In-law for their faith in me and allowing me to be as ambitious as I wanted. It was under their watchful eye that I gained so much drive and an ability to tackle challenges head on. In addition, I thank my In-laws family for

their constant encouragement, support and believe. Lastly my love for my Nephew and Niece, who always inspires me through their smiling face and cheerful activities.

Above all, I owe it all to Almighty God for granting me the wisdom, health and strength to undertake this research work and enabling me to its completion.

*Rishi Man Chugh*

Rishi Man Chugh

# Contents

---

1.	Chapter 1 Introduction.....	1-4
2.	Chapter 2 Review of Literature.....	5-24
	2.1 Tissue Engineered Skin.....	5
	2.2 Anatomy of the Normal Skin.....	5
	2.2.1 Structure of the skin.....	6
	2.2.1.1 Subcutis.....	6
	2.2.1.2 Dermis.....	7
	2.2.1.3 Basement membrane.....	8
	2.2.1.4 Epidermis.....	9
	2.3 Bioengineered Skin.....	12
	2.4 Bioengineered Skin Substitutes.....	13
	2.4.1 Apligraf®.....	13
	2.4.2 Integra.....	14
	2.4.3 Epicel®.....	14
	2.4.4 Dermagraft®.....	14
	2.4.5 OrCel®.....	15
	2.4.6 Alloderm®.....	15
	2.4.7 Transcyte®.....	15
	2.4.8 EZ Derm™.....	16
	2.4.9 Oasis Wound Matrix®.....	16
	2.4.10 PriMatrix™.....	16
	2.4.11 TissueMend®.....	16
	2.4.12 Celaderm®.....	17
	2.5 Burn Wound & Regeneration.....	17
	2.6 Feeder Cells.....	18
	2.7 Methods of Growth arrest of Swiss 3T3 feeder cells.....	20
	2.8 Mitomycin C.....	21
	2.8.1 Discovery of Mitomycin C.....	21
	2.8.2 Structure of Mitomycin C.....	21
	2.8.3 Mechanism of action of Mitomycin C.....	22
3.	Aims and Objectives.....	25
4.	Chapter 3 General Materials and Methods.....	26-29
	3.1 Swiss 3T3 fibroblast culture.....	26
	3.2 Keratinocyte-feeder Co-culture.....	28
5.	Chapter 4 Establishment and Validation of banking of Swiss 3T3 cells....	30-57
	4.1 Introduction.....	30

	4.2 Materials and Methods.....	32
	4.2.1 3T3 Fibroblast culture.....	32
	4.2.2 Subculture Schemes.....	32
	4.2.3 Generation of spontaneously transformed clone.....	34
	4.2.4 Growth Characteristic and Cell size measurements..	34
	4.2.5 Growth Arrest of 3T3.....	35
	4.2.6 Assessment of Feeder cell fate.....	35
	4.2.7 Anchorage-independent growth assay.....	36
	4.2.8 Keratinocyte-Feeder Co-culture.....	36
	4.2.9 Assessment of feeder contamination.....	37
	4.2.9.1 Non-Proliferative contamination.....	37
	4.2.9.2 Proliferative contamination.....	37
	4.2.10 Statistics.....	38
	4.3 Results.....	38
	4.3.1 Subculture schemes and response to Mitomycin C..	38
	4.3.2 Keratinocyte-Feeder Co-culture.....	41
	4.3.3 Feeder cell contamination.....	42
	4.3.4 Anchorage-independent growth.....	43
	4.3.5 Serial subculture and Response to Mitomycin C.....	46
	4.3.6 Transformed clone and response to Mitomycin C...	48
	4.3.7 Growth Characteristics.....	50
	4.3.8 Cell size measurements.....	52
	4.4 Discussion.....	54
<b>6.</b>	Chapter 5 Differential Growth Arrest by Exposure Cell Density titration	58-70
	5.1 Introduction.....	58
	5.2 Materials and Methods.....	60
	5.2.1 Swiss 3T3 Cell culture.....	60
	5.2.2 Growth Arrest Protocol.....	60
	5.2.3 Statistics.....	62
	5.3 Results.....	63
	5.4 Discussion.....	68
<b>7.</b>	Chapter 6 Differential Growth Arrest by Volumetric titration	71-88
	6.1 Introduction.....	71
	6.2 Materials and Methods.....	73
	6.2.1 Swiss 3T3 Cell culture.....	73
	6.2.2 Permutations of concentrations and doses of Mitomycin C	73
	6.2.2.1 Short Term Influence.....	75
	6.2.2.2 Long Term Influence.....	75
	6.2.3 Statistics.....	76
	6.3 Results.....	77



	6.3.1 Influence on Short-term viability.....	77
	6.3.2 Influence on Long-term extinctions.....	80
	6.4 Discussion.....	85
<b>8.</b>	<b>Chapter 7 Keratinocyte-Feeder Co-Culture</b>	<b>89-114</b>
	7.1 Introduction.....	89
	7.2 Materials and Methods.....	90
	7.2.1 Keratinocyte and fibroblast co-culture.....	90
	7.2.2 Feeder performance on Epidermal Keratinocyte at clonal density.....	91
	7.2.2.1 Colony forming Efficiency.....	91
	7.2.2.2 Digital Image Analysis.....	92
	7.2.2.3 BrdU labelling.....	93
	7.2.3 Feeder performance on mass culture of Epidermal Keratinocytes.....	94
	7.2.4 Statistics.....	94
	7.3 Results.....	96
	7.3.1 Colony Forming Efficiency.....	96
	7.3.2 Colony Forming Efficiency and Digital Image analysis	98
	7.3.3 BrdU Labelling Studies.....	104
	7.3.4 Feeder performance on mass cultures of epidermal keratinocytes.....	107
	7.4 Discussion.....	112
<b>9.</b>	<b>Chapter 8 Cultured Epithelial Sheets</b>	<b>115-133</b>
	8.1 Introduction.....	115
	8.2 Materials and Methods.....	116
	8.2.1 Establishment of Stratified Epithelium Culture.....	116
	8.2.2 Recovery of CEA from Confluent Culture of Keratinocytes.....	117
	8.2.3 Histological Evaluation.....	117
	8.2.4 Immunohistochemistry.....	118
	8.2.5 Feeder Contamination.....	119
	8.2.5.1 Non-proliferative Contamination.....	119
	8.2.5.2 Proliferative Contamination.....	119
	8.2.6 Hoechst staining.....	119
	8.2.7 In vitro Transformation assay.....	120
	8.2.8 Statistics.....	120
	8.3 Results.....	120
	8.3.1 Stratified Epithelium.....	120
	8.3.2 Histological Characterization.....	122
	8.3.3 Immunohistochemistry.....	124

	8.3.4 Feeder contamination.....	129
	8.3.4.1 Non-proliferative contamination.....	129
	8.3.4.2 Proliferative contamination.....	129
	8.3.5 Transformation Assay.....	131
	8.4 Discussion.....	131
<b>10.</b>	Chapter 9 Conclusions and Future scope of works.....	134-138
<b>11.</b>	References.....	139-154
<b>12.</b>	List of Publications/Patents	
<b>13.</b>	Brief Biography of the Candidate	
<b>14.</b>	Brief Biography of the Supervisor	

## List of Tables

---

<b>4.1</b>	Influence of various subculture schemes at P7 of Swiss 3T3 cells on anchorage-independent growth and responsiveness to Mitomycin C treatment.	40
<b>4.2</b>	Influence of serial subculture schemes at various passages of Swiss 3T3 Cells on anchorage-independent growth and responsiveness to Mitomycin C treatment	44
<b>4.3</b>	Influence of subculture on growth characteristics and cell Size in Swiss 3T3 cells	52
<b>5.1</b>	Outcome of exposure of Swiss 3T3 cells to a 2-hour pulse of various Mitomycin C doses showing their relationship with the respective concentration, exposure cell density and correlation coefficient of cell number with time	66
<b>6.1</b>	Quantitative details of Mitomycin C employed for treating Swiss 3T3 feeder cells with a two-hour pulse	78
<b>7.1</b>	Growth area measurement by quantitative image analysis of keratinocyte colonies grown by co-culturing 170 keratinocytes with various Swiss 3T3 feeders and colonies stained red with Rhodamine B	101
<b>7.2</b>	Growth area measurement by quantitative image analysis of keratinocyte colonies grown by co-culturing 340 keratinocytes with various Swiss 3T3 feeders and colonies stained red with Rhodamine B	103

## List of Figures

---

<b>2.1</b>	Mammalian skin (schematic)	07
<b>2.2</b>	Schematic drawing of the Epidermis	10
<b>2.3</b>	Schematic drawing of the epidermal proliferative unit (EPU)	11
<b>3.1</b>	The adopted two-tiered banking system	27
<b>4.1</b>	Flow chart depicting the experimental approach of testing the influence of varied subculture schemes in Swiss 3T3 cells at the denoted passage number	33
<b>4.2</b>	P6 and P7 cell yields and responsiveness to Mitomycin C	39
<b>4.3</b>	Feeder regrowth in 3K4D culture after Mitomycin C treatment	41
<b>4.4</b>	Influence of subculture schemes on responsiveness to Mitomycin C	42
<b>4.5</b>	Proliferative feeder cell contamination	45
<b>4.6</b>	Anchorage-independent growth assay	46
<b>4.7</b>	Cell yields during serial subculture	47
<b>4.8</b>	Establishment of spontaneously transformed clone	49
<b>4.9</b>	Failure of growth arrest in spontaneously transformed clone	50
<b>4.10</b>	Growth curves	51
<b>4.11</b>	Graphical representation of cell size distribution	53
<b>5.1</b>	Schematic representation of experimental derivation of doses from a given concentration of Mitomycin C by cell density titration in Swiss 3T3 cells	61
<b>5.2</b>	Influence of various concentrations of Mitomycin C on cell extinction/proliferation of Swiss 3T3 cells at various exposure cell densities	63
<b>5.3</b>	Scatter plot showing the four categories of trends of cell extinction/proliferation of Swiss 3T3 cells over a 20 days period following a two-hour pulsed exposure to various Mitomycin C doses/cell	67

<b>6.1</b>	Schematic representation of producing differential growth arrest by titrations of Swiss 3T3 cells with permutations of concentrations and those doses that were experimentally derived	72
<b>6.2</b>	Viable Swiss 3T3 cells from T25 flasks after 2-hour pulsed exposure to Mitomycin C solution	79
<b>6.3</b>	Differential periodic cell extinctions of Swiss 3T3 cells from 24-well plates after pulsed exposure to Mitomycin C in T25 flasks	81
<b>6.4</b>	Comparative cellularity of 3T3 cells on days 6 & 12 after they were re-plated into 24-well plates following a pulsed exposure to Mitomycin C in T25 flasks	82
<b>6.5</b>	Clustered column diagram showing differential periodic cell extinctions of 3T3 cells re-plated in 24-well plates following pulsed exposure to Mitomycin C in T25 flasks	84
<b>7.1</b>	Number of Colonies and Colony Forming Efficiency of keratinocytes	97
<b>7.2</b>	Separation of color in a Rhodamine B stained keratinocyte colonies over a substratum of feeder cells	99
<b>7.3</b>	Colony forming efficiency and Growth area analysis of Keratinocytes	100
<b>7.4</b>	Growth area analysis of keratinocytes	102
<b>7.5</b>	BrdU labelling in Keratinocytes	105
<b>7.6</b>	Number of BrdU Positive and Negative keratinocytes	106
<b>7.7</b>	BrdU labelling in Keratinocytes	106
<b>7.8</b>	Differential cell extinctions of Swiss 3T3 feeder cells	108
<b>7.9</b>	Growth patterns of Human Epidermal Keratinocytes	110
<b>7.10</b>	Growth patterns of Human Epidermal Keratinocytes	111
<b>7.11</b>	Growth patterns of Human Epidermal Keratinocytes	112
<b>8.1</b>	Recovery of culture epithelial sheet	121
<b>8.2</b>	Cultured Epithelia from different groups	121
<b>8.3</b>	Hematoxylin and Eosin staining of cultured epithelia-Low magnification	123

<b>8.4</b>	Hematoxylin and Eosin staining of cultured epithelia-High magnification	124
<b>8.5</b>	Expression of Cytokeratin 14 (CK-14) in cultured epidermis	125
<b>8.6</b>	Expression of Involucrin in cultured epidermis	126
<b>8.7</b>	Expression of Cytokeratin 10 (CK-10) in cultured epidermis	127
<b>8.8</b>	Expression of Filaggrin in cultured epidermis	128
<b>8.9</b>	Feeder cells contamination in Co-cultures	130
<b>8.10</b>	Demonstration of Proliferative feeder cell contamination by Hoechst staining	130

## Abbreviations

---

$\gamma$ -Irr	Gamma-Irradiation
ATCC	American Type Culture Collection
BSA	Bovine serum albumin
CO <sub>2</sub>	Carbon di oxide
cm	Centimeter
°C	Degree centigrade
CFE	Colony forming efficiency
CBS	Calf Bovine Serum
DMEM	Dulbecco modified eagle's medium
F-12	Ham's F-12 medium
ECNs	Exposure Cell Numbers
EDTA	Ethylene Diamine tetra acetic acid
EGF	Epidermal growth factor
FCS	Fetal Calf Serum
gm	Gram
HCl	Hydrochloric acid
hrs	Hours
IFA	Immunofluorescence assay
KCM	Keratinocyte culture medium
mg	Milli gram
ml	Milli litre
min	Minute
$\mu$ g	Micro gram
$\mu$ l	Micro litre
%	Percent
PBS	Phosphate buffered saline
$\rho$ g	Picogram
TAE buffer	Tris acetate EDTA buffer
TBS	Tris base saline

# **Chapter 1**

## **General Introduction**



## 1.1 Introduction:-

Cell culture based therapies are becoming more and more popular and the future for treating incurable diseases appears to be rapidly heading in the direction of adopting stem cell based therapeutics. The human keratinocytes culture for application in burns was one of the earliest recognized cell based therapeutic approaches using adult stem cells of the epidermis for application in burns (Rheinwald and Green, 1975 a; O'Connor et al., 1981; Gallico et al., 1984). This technique was further used in much larger burn wounds (over 95% of body surface area) and proved lifesaving (Gallico *et al.*, 1984). This is because in massive burn injuries with very limited donor skin, both the short term and long-term problems of the skin loss must be solved by alternative wound closure materials. It is necessary to wait a long time once healthy skin has been used for grafting before the same area becomes reusable. During the waiting period, the patient may die of sepsis or complications of internal organs. The wound should be closed as rapidly as possible in order to reform the water and infection barrier lost when skin is destroyed.

The need to achieve rapid wound closure in patients with massive burns and limited skin donor sites led to the investigation of in-vitro cellular expansion of keratinocytes. The use of cultured epithelial autografts (CEA) was first reported in the treatment of major burns in 1981 (O'Connor *et al.*, 1981). Since that time, support for the use of CEA has varied, ranging from 'a useful agent' (Rue et al., 1993) to having 'no demonstrable effect' (Cuono et al., 1986) on the outcome of extensively burned patients' (Wood et al., 2006).

The large quantities of cultured epithelial autografts for clinical use in the treatment of extensively burned patients are rapidly grown from the adult epidermal stem cells

(keratinocytes) by co-culturing with growth arrested mouse embryonic 3T3 dermal fibroblasts as feeder cells. It is well established that feeder cells are especially effective for the support of cells that are difficult to culture particularly the keratinocytes (Rheinwald and Green, 1975) and other stem cells (Lee et al., 2004; Chen et al., 2007).

Mouse embryonic 3T3 dermal fibroblasts should be irreversibly growth arrested before their use as feeders. The original method for growth arrest of 3T3 dermal fibroblast involved  $\gamma$ - irradiation of these feeders at 6000 rads using Co-60 as source. An alternative approach has been the treatment of 3T3 cells with an anti-cancer agent, Mitomycin C (MC), which is the general norm in the cultures of embryonic stem cells as well (Macpherson & Bryden 1971, Gregnani et al 2007; Liu et al 2007, Nieto et al 2007). In both of these growth arrest methods, feeder cells are stopped from proliferation, enabling their use as non-replicating supportive cells having finite viability. Because the feeder cells need to provide certain active signals, it is important to maintain them in a metabolically active state, allowing continued expression of specific ligands or cytokines (Roy A *et al.*, 2001) and gradually detach from the culture surface due to their finite life as the target cells multiply and occupy culture space (Navsaria et al 1994).

There are inconsistencies in both the growth arrest methods as highly varied conditions of treatment with growth arresting agents were reported (Navsaria et al., 1994; Ramirez et al 2001; Gregnani et al 2007; Liu et al 2007). The action of Mitomycin C was dependent on its concentration (Macpherson and Bryden, 1971), but use of a broad range of concentrations has been reported (Lechner et al 1981; Baroffio et al 1988; Soriano et al 1995; Ponchio et al., 2000; Ramirez et al 2001; Gragnani et al 2003 Takano et al 2008; Fleischmann et al., 2009). The concentrations were either high or low and there was no

general consensus on a single optimal concentration. It was not clear whether the range of Mitomycin C concentrations employed by various investigators would yield similar extent of attenuation with equivalent feeder-cell efficiencies and fool-proof inactivation in the generated feeders. Additionally, exposure cell densities were also inconsistent in these studies, complicating the growth arrest procedure; because the action potential of a cell proliferation-blocking agent was shown to arithmetically depend on exposure cell density (Yerneni and Jayaraman 2003). Hence, there is an unmet need to identify a uniform growth arrest protocol that exerts optimal and reproducible growth supporting activity. It is, therefore, proposed that the inadequacies in Mitomycin C induced growth arrest could perhaps be overcome at first, by an experimental strategy of varying the exposure cell number of feeder cells for any given concentration. Secondly, a range of values consisting of permutations of Mitomycin C concentrations and the doses per cell can be arithmetically derived. This could ultimately lead to the identification of a growth arresting protocol in which a fixed exposure cell number would be treated with an optimal Mitomycin C concentration in a way to deliver an optimal dose per cell.

It was reported that the growth arrested 3T3 cells were able to survive both in vitro and in vivo which turned out to be immunogenic after transplantation resulting in complete graft breakdown (Hultman 1996). However, it was not clear whether the surviving feeders resulted from the failure of growth arrest or remained as non-replicating contaminants. Such a failure of growth arrest in 3T3 cells could possibly arise if variants expressing reduced sensitivity to growth arresting agents gradually accumulate during the routine sub-culturing. The inadequate growth arrest can lead to a risk of viable and proliferative feeder cell contamination during the successive passages of target cells. Therefore, it is of primary

importance to validate the banking procedure for 3T3 cells to avoid inclusion of such variants.

In view of the above observations, this Ph.D. work has been aimed at establishing a procedure for subculturing and banking of 3T3 cells, achieving foolproof growth arrest in the banked 3T3 cells through the use of arithmetically derived permutations of concentrations and doses of Mitomycin C. Further, the work comprised of testing the growth stimulatory influence of those feeders that were growth arrested with such concentration-dose permutations of Mitomycin C on the in vitro growth of human epidermal keratinocytes cells and secondly, characterizing the cultured keratinocytes and the epidermal sheets produced by these, growth arrested feeders in order to identify the best feeder batch.

## **Chapter 2**

# **Review of Literature**

## **2.1 Tissue-Engineered Skin**

Tissue engineering applies principles of biology and engineering to the development of functional substitutes for damaged or lost tissues. Tools for the neo-generation of tissue in tissue engineering research include cells, biomaterials and soluble factors. One main obstacle in tissue engineering is the limited availability of autologous tissue specific progenitor cells. The standard therapy for large burn wounds or chronic wounds is unsatisfactory in terms of quality and rate of healing. Therefore, there is a high demand for tissue- engineered skin that improves wound healing. For the development of tissue-engineered skin, knowledge of the normal skin architecture is important. It shows which components should be replaced by skin substitutes. Several Bioengineered skin grafts or substitutes (also known as tissue-engineered skin substitutes, artificial skin, living skin equivalents, human skin equivalents, or skin alternatives) are available. They are most commonly used to treat chronic wounds, severe burns, and rare skin conditions such as recessive dystrophic epidermolysis bullosa.

## **2.2 Anatomy of the Normal Skin:**

The human body has two systems that protect it from the harmful organisms existing in the environment. The internal defense system destroys microorganisms and bacteria that have already attacked the body. The external defense system prevents microbial microorganisms to enter the body. Skin is biggest external defense system. Skin covers the outside of the body but has other functions beside the defense mechanism. It serves as a mechanical barrier between the inner part of the body and the external world (Sherwood,

2007). Temperature of skin varies in a range of 30 to 40 °C depending on the environmental conditions (Noble, 1993).

The human skin covers a body surface of 1.5 to 2 meter<sup>2</sup> and has a weight of up to ten kilograms. Therefore, it is the largest organ of the human body. It helps maintaining a constant body temperature, serves as a sensory organ and also takes part in communication. Although, the most important function of the skin is to protect the body from the loss of water and to communicate with the environment. The skin also shields against infections by pathogens and against UV radiation (Rongone, 1987; Schaeffler and Schmidt, 1995).

### **2.2.1 Structure of the skin:**

The skin of mammals in general consists of four different layers (Figure 2.1):

- The subcutis
- The dermis
- The basement membrane
- The epidermis

#### **2.2.1.1 Subcutis:**

The innermost layer of the skin is the subcutis. It attaches the dermis to periosteum and fascia and consists mainly of loose connective and fat tissue. Major purpose of the subcutis is to provide structural support and to supply the dermis with blood vessels and nerves. Fat tissue is embedded as islets inside the connective tissue and mainly serves as a storage of nutrients, protection against impact and insulation (Schaeffler and Schmidt, 1995).

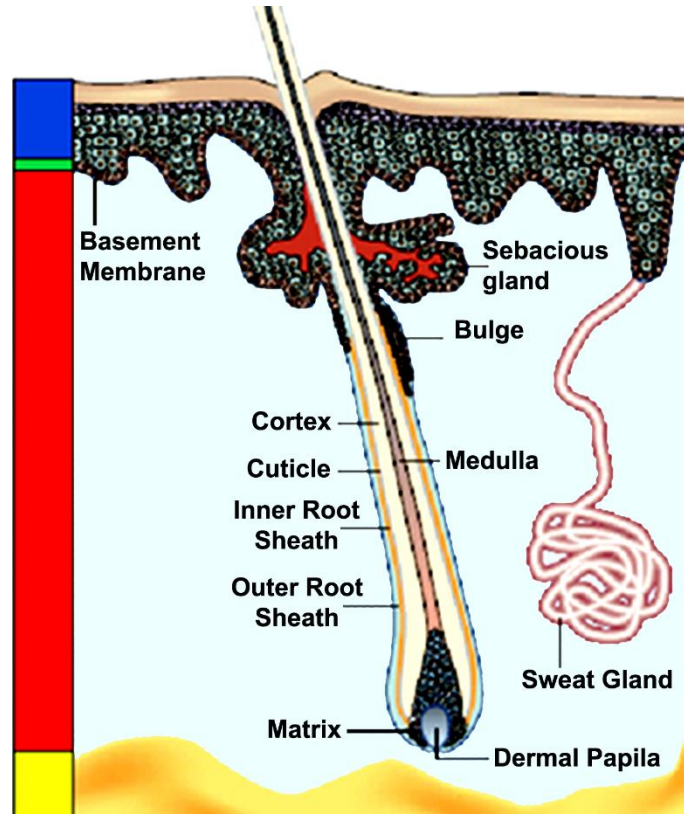


**Figure 2.1** *Mammalian skin (schematic).* Epidermis (blue), basement membrane (green), dermis (red), and subcutis (yellow). (Fuchs and Raghavan, 2002, modified).

### 2.2.1.2 Dermis:

The human dermis is 0.3 to 2.4 mm deep, rich in collagen fibers, predominantly type I and III, and cushions the body from stress and strain. The dermis is divided by a vascular plexus into papillary layer and reticular layer.

#### 2.2.1.2.1 Papillary Layer:

It consists of loose connective tissue and it is teathed to the epidermis by papillae. Blood vessels in the papillae provide support to the basement membrane and the epidermis.



#### **2.2.1.2.2 Reticular layer:**

It consists of irregular dense connective tissue. The protein elastin is expressed more abundant than in the papillary layer and therefore responsible for the elastic properties of the dermis (Schaeffler and Schmidt, 1995). The main cell type found in the dermis is fibroblasts, which synthesize and secrete the structural proteins of the dermis. Both dermal layers consist in general of collagen, elastin, proteoglycans and glycoproteins, but in both layers different types of proteins are predominantly expressed.

The loose tissue is primarily characterized by a high ratio of type III collagen to type I, whereas the dense reticular layer is characterized by more type I collagen in comparison to type III. Additionally type IV collagen is expressed exclusively in the reticular layer of dermis. Among the proteoglycans, decorin is expressed in the papillary layer and versican in the reticular layer of the dermis. The glycoprotein tenascin-C is characteristically found in the papillary dermis, whereas tenascin-X is restricted to the reticular dermis (Sorrell and Caplan, 2004). Sebaceous glands and hair follicles reach deep into the dermis but are actually parts of the epidermis (Schaeffler and Schmidt, 1995).

#### **2.2.1.3 Basement membrane:**

The cutaneous basement membrane is a specific type of ECM and connects the dermis with the epidermis (McMillan et al., 2003). In contrast to the ECM the major collagen component of the basal lamina is type IV collagen, thus forming a sheet-like structure instead of thin fibrils build by type I collagen (Lodish et al., 1999a).

Other important components are different laminins, fibronectin, entactin and perlecan (Bosman and Stamenkovic, 2003). The basement membrane is around 100 nM thick and can be divided into three layers, the sub-basal dense plate adjacent to the basal keratinocytes of the epidermis, the lamina lucida and the lamina densa.

#### **2.2.1.4 Epidermis:**

The epidermis is the outermost part of the skin. It is keratinized, not vascularized and between 30 µm to 4 mm thick. The epidermis is divided into five striated layers: the Basal layer or germinativum layer, the Spinous layer, the Granular layer, the lucidum layer and the outermost layer the cornified layer. The lucidum layer is only found in thick epidermal areas, i.e. palm and sole (Wokalek, 1992; Schaeffler and Schmidt, 1995) (Figure 2.2).

The keratinocytes are anchored via hemidesmosomes to the basement membrane; the intracellular keratin intermediate filaments are connected through integrins to a laminin 6/10 complex and laminin 5 in the lamina densa. These laminins are cross-linked to type IV collagen by entactin. Entactin is one among a variety of small bridging molecules, the most important being perlecan, which also cross-links laminins to type IV collagen, and fibronectin, which connects the lamina densa via type VII collagen to type I collagen bundles of the dermis (McMillan et al., 2003).

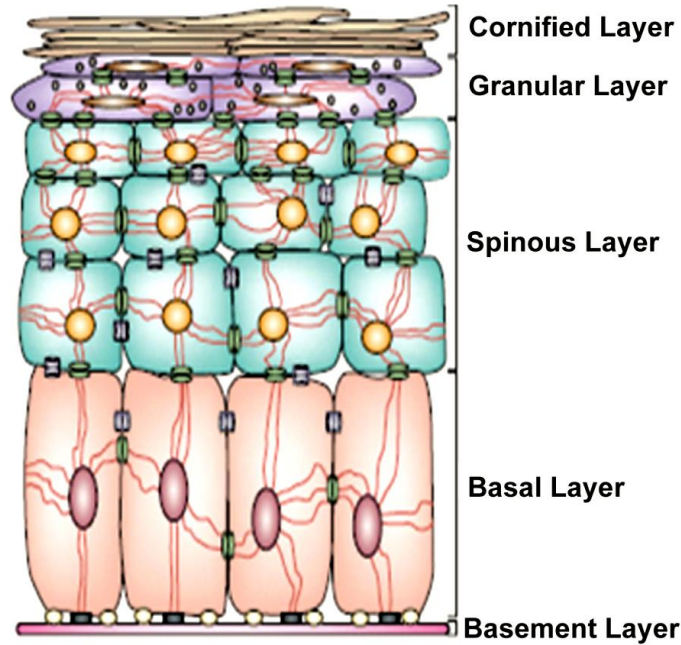


**Figure 2.2:** *Schematic drawing of the epidermis. Striated layers of the epidermis and intercellular connections like desmosomes (Fuchs and Raghavan, 2002).*

Keratinocytes are present in all layers of the epidermis. Other, less numerous cells, are melanocytes, antigen-presenting and Langerhans-cells. Melanocytes synthesize melanin, which is transferred to keratinocytes, where it is responsible for protecting the DNA of nuclei from UV-radiation. Therefore, melanin is responsible for the color of the skin (Schaeffler and Schmidt, 1995).

It is well known that epidermal stem cells exist only in the Basal layer where they proliferate but it is still not clear whether all cells within the basal layer are stem cells or whether only a small number of stem cells exist within this layer. The epidermal proliferative unit (EPU) has been architecturally defined as a bed of 10 tightly packed basal cells yielding a stack of increasingly larger and flatter cells that culminate with a single hexagonal surface cell (Potten, 1974) (Figure 2.3). This has led to the hypothesis that there

is one self-renewing stem cell per EPU and that the other basal cells are so-called transit-amplifying (TA) cells (i.e., committed cells) that divide several times and then exit the basal layer, increasing keratinization occurs during their migration and differentiation through the suprabasal layers. Moreover, in the epidermal basal layer, the PCNA positive cells are found at regular intervals (Tan et al, 2013). It was suggested that the integrin expression profile which varies both in stochastic and deterministic manner influences the division capability of basal cells and when its expression drops to specific levels the cells migrate upwards and differentiation sets in, whereas the label retaining stem cells remain clustered in the basal layer. The long-term repair of burn injuries with human cultured epidermis is a success story of epidermal stem cell therapy wherein stem cells are maintained and expanded in culture. (Green H, 2008)

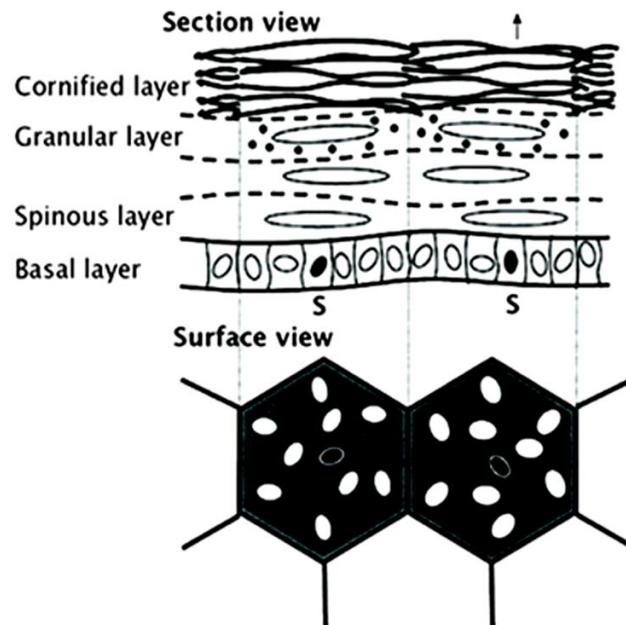


**Figure 2.3** *Schematic drawing of the epidermal proliferative unit (EPU), architecturally defined as a bed of 10 tightly packed basal cells yielding a stack of increasingly larger and flatter cells that culminate with a single hexagonal surface cell [Potten, 1974].*

The keratinization is the character of keratinocytes and is associated with changing expression patterns of keratins, condensing of cytoplasm and loss of nuclei and organelles. Basal cells express keratins K5 and K14, whereas during further differentiation and keratinization keratins K1 and K10 are produced (Byrne et al., 1994). In the end, terminally differentiated keratinocytes are referred to as corneocytes and sloughed off in the cornified layer (Polakowska et al., 1994; Ishida-Yamamoto et al., 1997). In the corneocytes, intracellular proteins like involucrin, loricrin, filaggrin and keratins are covalently cross-linked and form the cornified cell envelope. Together with secreted inter corneocyte lipids the cornified cell envelope builds the so-called “bricks and mortar” system. Hence, the body is protected from losing water and pathogens from the environment face a first barrier (Nemes and Steinert, 1999).

The Basal layer is one cell-layer thick and here the keratinocytes are anchored to the basement membrane by hemidesmosomes. Structural shaping connections between keratinocytes are established by desmosomes, adherens junctions and also tight junctions (Jamora and Fuchs, 2002; Morita and Miyachi, 2003). Gap junctions as communicating connections are building up by different connexins dependent on the epidermal layer (Salomon et al., 1994).

### **2.3 Bioengineered skin:**

Bioengineered skin may be composed of a dermal (inner) layer, an epidermal (outer) layer, or a combination of both, which is embedded into a cellular or acellular matrix (a support structure). Acellular matrices do not contain living cells, but are rather composed

of materials such as collagen, hyaluronic acid, and fibronectin. Cellular matrixes contain living cells obtained from humans (patient or other individual) or another species.

Bioengineered skin can be created using the following substances:

- i. Human tissue (autologous): Derived from the patient's own cells
- ii. Human tissue (allogeneic): Derived from a human other than the individual themselves. A common practice is to utilize cells derived from neonatal foreskin (skin obtained from newborn babies during circumcision)
- iii. Non-human tissue (xenographic): Derived from non-human organisms such as cows, pigs, and horses
- iv. Synthetic materials: A laboratory-produced product derived from man-made materials such as collagen, polymers, and silicone
- v. Composite: Derived from any mixture of materials listed above

## **2.4 Bioengineered skin substitutes:**

Bioengineered skin can serve as either temporary or permanent wound coverings. There are various manufacturers that produce bioengineered skin substitutes including: Apligraf®, Integra®, Epicel®, Dermagraft®, AlloDerm®, OrCel®, and TransCyte (NCDHHS, 2010). Each product is different and requires specific indications.

**2.4.1 Apligraf®** (Organogenesis, Canton, MA, USA) graft skin is a culture-derived human skin equivalent (HSE). Like human skin, it has two layers. The upper epidermal layer is made of living human keratinocytes. The bottom dermal layer consists of human fibroblasts combined with bovine collagen to produce a matrix of proteins. This living skin construct is similar in cell proliferation to human

skin. It is used to treat both diabetic foot ulcers and venous leg ulcers. Since Apligraf is constructed in small size, large wounds may require multiple applications. It is more expensive (\$15000/ft<sup>2</sup>) than other bioengineered products and have 5-day shelf life.

**2.4.2 Integra** (Integra Life Sciences Corporation) is a bilayered membrane system made of a porous matrix of fibers that crosslink bovine tendon collagen and glycosaminoglycan. The epidermal substitute layer is made of a thin poly silicone layer to control moisture and it is used for partial and full-thickness wounds, pressure ulcers, venous ulcers, diabetic ulcers, chronic vascular ulcers, surgical wounds (donor sites/grafts, post-Moh's surgery, post-laser surgery, podiatric, wound dehiscence), trauma wounds (abrasions, lacerations, second-degree burns, and skin tears) and draining wounds. The use of Integra requires complete wound excision. Since it is avascular, there is a high risk of infection and graft loss.

**2.4.3 Epicel®** (Genzyme Biosurgery, USA) uses autologous keratinocytes from a recipient's healthy skin tissue that are cultured to form cultured epidermal autografts (CEA). The autografts are processed into sheets that are attached to a petrolatum gauze backing using stainless steel surgical clips. The autograft is applied directly to the burn wound. It has long culture time of 3-4 weeks with a shelf life of this product is one day. The cost of Epicel is USD 14/cm<sup>2</sup>.

**2.4.4 Dermagraft®** (Advanced BioHealing, Inc., La Jolla, CA) is a single layer biosynthetic dermal substitute made of human fibroblasts. The fibroblasts are obtained from neonatal foreskin and cultured on a bioabsorbable polyglactin mesh for several weeks. Matrix proteins are secreted during the culture period

that includes human dermal collagens and soluble factors, which creates a three dimensional matrix that is used as a dermal replacement or temporary skin substitute in diabetic foot ulcers (DFUs) and venous leg ulcers (VLUs). Dermagraft is used only for temporary coverage, which is the main disadvantage of this product and it has a shelf life of 6 months.

**2.4.5 OrCel®** (Forticell Bioscience, Inc. New York) formally known as composite cultured skin is a living skin equivalent. This bilayered cellular matrix is made of human dermal cells cultured in bovine collagen sponge. The absorbable matrix is used as a wound dressing. It is indicated in chronic diabetic and venous wounds. It is a cryopreserved product.

**2.4.6 Alloderm®** (Life Cell Corporation, NJ) is skin tissue donated from cadavers to make an acellular dermal matrix that has been freeze dried after processing. It is used to serve as a scaffold for normal tissue remodeling. The collagen framework provides strength to the skin and contains no cells that can cause rejection or irritation. Alloderm has been researched as a support mechanism for breast reconstruction, difficult hernia repairs and after parotidectomy to avoid Frey's syndrome. It requires two procedures and has inability to replace both dermal and epidermal components simultaneously.

**2.4.7 Transcyte®** (Advanced BioHealing, Inc., La Jolla, CA; previously available through Advanced Tissue Sciences, La Jolla, CA) is a bilaminate skin substitute made of human fibroblasts cultured on a silicone covered nylon mesh and combined with a synthetic epidermal layer. TransCyte is intended to be used as a



temporary covering over burns until autografting is possible. It can also be used as a temporary covering for some burn wounds that heal without autografting.

**2.4.8 EZ Derm™** (Molnlycke Health Care, US, LLC, Norcross, GA) is a porcine (pig) derived xenograft (non-human skin graft) of collagen that has been chemically cross linked with aldehyde (non-human skin graft) to provide strength and durability. This skin substitute has the reliability of a long shelf life at room temperature. It is designed as a biosynthetic temporary wound covering.

**2.4.9 Oasis Wound Matrix®** (Health point, Fort Worth, TX) is an acellular skin substitute made from porcine small intestine. The matrix is composed of submucosa acellular collagen and acts as a wound covering. It accommodates the remodeling of host tissue by providing an acellular dermal scaffold for tissue growth. It is used for the treatment of chronic, non-infected, partial or full-thickness lower extremity skin ulcers due to venous insufficiency, which have not adequately responded following a one-month period of conventional ulcer therapy.

**2.4.10 PriMatrix™** (TEI Biosciences Inc. Boston, MA) (formerly known as Dress Skin) is an acellular collagen dermal tissue matrix made from fetal bovine skin. It is cell-friendly, strong and vascularizes quickly to provide a scaffold for new tissue development. It was developed to be used in the management of skin ulcers, second-degree burns, surgical wounds, and trauma wounds.

**2.4.11 TissueMend®** (TEI Biosciences Inc. Boston, MA) it is composed of pure, non-denatured collagen, TissueMend is indicated for tendon repair surgery, including

reinforcement of the rotator cuff, patella, Achilles, biceps, quadriceps, or other tendons.

**2.4.12 Celaderm®** (Advanced BioHealing, Inc. in New York, NY) is an allograft that contains active keratinocytes made from epithelial cells of the foreskin. Although metabolically active, they are not capable of proliferating. Celaderm used to accelerate healing of venous leg ulcers.

In the present study, the major focus is on the cost-effectiveness without compromising with the rapid proliferation of human epidermal keratinocyte cells by using growth arrested Swiss 3T3 dermal fibroblast cells. The above mentioned bioengineered skin substitutes have some limitations for their use, in which most of the products have been used in treating diabetic foot ulcer/venous leg ulcer or small burn wounds but only Epicel has the capacity to treat large burn wounds ( $\geq 30\%$ ). However, its use in major burn wounds ( $\geq 50\text{-}60\%$  total body surface area) is limited by the high costs of production. The present study has a major concern over cost/time of production of cultured sheets enabling their use in the developing countries where most of the burn casualties occur.

## **2.5 Burn wound and Regeneration:**

In our country, burn casualties are more frequent and burn centers are not equipped to adopt modern approaches like cultured epithelial grafting leading to high morbidity and mortality. In-vitro cultured epidermis is employed for early closure of burn wounds as an alternative to conventional temporary wound closing material to counter infection and loss of fluids that are major causes for high mortality rates in burn patients. The epidermal culture technique is a well-established technique in many western countries (Teepe et al.,

1990; Daniels et al., 1996; Paddle-Ledinek et al., 1997; Carsin et al., 2000; Elliott and Vandervord, 2002; Atiyeh et al., 2007) and has not yet been the clinical practice in India.

Large numbers of cultured epithelial autografts for clinical use in the treatment of extensively burned patients are rapidly grown from the adult epidermal stem cells (keratinocytes) by co-culturing in the presence of the growth arrested mouse embryonic 3T3 dermal fibroblasts as feeder cells.

## **2.6 Feeder Cells:**

3T3 cells are often used in the cultivation of human keratinocyte cells. The 3T3 cells are a standard fibroblast cell line established from embryonic skin of Swiss mouse in 1962 by two scientists George Todaro and Howard Green at the Department of Pathology, School of Medicine; New York University. The '3T3' designation refers to the abbreviation of "3-day transfer, inoculum of  $3 \times 10^5$  cells which is shortly termed as the '3T3 protocol'.

It was Puck and Marcus (1955) who proposed for the first time that feeder cells grown as a confluent monolayer to make the surface suitable and even selective for attachment of other cells. It is now well established that feeder cells are especially effective for the support of cells that are difficult to culture particularly the keratinocytes (Rheinwald and Green, 1975) and other stem cells (Lee et al., 2004; Chen et al., 2007). They are known to provide a suitable environment in the co-culture with a variety of cell types through cell-to-cell interactions and by producing soluble growth factors and removal of toxicants from the culture medium (Rajabalian et al., 2003).

The most popular feeder cell is the mouse embryonic 3T3 fibroblast that displays persistent keratinocyte or induced pluripotent stem cells promoting activity even after their

fixation in glutaraldehyde or formaldehyde indicating that the growth promoting factor(s) is/are probably bound to plasma membrane (Yaeger et al., 1991, Yue et al., 2012). The epidermal keratinocytes culture in the presence of feeder layer showed a very high growth rate along with significant increase in quantitative expression of protein when compared to cell growth without feeder cells or with conditioned medium (Hunyadi et al., 1989; Parnigotto et al., 1993). Further, studies with keratinocytes grown in basal medium, conditioned medium derived from fibroblast culture, and in the presence of feeder layer revealed significant differences in the qualitative as well as quantitative expression of the keratin pattern (Parnigotto et al., 1994). Keratinocytes cultured with the feeder layer expressed seven keratin types (58, 57, 53, 52, 50, 48 & 45 KDa). Those grown with conditioned medium expressed five Keratin types (58, 53, 52, 48 & 45 KDa). Those with basal medium expressed only one Keratin type (45 KDa). These observations confirm that the rapid growth of the keratinocytes depends on feeder cells layer because epithelial cells cultured on a 3T3 fibroblast feeder layer perceive a softer substrate than those on plastic, which might impact on mechano-transduction pathways (Pellegrini et al. 2014) and the growth potential of keratinocyte also increases in the presence of feeder layer. Culture systems without feeder cells (Hefton et al., 1983) failed to achieve the required expansion in cell numbers because in feeder less system the keratinocytes rapidly showed signs of terminal differentiation and they stopped proliferating after a limited number of passages (Bisson et al. 2013).

The 3T3 feeder layer have been employed successfully for growing large quantities of cultured epithelial autografts with enormous clinical potential in the treatment of extensive burns through drastic reduction in cultivation time of keratinocytes, which is necessary for

fast growth of sufficient quantities of cultured epithelium (Rheinwald and Green, 1975). The 3T3 cells in contrast to human dermal fibroblasts are reported to enhance the culture of keratinocytes since non-proliferating 3T3 fibroblasts are known to generate factors necessary for enhanced proliferation of human keratinocytes (Blacker et al., 1987). The 3T3-J2 strain, which is known to bring about rapid turnover of keratinocytes enabling optimal clinical utilization by reducing the waiting period for culture, is only available with the inventors (Pellegrini et al., 2001) although other available strains, NIH or Balb/C, are known to work adequately (Navsaria et al., 1994).

### **2.7 Methods for Growth arrest of Swiss 3T3 feeder cells:**

The 3T3 cells before using as feeders should be growth arrested in a way to irreversibly prevent them from proliferation but remain finitely live. The original growth arrest method involved  $\gamma$ - irradiation of Swiss 3T3 feeders at 6000 rads using Co-60 as source. The other convenient alternative approach has been the treatment of 3T3 cells with an anti-cancer agent, Mitomycin C (MC). However, there has been a controversy over the efficacy and safety of the Mitomycin C method, because of varied plating efficiency of the stem cells seeded over these generated feeders and recurrent failure of growth arrested feeder cells following Mitomycin treatment. The controversy appeared to have stemmed from the fact that there has been an inconsistency in the adoption of exposure conditions of feeders with Mitomycin C. Moreover, various groups (Ramirez et al., 2001; Gregnani et al., 2007; Liu et al., 2007) have used a wide range of effective concentrations from 4 – 15  $\mu\text{g}$  Mitomycin C per ml of medium for 2 hours at 37<sup>0</sup>C for the growth arrest of 3T3 feeders creating an overall uncertainty in the method. It may thus be hypothesized that the inadequacies in Mitomycin C induced growth arrest could be the consequence of varied initial cell number

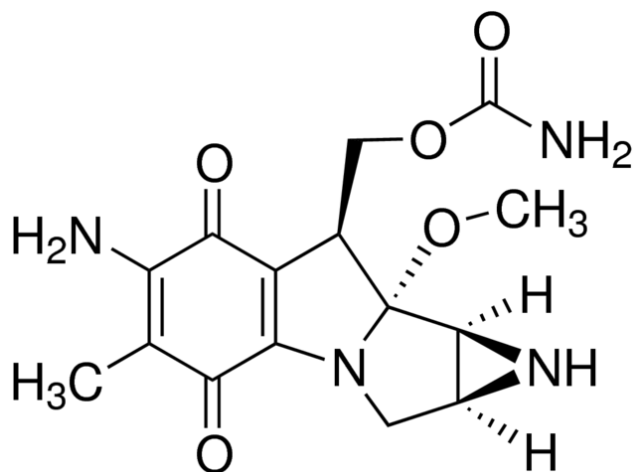
of feeder cells at the time of exposure since the action of cell proliferation inhibiting agents has been shown earlier (Yerneni and Jayaraman, 2003), to depend upon the exposure cell density in an arithmetic manner.

## 2.8 Mitomycin C:

### 2.8.1 Discovery of Mitomycin C:

The Mitomycins are a family of aziridine-containing natural products isolated from *Streptomyces caespitosus* or *Streptomyces lavendulae*. The Mitomycins were first discovered by Hata et al (Hata T. et al 1956) in 1956. Four Mitomycins occur naturally i.e. Mitomycin A, B, C and porfiromycin. All are antibiotics effective against both gram positive and gram negative bacteria (Szybalski & Iyer, 1967), but only Mitomycin C and porfiromycin have appreciable anticancer activity. Wakaki et al. (1958) isolated the Mitomycin C from *Streptomyces caespitosus*.

### 2.8.2 Structure of Mitomycin C:



The Mitomycin C has a molecular formula of  $C_{15}H_{18}N_4O_5$  and molecular weight of 334.33. It contains three anticancer moieties, quinone, urethane, and aziridine groups.

### 2.8.3 Mechanism of action of Mitomycin C:

In tissue culture system Mitomycin C has been known to inhibit mitosis, reduces cell viability and produces nuclear disorganization (Utzat et al 2005). Mitomycin C is capable of arresting cells in G1, S and G2 phases of the cell cycle while the cells remain viable (Nieto et al., 2007). Mitomycin C is a chemotherapeutic agent that avoids DNA double strand separation during cell replication by forming covalent cross-links between DNA opposite strands. It forms crosslinks with high efficiency and absolute specificity for the guanine nucleoside sequence (5'-CpG-3'), while RNA and protein synthesis continue (Verweji and Pinedo, 1990; Tomasz, 1995, Llames et al., 2015).

The damage of the DNA induced by Gamma-Irradiation is not fully understood although it is commonly accepted that Gamma-Irradiation treatment leads to DNA strand breaks and both the approaches inhibit cell replication without interfering with metabolism.

It was described that the treatment with Mitomycin C could successfully bring about growth arrest of 3T3 cells and such growth arrested feeders were employed in culturing of human epidermal keratinocytes (Navsaria et al., 1994) and ocular epithelial cells (Fernandes et al., 2004). However, there has been a debate for growth arrest methods in between Mitomycin C and Gamma-Irradiation treatments. The other growth arrest methods involve the use of X-rays, UV-rays and ultra-electric pulses (Schoenbach et al., 2004; Xu et al., 2009; Browning et al., 2010). The effect of some growth arrest methods in the order of highly to less effectiveness is as follows: Gamma rays > Mitomycin C > X-rays > UV-rays as observed by Schrader, (1999) who concluded that Mitomycin C was adequate although not as efficient as Gamma-Irradiation. Roy et al., (2001) concluded that

Mitomycin C treatment of feeder cells is qualitatively equivalent to Gamma-Irradiation. On the other hand, it was recommended that Mitomycin C could become a better alternative to Gamma-Irradiation to inhibit the feeder layer in long-term culture conditions (Blacker et al., 1987; Ponchio et al., 2000). Earlier, it was reported that cell populations greatly differ in their susceptibility to Mitomycin C and Gamma-Irradiation, indicating that the effect of such treatments should be evaluated for each specific stimulator cell type being used (Webb et al., 1985 and Malinowaski et al., 1992).

It becomes apparent that the choice on the effectiveness of both the methods originates from the fact that the conditions of treatment are so varied from one group of investigators to the other (Navsaria et al., 1994; Ramirez et al 2001; Gregnani et al 2007; Liu et al 2007). The most important guiding factor in any center involved with stem cell culture is the choice of Gamma-Irradiation or Mitomycin C treatment. Since the availability and cost of whether Gamma-Irradiation equipment, which is expensive and time consuming or Mitomycin C reagent which is readily available at low cost are often the matter of concern (Ponchio et al., 2000, Llames et al., 2015).

Macpherson and Bryden (1971) reported that the action of Mitomycin C was dependent on its concentration. However, it is not clear from the existing data on this subject whether the range of Mitomycin C doses would yield similar extent of growth arrest with equivalent metabolic states (feeder efficiencies) and with adequate growth arrest. It will be more damaging if the growth arrest is inadequate which inadvertently would end up in the resumption of feeder cell proliferation (recovery) and consequently contaminating the target cells. This scenario could be more devastating while dealing with human epidermal cultures that are destined for autologous clinical application. On the other hand, if the



growth arrest of feeders were achieved with higher concentrations of Mitomycin C, the feeder efficiency would be lower than optimal. Thus, the suboptimal growth arrest could ultimately contribute to ineffective growth and differentiation support reflecting both quantitative and qualitative character of target cells particularly in case of clinically significant applications like cultured epithelial autograft in burn patients or even total failure in growth arrest, which is a serious impediment in a clinically significant production line.

In view of the undefined dogma pertaining to optimal growth arrest of 3T3 feeders, it is necessary to; establish the right mode of growth arrest by fixing accurate dosing. Thus this study is aimed at understanding the correct dosing of Mitomycin C. The experiments are designed on the assumption that the outcome of Mitomycin C induced growth arrest could be dependent on concentration of Mitomycin C present in the medium as well as the cell number present at the time of exposure. Additionally to verify the growth stimulatory influence of such foolproof growth arrested feeders on human epidermal keratinocytes followed by characterization of human epidermal keratinocytes and epidermal sheets produced in this manner.

In this study we experienced that it is the method of achieving successful irreversible growth arrest which is more vital for not only preventing the risk of recovery of feeder cell proliferation but also for effective growth support that they render on the human keratinocytes in culture.

# **Aims and Objectives**

**Aims and Objectives:**

1. To optimize exposure conditions for Mitomycin C induction of 3T3 feeder cell attenuation through arithmetic derivation of effective doses based on cell number.
2. To verify cell proliferative influence of such distinctively growth arrested 3T3 cells on human epidermal keratinocytes.
3. To characterize the human epidermal keratinocytes and epidermal sheets cultivated using such optimally growth arrested 3T3 cells.

## **Chapter 3**

# **General Materials and Methods**

**General Materials and Methods:**

All the following chapters in this thesis involved the following common materials and methods while the additional pertinent methods are described under each specific chapter.

**3.1 3T3 fibroblast culture:**

The frozen vial of SWISS 3T3 cells (CCL-92) were purchased from ATCC. The Swiss 3T3 culture supplied at 115<sup>th</sup> passage (designated as zero passage in our laboratory) was cultured in Dulbecco's modified eagle medium (DMEM) (Gibco-Invitrogen) containing 10% (Volume/volume) donor calf serum (Hyclone) and 1.5 grams of sodium-bi-carbonate (Himedia) under cell culture conditions of a constant temperature of 37°C and humidified 5% CO<sub>2</sub> atmosphere. The cells were trypsinized using 0.25 % trypsin (Sigma) and 0.03 % Ethylene-Diamine-Tetra Acetic acid (EDTA) (Sigma) in phosphate buffered saline (PBS) (Himedia) for sub-culturing. The cells were subjected to serial sub-culture as per a protocol validated for absence of spontaneously transformed variants (Chugh et al, 2015). Initially, the supplied culture was subcultured for 4 passages to establish a cryo-preserved master bank which was denoted as 4<sup>th</sup> passage (Figure 3.1).

A working bank was then generated from a frozen vial of master bank (4<sup>th</sup> passage vial) by sub-culturing two more times until 6<sup>th</sup> passage and cryo-banked. The cultures were tested for Mycoplasma (Kumar et al 2008), doubling time, saturation density and absence of growth in methyl-cellulose (Sigma-Aldrich) (Jose Russo et al, 1988). The sub-culture dilutions adopted throughout the banking procedure ranged from 1:6 to 1:10 while

maintaining a seeding density of about  $3 \times 10^3$  cells per  $\text{cm}^2$  as recommended by supplier and the cultures were never allowed to reach more than 50% confluence.

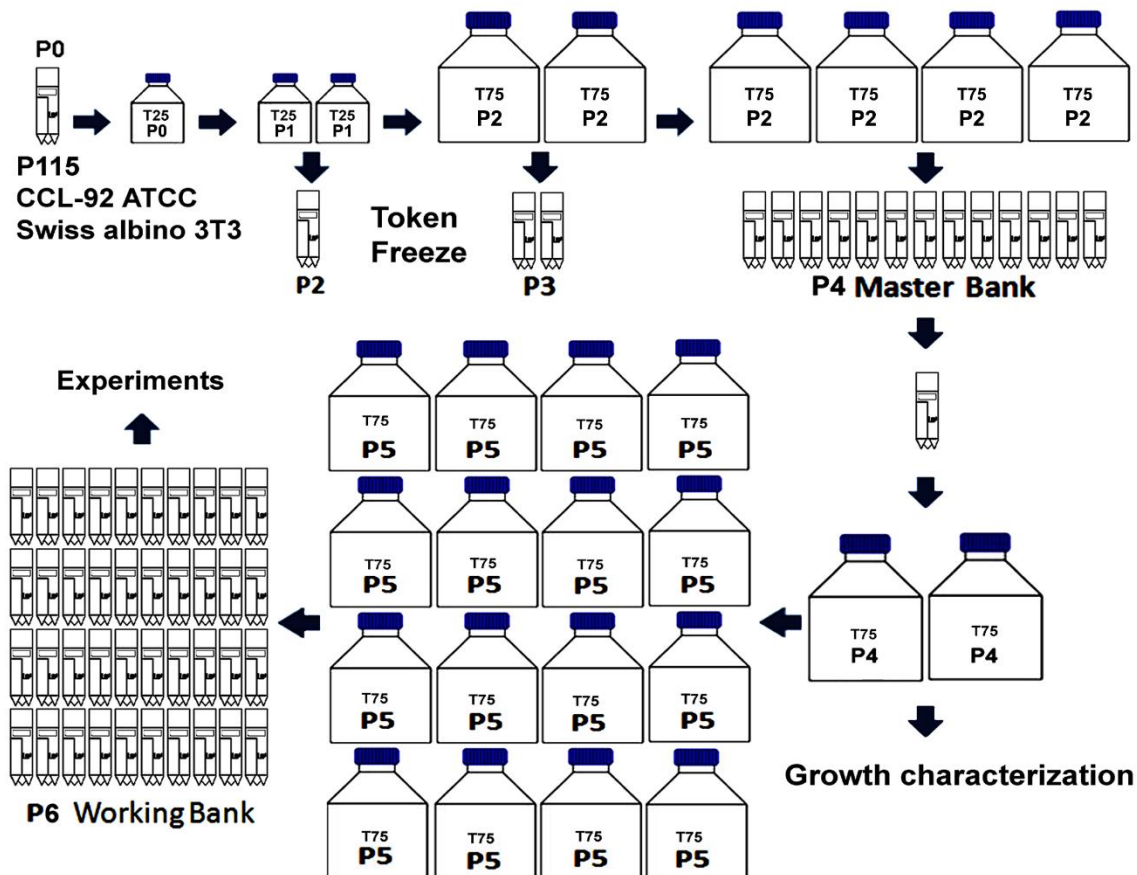


**Figure 3.1** *The adopted two-tiered banking system.* Flow chart illustrating establishment of a two-tiered banking from Swiss 3T3 cells (CCL-92) purchased from ATCC, Cryovial was supplied at 115<sup>th</sup> passage, designated as zero passage and expanded through additional 6 passages at our laboratory.

The 6<sup>th</sup> passage cultures were initiated from cryo-preserved working bank cells after they were rapidly thawed (% viability of  $81.4 \pm 1.1$ ; n=22) and incubating 225,000 cells for 4 days in T75 culture flasks; the output ( $17.90934 \pm 5.3809 \times 10^4$ ; n=22) was further sub-cultured by incubating same number of cells for 3 days; the resultant 7<sup>th</sup> passage output cells ( $17.60247 \pm 4.2266 \times 10^4$ ; n=22) were batch-tested for irreversible growth arrest by

maintaining them until all cells disintegrated subsequent to their pulse exposure to 40 µg of Mitomycin C (Sigma-Aldrich, Catalogue number M4287) in 10 ml of culture medium by diluting a stock solution of 200 µg per ml of HEPES Buffered Earl's Salt (HBES). The other identically generated 7<sup>th</sup> passage cells from parallel working bank vials were designated as qualified feeder cells and the same were used for growth arrest experiments in subsequent chapters.

### **3.2 Keratinocyte-feeder Co-culture**

Primary keratinocytes cells were purchased from Genlantis-USA (Cat No. PH10205A, [www.genlantis.com](http://www.genlantis.com)). The supplied cells received in liquid nitrogen were originally cryo-preserved at the end of first culture of epidermal cells that were isolated from healthy adult human skin biopsy and grown in a feeder-free and serum-free culture system. The cells were used for co-culture experiments with the growth arrested feeders as described by adopting the basic Rheinwald-Green (1975) technique (Navasaria et. al.1994). The keratinocyte growth medium (KGM) comprised of Dulbecco's modified eagle medium (DMEM) (Gibco-Invitrogen) and Ham's F-12 (Gibco-Invitrogen) at 3:1 ratio, 10 % (Volume/Volume) Fetal Calf Serum (Hyclone), 10 µg/ml ciprofloxacin. The following additional growth factors i.e. 5 µg/ml of Insulin (Sigma), 110 µg/ml L-Glutamine (Sigma), 1.0µg/ml of dexamethasone (Sigma), 24.32 µg of adenine (Sigma), 20 µg of L-serine (Sigma), 0.4 µg/ml of hydrocortisone (Sigma), 10 ηg/ml of Cholera toxin (Sigma), 1.346 ηg/ml of Tri-Iodo-thyronine (Sigma) and 5 µg/ml of Transferrin (Sigma) were added in the KGM. While 10 ηg/ml of Epidermal Growth Factor (EGF) (Sigma) were added in the culture medium on day 2.

The keratinocyte co-cultures were passaged by initially treating with 0.03 grams of EDTA per 100 ml of PBS to remove the remaining feeder cells followed by trypsinization of keratinocytes using 0.08 grams of trypsin together with 0.01 grams of EDTA and 0.025 grams of glucose, each of which is per every 100 ml of the respective final solutions and viable cells were counted by trypan blue exclusion method.



## **Chapter 4**

### **Establishment and Validation of**

### **Banking of Swiss 3T3 Cells**

#### **4.1 Introduction:**

Large quantities of cultured epithelial autografts (CEA) for clinical use in the treatment of extensively burned patients are speedily grown from the adult epidermal keratinocytes over the growth arrested Swiss mouse embryonic 3T3 dermal fibroblasts (Rheinwald and Green 1975). These cells are superior in supporting the growth of other target cells as well (Lechner 1981; Navasaria et al 2004). The original inactivation method involved Gamma-Irradiation, although a more convenient option has been the treatment with Mitomycin C (Navasaria et al 2004). The growth arrested 3T3 fibroblasts reportedly survived in CEA and elicited immunogenicity in recipient resulting in complete graft breakdown (Hultman 1996). Reasonably the viable feeders can result either from the mitotically inactive yet surviving feeders or the proliferating ones. Although, there is an evidence of proliferation in other growth arrested mouse embryonic feeders, but there are no specific studies to link the persistence of the viable 3T3 feeders with the failure of growth arrest (Connor 2000).

The 3T3 cells have the potential to undergo spontaneous transformation depending on subculture, confluence state, and type and concentration of serum (Rubin and Xu 1989; Bowen-Pope et al 1994). Repeated and inconsistent passaging of cell cultures leads to the accumulation of specific transformed variants and display of altered characteristics (Takeuchi et al. 2008). Selective accumulation of such variants, particularly in late passage cultures of 3T3 is a strong possibility as they have been extensively subcultured due to their popularity and wide distribution through several channels in the world (Takeuchi et al. 2008). But indications of transformation such as loss of contact inhibition and presentation of phenotypic differences may not readily be apparent, when the transformed variants are less frequent. However, few variants with innate resistance to growth arrest

may continue to even after exposure to MC. Such proliferative feeders then become visible and contaminate the target cell cultures. It may therefore, be hypothesized that the presence of such variants in 3T3 cell cultures is a potential cause for failure of growth arrest.

It is, therefore, proposed to investigate if the proliferative feeder contamination of target cells is dependent on the adopted subculture protocol for 3T3 cells and identify preventive strategies. The identified solutions can help in eliminating apprehensions on feeder dependent culture system (Mallon et al 2006), which is the most efficient and economical method to culture stem cells compared with feeder-free systems (Lamb and Ambler 2013).

In brief, the experimental strategy included adoption of various sub-culture schemes on Swiss 3T3 cells which were tested at every passage for growth in agar-methyl cellulose (suspension culture) and treated with a two-hour pulse of Mitomycin C. The treated cells were evaluated for (1) complete disintegration over a finite time period, (2) epidermal keratinocyte growth support in a co-culture system and (3) presence of viable and proliferative feeder contaminants in the subsequent keratinocyte sub-cultures. Similarly, a transformed clone, established by single cell cloning of transformation foci induced by altering the culture condition was used for comparison. The results indicated the necessity to validate each lot of the growth arrested 3T3 cells through confirmation of the complete disintegration of feeders before qualifying them as safe feeders.

## **4.2 Materials & Methods**

### **4.2.1 3T3 fibroblast culture**

The SWISS 3T3 fibroblast cells (CCL-92) were cultured and cryopreserved as described in Chapter 3. In brief, frozen vial obtained from ATCC at 115<sup>th</sup> passage (**designated as zero passage in our laboratory**) was quickly thawed and grown in 3T3 culture medium and incubated in a humidified 5% CO<sub>2</sub> atmosphere at 37°C. The cells were subcultured until 6 passages to establish a cryopreserved master and working banks (Figure 3.1). The cultures were tested for Mycoplasma contamination (Kumar et al 2008) and anchorage independent growth (Jose Russo et al, 1988). All the experiments in this chapter were initiated with the frozen stocks of the working bank.

### **4.2.2 Subculture schemes**

The working bank cultures were subjected to specific subculture schemes which were determined after several rounds of preliminary experiments. Initially, 7<sup>th</sup> passage (P7) cultures were setup in T75 flasks (Nunc) from working bank by seeding 3000 cells per cm<sup>2</sup> and were subjected to varied subculture schemes as depicted in the flow chart (Figure 4.1). Two of the subculture schemes denoted as 3K3D and 3K4D, represented incubation of 3000 plated cells per cm<sup>2</sup> for 3 and 4 days, respectively. The third scheme of 4K3D involved 3 days incubation of 4000 cells plated per cm<sup>2</sup>. The resultant cells were tested for anchorage-independent growth using agar-methocel and stability of growth arrest by Mitomycin C treatment. Further, the 3K3D cells that exhibited irreversible growth arrest and no anchorage-independent growth were repeatedly subcultured by 3K3D procedure to determine the number of passages that these characters persisted. Simultaneously, the cells

were also passaged serially by the 4K3D scheme for comparison to match with the same subculture interval (3 days). The subcultures were continued in T25 flasks until the cells exhibited an obvious 3-dimensional anchorage-independent growth in agar-methocel.

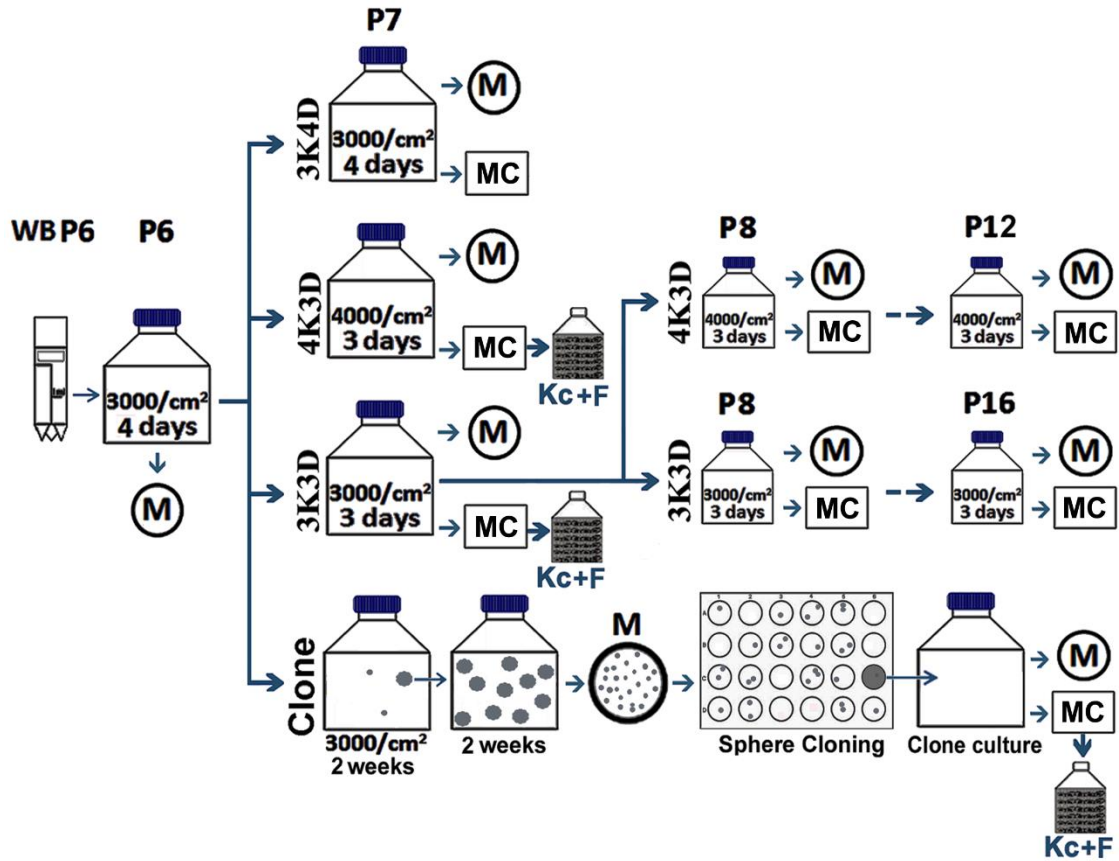


**Figure 4.1** Flow chart depicting the experimental approach of testing the influence of varied subculture schemes in Swiss 3T3 cells at the denoted passage number (P). P6 cultures were uniformly set up by incubating 3000 cryo-preserved working bank (WBP6) cells plated per cm<sup>2</sup> for 4 days in 3T3-CBS medium. The subsequently initiated P7 cultures were subcultured by three schemes. They were 4K3D and 3K3D, representing 3 days incubation of 4000 and 3000 cells plated per cm<sup>2</sup>, respectively and 3K4D denoting 4 days incubation of 3000 cells plated per cm<sup>2</sup>. Parallel cultures from each scheme were tested for anchorage-independent growth in methyl cellulose (M) and responsiveness to Mitomycin C (MC). Subsequently, the 3K3D cells that exhibited no resistance to MC were further serially subcultured as per 3K3D and 4K3D schemes until the presentation of growth in methylcellulose while simultaneously testing for resistance to MC in parallel

*cultures. A separate P7 culture was grown in 3T3-FCS medium for 2 weeks and subcultured once to induce transformation foci which formed spheres in methylcellulose. A culture established by single sphere cloning was tested for MC resistance. The MC treated cells of 4K3D, 3K3D, and the clone were used to co-culture with epidermal keratinocytes (Kc+F).*

#### **4.2.3 Generation of spontaneously transformed clone**

A transformed clone of 3T3 cells was derived from a spontaneously induced transformation focus in a confluent culture of 3T3 cells (Figure 4.1). The transformed focus is a discrete pile of tightly packed proliferating cells that was established by incubating 3000 cells per cm<sup>2</sup> in 3T3-FBS medium containing 10% Fetal Bovine Serum (Hyclone) (Rubin and Xu 1989). The frequency of foci forming cells was increased by sub-culturing a large focus, which was scraped with a cell scraper. Subsequent culture was trypsinized and thousand cells were incubated in agar-methocel for two weeks. The discrete spheres formed by the transformed variants were subjected to the single sphere cloning in 24-well plates. Before experimentation a cryo-preserved bank was established from a proliferating clone by subculturing it additional two more passages.

#### **4.2.4 Growth Characteristics and Cell size measurements**

The P6 cell output was subcultured as per the 3K3D and 4K3D schemes in T25 flasks and counted on each day until confluence. Lag period, doubling time and saturation density were estimated by the standard growth curve method. Similar estimations were made for the cells of P5 and the clone after plating them at a density of 3000 cells per cm<sup>2</sup>. The saturation density of 3K3D and 4K3D cells was additionally estimated in T75 flasks.

The 3<sup>rd</sup> day cells were analyzed for cell size using Cellometer Vision (Nexcelom Bioscience LLC, Lawrence, MA, USA) which was previously calibrated with beads of known sizes. In brief, the trypsinized cells were pipetted into the disposable counting chambers, bright-field images were automatically captured and the pixel area of the captured cells was converted to corresponding cell diameter.

#### **4.2.5 Growth arrest of 3T3**

The cultures intended for growth arrest were treated for two hours with 4 $\mu$ g per ml of Mitomycin C (Catalogue No. M4287, Sigma-Aldrich) which was prepared in 3T3-CBS medium by diluting a stock solution of 200  $\mu$ g per ml of HEPES Buffered Earl's Salt (HBES). Subsequently, cultures were washed 3-times with 3T3-CBS medium followed by phosphate buffer saline (PBS) with 5-minutes incubation at each step. The cells were detached using 0.25% trypsin (Sigma-Aldrich) + 0.03% EDTA (Sigma-Aldrich) solution and counted by trypan blue (Himedia) exclusion. The cells were replated alone at a density of 14000 cells per cm<sup>2</sup> or co-cultured with epidermal keratinocytes in triplicate T25 flasks and incubated in keratinocyte growth medium (KGM). The medium was renewed every 3 days. The cultures beyond 8<sup>th</sup> passage were exposed to Mitomycin C at every passage, washed three times with 3T3-CBS medium and continued incubation in the same culture flasks in KGM. The responsiveness of serial cultures to Mitomycin C was tested until the cells showed anchorage-independent growth for two consecutive passages.

#### **4.2.6 Assessment of Feeder cell fate**

The Mitomycin C treated cells were microscopically assessed on a weekly basis, assigned as completely disintegrated or proliferating and the duration elapsed was

recorded. Criteria considered for complete disintegration were the absence of healthy cells and presence of a very low density of cells that exhibited vacuolated cytoplasm and/or loss of membrane integrity. The visual assessment was performed by three observers. Complete disintegration was verified by transferring the remaining attached cells by trypsinization to a fresh flask and observing for cell attachment. On the other hand, the cultures were designated as proliferating if one or more proliferative foci were observed and continued the incubation of these cultures until confluence.

#### **4.2.7 Anchorage-independent growth assay:**

$10^3$  to  $10^5$  3T3 cells at every passage were suspended in methylcellulose (Methocel, Sigma-Aldrich) which was prepared at a final concentration of 0.8% in 3T3-CBS medium, poured over a base of 0.6% agar in 35 mm dish and incubated under standard culture conditions in triplicate for 2 weeks with periodic examination under Nikon inverted phase contrast microscope.

#### **4.2.8 Keratinocyte - feeder co-culture:**

Primary Human epidermal keratinocytes (Catalogue No. PH10205A) purchased from Genlantis-USA were co-cultured with feeder cells by the basic Rheinwald-Green (1975) technique. The keratinocyte growth medium (KGM) consisted of DMEM with 1/3 volume Ham's F12, 10% FBS, adenine (Sigma-Aldrich) ( $1.8 \times 10^{-4}$ M), transferrin (Sigma-Aldrich) (5  $\mu$ g/ml), Triiodo-L-thyronine (Sigma-Aldrich) ( $2 \times 10^{-9}$  M), dexamethasone (1 $\mu$ g/ml), hydrocortisone (Sigma-Aldrich) (0.4  $\mu$ g/ml), insulin (Sigma-Aldrich) (5  $\mu$ g/ml), Cholera Toxin (Sigma-Aldrich) ( $1 \times 10^{-10}$ M), L-serine (Sigma-Aldrich) (20  $\mu$ g/ml) and L-glutamine (100  $\mu$ g/ml). EGF (Invitrogen) (10 $\eta$ g/ml) was added to the medium 2 days after culture



initiation. Flasks containing 14,000 cells per cm<sup>2</sup> feeder cells were inoculated with 2000 cells per cm<sup>2</sup> keratinocytes and incubated at standard culture conditions for 7-10 days. The cultures were then treated with 0.03% EDTA to remove feeder cells followed by detachment of keratinocytes using 0.08% trypsin + 0.01% EDTA + 0.008% glucose (Rheinwald and Green, 1975) and the viable cells were counted by trypan blue exclusion.

#### **4.2.9 Assessment of feeder contamination**

The isolated keratinocyte suspension was assessed for both (a) non-proliferative and (b) proliferation feeder cell contamination by Hoechst staining.

##### **4.2.9.1 Non-Proliferative contamination:**

The detached keratinocytes were plated in 60 mm dishes without feeders at a density of 1000 cells/dish, allowed to attach by overnight incubation in KGM and feeder cells were counted after Hoechst staining.

##### **4.2.9.2 Proliferative contamination:**

The detached keratinocytes were plated in T25 flasks at a density of 50,000 cells / flask and incubated in KGM for a period of 3 weeks and processed for Hoechst staining.

The cultures were fixed in a chilled solution of three parts of methanol and one part of glacial acetic acid stained with 0.125 µg Hoechst 33258 (Sigma, H-6024) per ml of Hank's balanced salt solution in the dark for 10 minutes, washed with distilled water and observed in an inverted fluorescence microscope (Nikon Diaphot 300) fitted with excitation filter of 330–380 nm and emission filter of 420 nm. The 3T3 cells were distinguished from

Keratinocytes on the basis of their nuclear size, morphology and fluorescence pattern type (Alitalo et al., 1982).

#### **4.2.10 Statistics:**

The experiments of growth arrest, co-culture, anchorage-independent growth assays and feeder cell contamination assays were performed in triplicates. The cell yields among different groups were compared by Student's t test while the linearity of cell yields in serial subcultures was tested by regression. Skew, Kurtosis, Confidence level for mean of cell size distribution were calculated in Microsoft Excel (2007).

### **4.3 Results**

#### **4.3.1 Subculture schemes and response to Mitomycin C**

The P6 cultures yielded  $1,771,851 \pm 36,695$  cells that corresponded to 40% confluence. The subsequent subcultures as per 3K3D, 3K4D and 4K3D schemes yielded  $1,759,950 \pm 64,089$ ,  $2,276,700 \pm 63,580$  and  $2,103,675 \pm 27,152$  cells, respectively (Figure 4.2) which corresponded to confluence levels of 42%, 52% and 48%, respectively. As expected for the higher seeding density or longer the incubation period, the P7 cell yields of 4K3D and 3K4D schemes, were significantly higher ( $P < 0.05$ ) than the 3K3D scheme.

There was a resumption of cell division in Mitomycin C treated 3K4D and 4K3D flasks as evident by the formation of proliferative foci, whereas 3K3D cultures exhibited irreversible growth arrest (Table 4.1). The formation of proliferation foci in 4K3D cells was rapid which was noticed as early as in 1 week after re-plating. However, it was noticed in 3K4D only after 4 weeks by which time the disintegration of susceptible cells was

extensive (Figure 4.3 A). Initially, the foci in reviving cultures were less apparent and showed diffuse zones of bipolar cells among a mix of large attached cells with or without vacuolated cytoplasm and floating cellular debris. Most of such zones, but not all, progressively turned into distinct proliferative foci of polygonal cells with high nucleus to cytoplasm ratio (Figure 4.3 B).

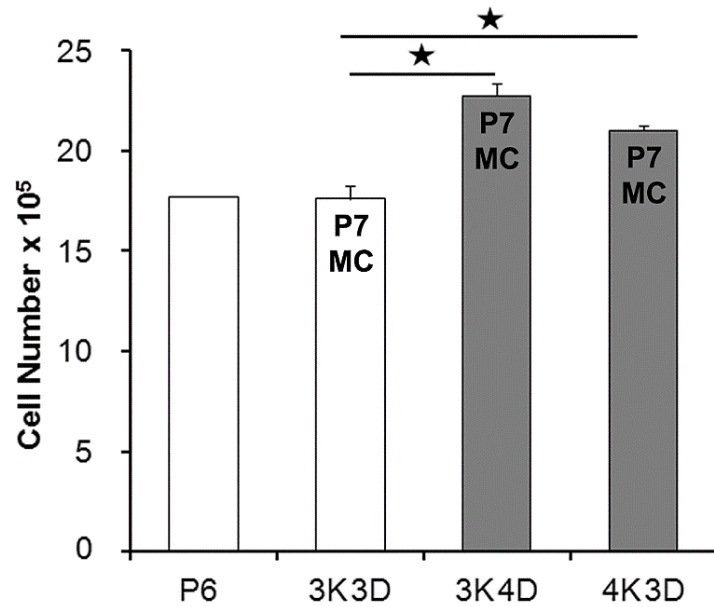


**Figure 4.2** *P6 and P7 cell yields and responsiveness to Mitomycin C.* Column chart representing the influence of subculture schemes on Swiss 3T3 cell outputs in T75 flasks at 7<sup>th</sup> passage (P7) and responsiveness to Mitomycin C (MC). The uniformly set up 6<sup>th</sup> passage (P6) cultures from a working bank were subcultured to P7 by schemes of 3K3D, 3K4D and 4K3D (\* $P < 0.05$ ). Shaded columns represent exhibition of resistance to MC and each column represents a mean value from 3 flasks with the standard deviation.

**Table 4.1: Influence of various subculture schemes at P7 of Swiss 3T3 cells on anchorage- independent growth and responsiveness to Mitomycin C (MC) treatment.**

<b>Subculture Scheme</b>	<b>Growth in methyl-cellulose</b>	<b>Post-MC incubation period (Weeks)</b>	<b>Cells attached after subculture</b>	<b>Post-MC status of culture</b>
3K3D	Nil	6	No	D*
3K4D	Nil	4	-	P#
4K3D	Nil	1	-	P

\*D = Disintegrated cultures; #P = Proliferative cultures

The frequency of proliferative foci at any given time point appeared to vary among replicates. But, it was not possible to accurately estimate the number of foci because they were more frequent at the periphery of the culture flasks making the observation difficult. Not all the proliferative zones were progressed into distinct foci, but a few remained stable or even disintegrated. Several new foci were appeared intermittently while a number of old ones grew larger and coalesced. All the cultures showing progressive proliferation with the new cellular phenotypes became confluent in additional 8-12 weeks. On the other hand, the MC-exposed fibroblasts from 3K3D showed progressive irreversible disintegration and presented extensive vacuolization and completely disintegrated in 6 weeks (Figure 4.4 top left; Table 4.1). So far, we have validated the 3K3D subculture scheme on 22 out of 40 working bank stocks vials for irreversible growth-arrest.

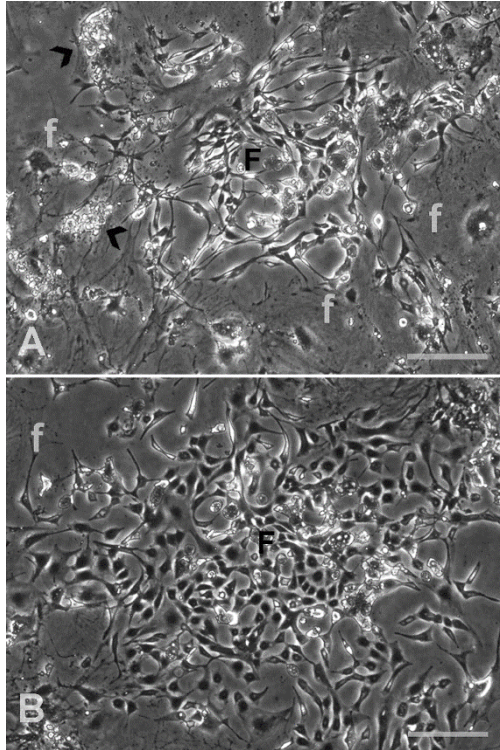


**Figure 4.3 Feeder regrowth in 3K4D culture after Mitomycin C treatment.** The newly formed bipolar cells (F) appeared amidst the attached MC treated large cells (f) and the floating cellular debris (arrowhead, A) after four weeks of post-treatment period. Five weeks later, the same field showed a distinct large collection of multipolar cells with high nucleus to cytoplasm ratio (B). Scale bar: 100  $\mu$ m.

#### 4.3.2 Keratinocyte - feeder Co-culture

One week old co-cultures that was initiated with the 3K3D feeder cells revealed discrete keratinocyte colonies surrounded by the non-proliferating feeder cells which presented the signs of disintegration (Figure 4.4). But the 4K3D feeders that showed failed growth arrest as early as one week after they were plated alone, similarly revived and produced several proliferative foci in co-cultures. The newly proliferated 3T3 fibroblasts were easily identified by their characteristic narrow cell bodies compared with the large disintegrating

cells that presented cytoplasmic vacuolization or nuclear fragmentation (Figure 4.4 bottom left).

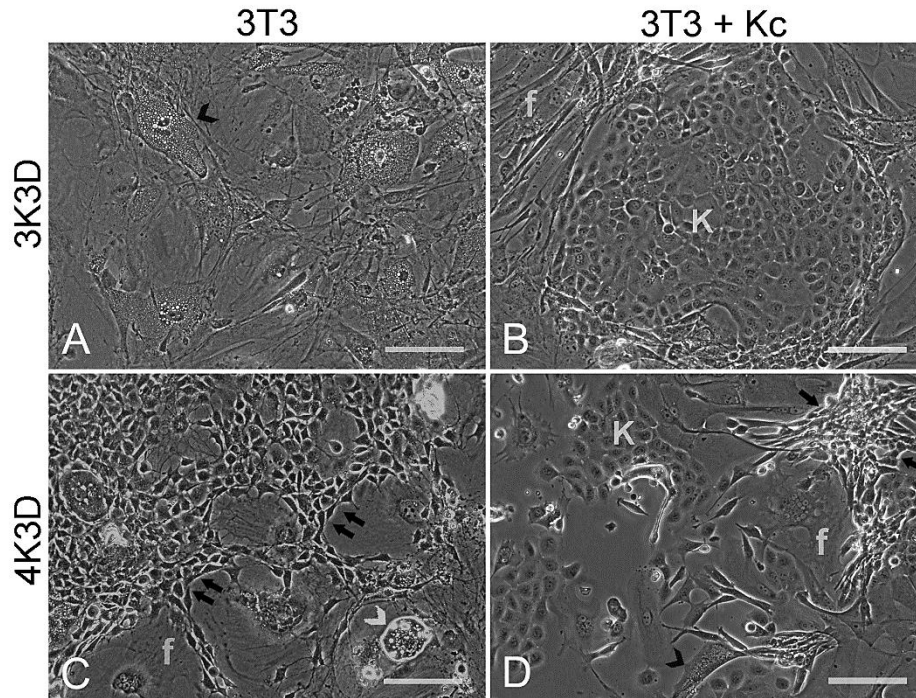


**Figure 4.4 Influence of subculture schemes on responsiveness to Mitomycin C.** The 3K3D feeders (3T3) plated either alone (A) or co-cultured with human epidermal keratinocytes (3T3 + Kc) (B) showed degeneration of feeders (arrowhead) and a large well circumscribed keratinocyte (K) colony surrounded by inactivated feeders. The 4K3D feeders plated alone (C) exhibited newly formed compact proliferative feeder cells with high nucleus to cytoplasm ratio (arrows) over a background of enlarged (f) and degenerating cells (white arrow head). The co-culture with human epidermal keratinocytes showed the proliferative foci (arrows) (D). The 3T3 alone and the co-cultures were 2 and 1 weeks old, respectively. Scale bar: 100  $\mu$ m.

### 4.3.3 Feeder cell contamination:

The feeder contaminants after Hoechst-staining displayed large nuclei with brightly stained coarse chromatin as compared with the small and dull nuclei of keratinocytes (Figure 4.5). The frequency of non-proliferative feeder contamination with 3K3D and

4K3D feeders was uniform at  $28 \pm 4$  per 1000 cells counted. However, when the proliferative capability was assessed, it was found that the 3K3D contaminants progressively disintegrated, whereas the keratinocytes showed a limited proliferation (Figure 4.5 Left panel). In contrast, the 4K3D feeder contaminants proliferated to generate a large population of small cells (Figure 4.5 Right panel). The invading new feeder cells, presenting several dividing cells, tightly enveloped the keratinocyte colonies and the few large non-proliferative feeder cells.

#### **4.3.4 Anchorage-independent growth:**

There was no cultures until P7 that showed an anchorage-independent growth in any of the dishes of methyl cellulose (Table 4.1). Similarly, the serially passaged cultures from P8 to P14 of 3K3D scheme and P8 to P10 of 4K3D scheme failed to grow in suspension cultures (Table 4.2). However, the 3K3D cells showed linear and 3-dimensional growth at P15 and P16, respectively (Figure 4.6) while the 4K3D cells produced similar growth at earlier passages of P11 and P12, respectively. The cells of these cultures exhibited angular outlines with a shallow contrast, as opposed to the smooth outlines of single cells in non-proliferating cultures. The growth of cells in dishes plated with 50,000 cells was observed within 4-6 days of incubation as compared with two weeks in at least one of the dishes that were plated with 1000 cells.

**Table 4.2: Influence of serial subculture schemes at various passages of Swiss 3T3 cells on anchorage-independent growth and responsiveness to Mitomycin C (MC) treatment.**

Subculture Scheme	Passage	Growth in methylcellulose	Post-MC incubation period (Weeks)	Cell attachment after subculture	Post-MC status of culture
<b>3K3D</b>	8	Nil	8	No	D
	9-11	Nil	10	No	D
	12	Nil	11	-	P
	13	Nil	19	Yes*	D
	14	Nil	4	-	P
	15	Linear	3	-	P
	16	3-D	2	-	P
<b>4K3D</b>	8-10	Nil	1	-	P
	11	Linear	1	-	P
	12	3-D	1	-	P

D = Disintegrated cultures; P = Proliferative cultures; \* Few loosely attached vacuolated cells completely disintegrated in 7 days.



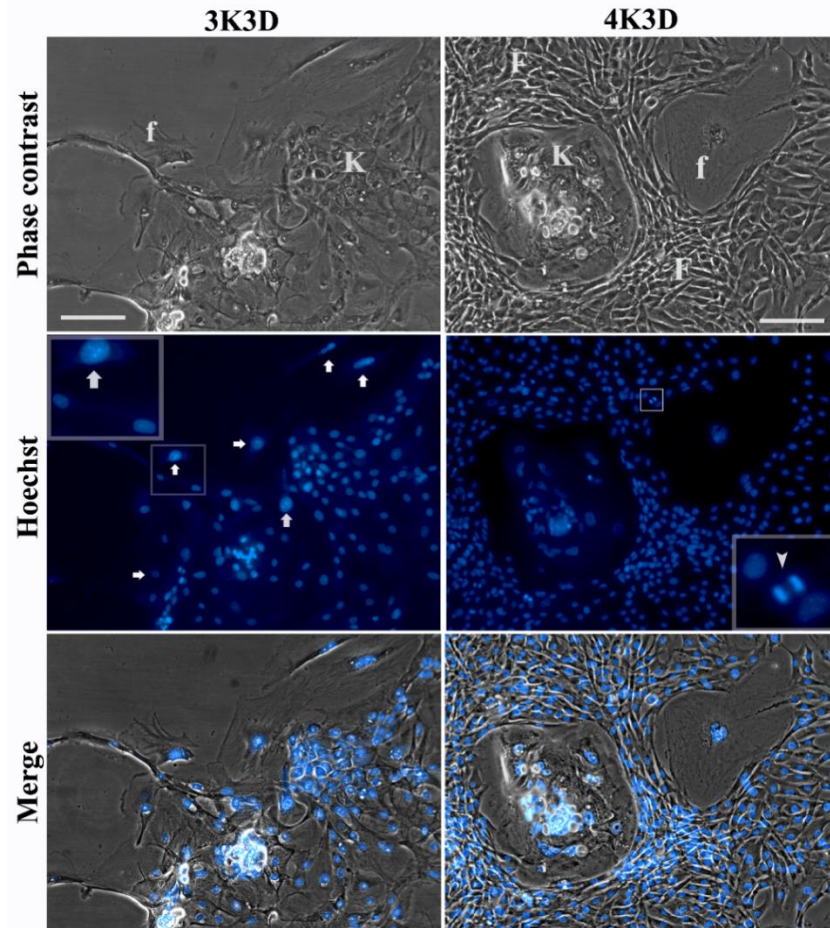


**Figure 4.5 Proliferative feeder cell contamination.** Keratinocyte cultures plated alone without the feeders showing cytological features of attached keratinocytes (K) and the contaminating non-proliferative (f) and proliferative feeders (F). The 3K3D feeder cells that came along with the keratinocytes as contaminants (Left panel) presented no dividing cells and were broad with large nuclei in phase contrast and showed coarse chromatin aggregates (arrows) that stained bright in Hoechst (inset of Hoechst image). The keratinocytes comprised of a mix of small polygonal or broad terminally differentiated cells which presented the dull small nuclei. The 4K3D contaminating feeder cells (Right panel) consisted of well circumscribed keratinocyte colonies (K) enveloped by numerous newly formed narrow-bodied feeder cells (F) with several cell divisions (inset of Hoechst image) in addition to a few broad non-proliferating feeder cells (f) showing vesicular nuclei. Scale bar: 100  $\mu\text{m}$ ; Left inset: 200  $\mu\text{m}$ ; Right inset: 450  $\mu\text{m}$ .

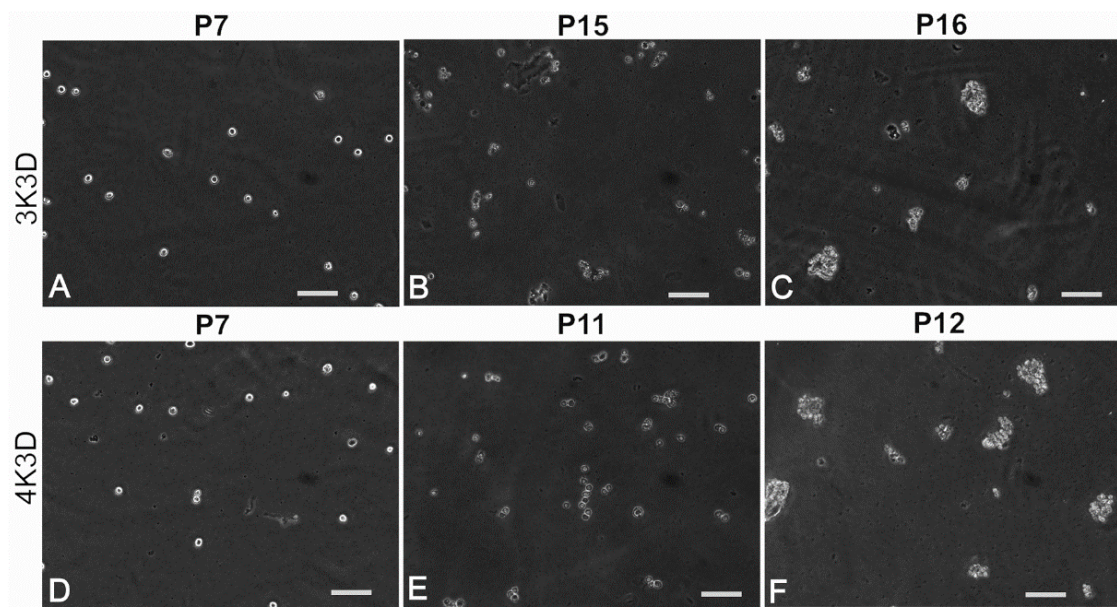


**Figure 4.6 Anchorage-independent growth assay.** Swiss 3T3 fibroblasts from different passages during serial subculture by the 3K3D and 4K3D schemes were plated in methylcellulose. Discrete cells from 7<sup>th</sup> Passage (P7) cultures of 3K3D (A) and 4K3D (D) subculture schemes showed smooth outline. Cells with angular outlines having a shallow contrast were observed at P15 of 3K3D (B) and P11 of 4K3D (E) with occasional linear aggregates. Conspicuous 3-dimensional spheres appeared in the subsequent passages of P16 (C) and P12 (F). Scale bar: 100  $\mu\text{m}$ .

#### 4.3.5 Serial subculture and Response to Mitomycin C:

The cell yields of serial cultures passaged by either 3K3D ( $R^2=0.125$ ) or 4K3D ( $R^2=0.012$ ) scheme did not exhibit any significant trend (Figure 4.7). The average 4K3D cell output of  $6.62 \pm 0.69 \times 10^5$  was significantly ( $P<0.001$ ) higher than  $4.84 \pm 0.44 \times 10^5$  of 3K3D (Figure 4.7 inset) and these values corresponded to 72% and 51% confluence, respectively.

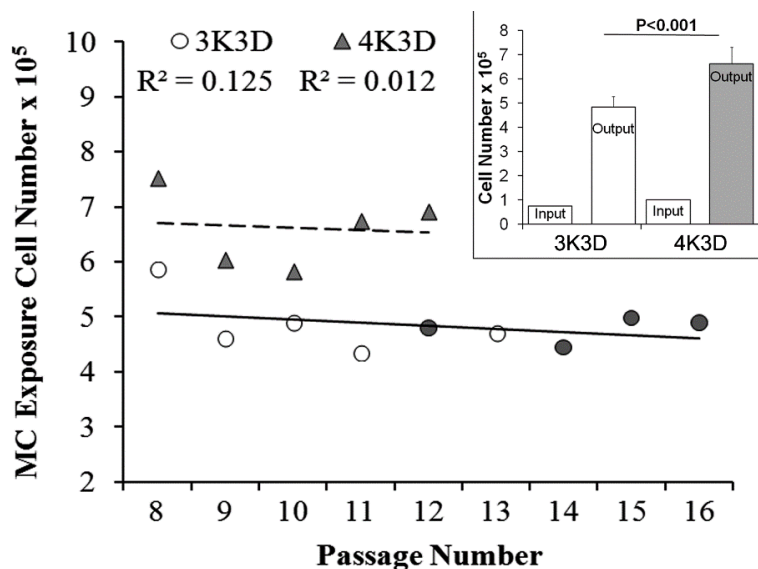


**Figure 4.7 Cell yields during serial subculture:** Scattered plot showing the influence of serial subculture of Swiss 3T3 fibroblasts by schemes of 3K3D and 4K3D on cell outputs and responsiveness to Mitomycin C treatment at each passage. The 3K3D cultures were serially subcultured either by the same scheme or the 4K3D scheme. Shaded markers denote passages at which MC treated cells showed proliferative foci. The columns in the inset represent the number of cells seeded (Input) and yield (Output). Each column represents average cell number of all the passages from each scheme. The shaded column represents consistent resistance to Mitomycin C at all passages.

The serial cultures of the 3K3D scheme from P8 to P11 exposed to MC exhibited total cellular disintegration that took 8-10 weeks (Table 4.2). But the subsequent subcultures were exhibited the conspicuous proliferation foci with the exception of P13, which was disintegrated slowly over more than 19 weeks of post-MC incubation. The time period for the proliferating cells to appear during post-MC incubation gradually decreased with increase in passage number. It was 11, 4, 3 and 2 weeks for P12, P14, P15 and P16 cultures, respectively. On the other hand, the 4K3D cultures persistently resumed post-MC cell proliferation at all the tested passages within a week.

#### **4.3.6 Transformed clone and response to MC**

A clone was established from a transformation focus in a super-confluent culture of Swiss 3T3 fibroblast. Initially, few foci of heterogeneous cells appeared in a 3K3D culture after two weeks of incubation in FBS containing medium (Figure 4.8 A-C). The cells from a large focus isolated by scraping and trypsinization were able to induce more of such foci in a subsequent culture. Each focus was a discrete collection of small cells characterized by high nucleus to cytoplasmic ratio (Figure 4.8 D-F). The single cell suspension from this culture were incubated in methyl cellulose grew into three-dimensional spheres (Figure 4.8 G). A single cloned sphere produced a large homogeneous colony with irregular margins after ten days of incubation (Figure 4.8 H-K). The colony was further expanded by two subcultures in culture flasks. The resultant cell population predominantly consisted of narrow bipolar and tripolar cells (Figure 4.8 L).

The MC-exposed clone cells after two weeks showed several pockets of newly formed small cells in the midst of enlarged and degenerating cells (Figure 4.9 A). Similarly, the epidermal keratinocytes co-cultured with the MC-treated clone cells showed the presence of the newly proliferating and the disintegrating cells. Both the cell types were easily distinguishable from the discrete keratinocyte colonies within a week under the phase contrast (Figure 4.9 B).

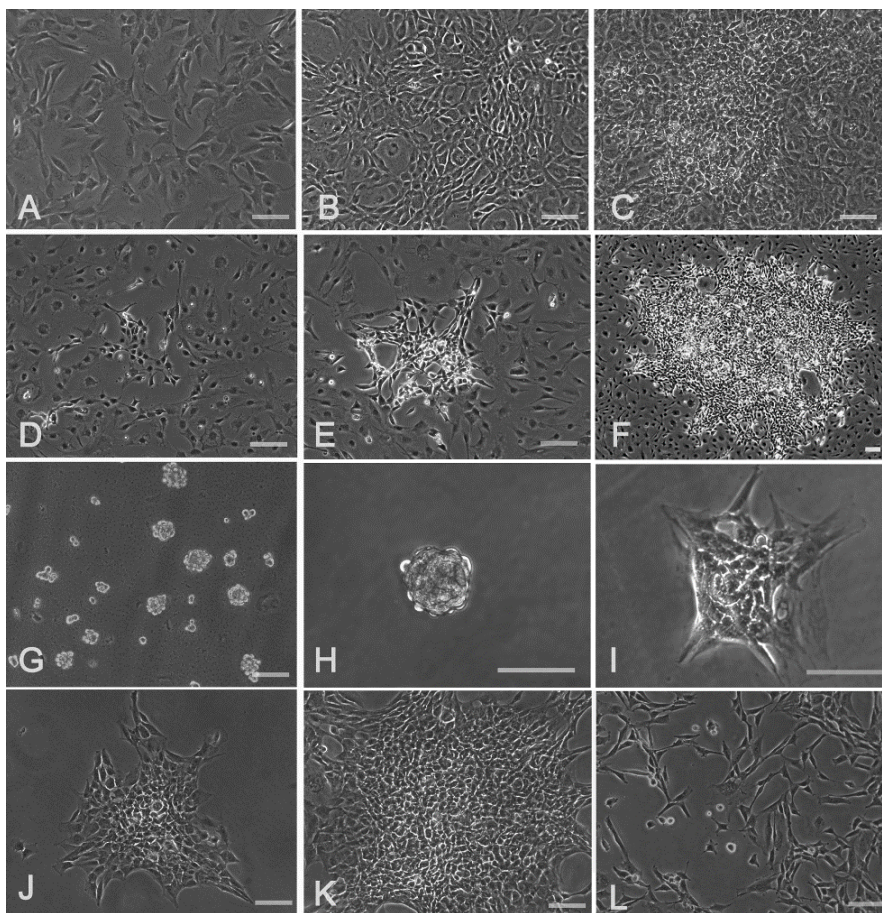


**Figure 4.8** *Establishment of spontaneously transformed clone.* The culture of 7<sup>th</sup> passage Swiss 3T3 fibroblasts initiated with 3000 cells per cm<sup>2</sup> after 3 days showed cells with uniform morphology (A) which reached confluence in five days (B) and formed few transformation foci in ten days (C). After two weeks, the cells from such foci were scraped, trypsinized briefly and the single cells were re-plated in a fresh flask. Several discrete clusters of small cells with compact cell bodies and high nucleus to cytoplasm ratio appeared in two days (D) which grew steadily forming conspicuous colonies in four days (E) and enlarged further in ten days (F) over a background of normal looking broad cells. Two weeks later, the trypsinized cells from this culture formed discrete spheres in methyl cellulose (G) which were subjected to the single sphere cloning in 24-well plates (H). The spheres readily anchored overnight (I), spread out to form small colonies in three days (J) and established as large dense colonies in ten days (K). One such colony further expanded in flasks presented narrow bipolar and tripolar cells (L). Scale bar: 100  $\mu$ m.

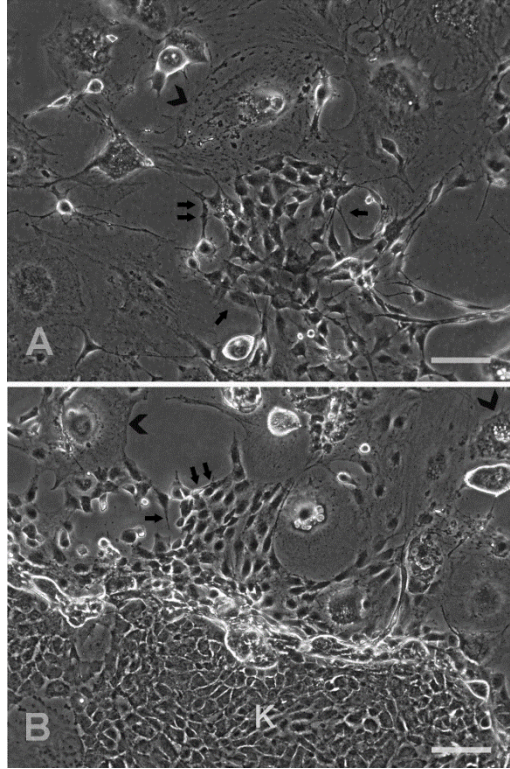


**Figure 4.9** *Failure of growth arrest in spontaneously transformed clone. The 2<sup>nd</sup> passage culture of the clone exposed to Mitomycin C and replated alone (A) exhibited the proliferative focus consisting of the newly formed compact cells (small arrows) surrounded by the broad cells (arrowhead) after 14 days of incubation. The co-culture of the growth-arrested clone cells with the human epidermal keratinocytes (B) presented the well-spread out degenerating cells (arrowhead) and the newly formed cells (small arrows) at the periphery of a large colony of keratinocytes (K) after 7 days. Scale bar: 100  $\mu$ m.*

#### 4.3.7 Growth Characteristics

The growth curves of 3K3D and 4K3D were more or less similar (Figure 4.10). The lag phases of 3K3D and 4K3D cells were 32.4 and 30.0 hours, respectively; the doubling times were 38.2 and 38.5 hours, respectively; the saturation densities in T25 flasks were 37,800 and 36,700 per  $\text{cm}^2$ , respectively while they were 1.48 times higher at 56,000 and 1.6 times higher at 58,700 per  $\text{cm}^2$  in T75 flasks, respectively (Table 4.3). This was in

contrast to the P5 cells which exhibited 26.5 hours of lag phase; 17.7 hours of doubling time and T25 saturation density of 26,800 cells per cm<sup>2</sup>, while it was 1.81 times higher at 48,500 in T75. On the other hand, the spontaneously transformed clone cells exhibited the longest lag phase of 67.7 hours with a prolonged pre-exponential phase, a doubling time of 26.7 hours and attained a much higher density of 159,200 cells per cm<sup>2</sup> after 10 days in culture exhibiting transformation foci.

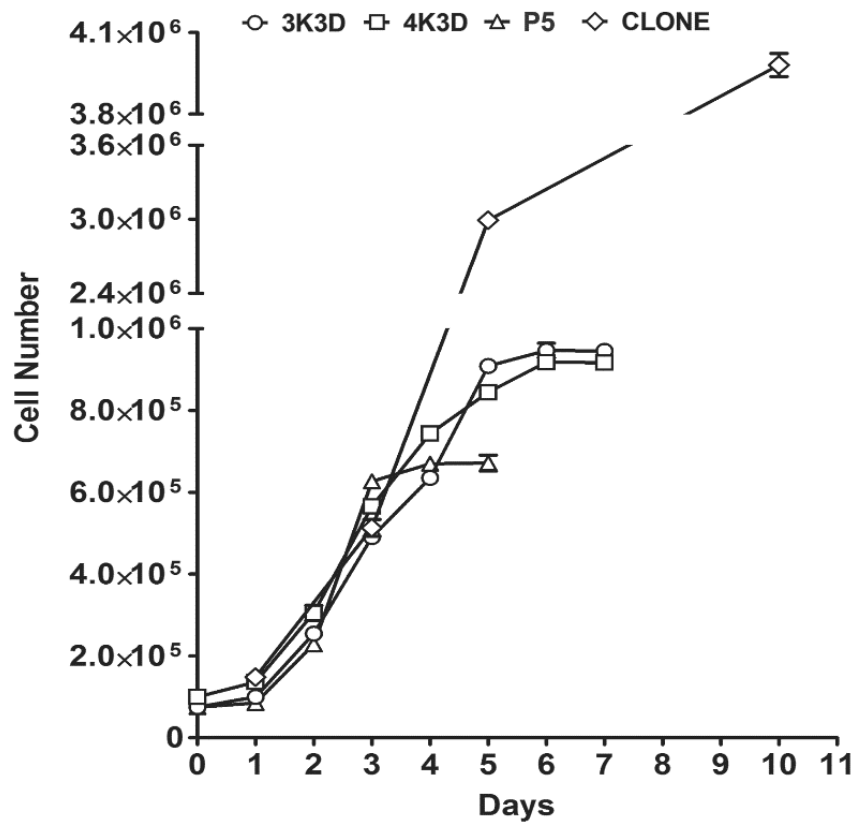


**Figure 4.10 Growth curves.** Growth curves of Swiss 3T3 cells of P5, spontaneously transformed clone and the P7 cells produced by subculture schemes of 3K3D and 4K3D.

**Table 4.3 Influence of subculture on growth characteristics and cell size in Swiss 3T3 cells.**

Characteristics	3K3D	4K3D	P5	Clone
<b>Lag phase (Hr)</b>	32.4	30.00	26.5	67.7
<b>Doubling time</b>	38.2	38.5	17.7	26.7
<b>Saturation density - cells/cm<sup>2</sup> (T25)</b>	37,800	36,700	26,800	>1,59,200*
<b>Saturation density - cells/cm<sup>2</sup> (T75)</b>	56,000	58,700	48,500	
<b>Sample size</b>	1,924	3,053	2,600	2,619
<b>Minimum</b>	5.04	5.04	5.45	5.45
<b>Maximum</b>	33.89	45.17	51.83	51.91
<b>Mean</b>	11.92	15.44	20.48	21.21
<b>Median</b>	11.27	15.13	17.59	17.95
<b>Mode</b>	7.28	14.92	15.40	15.40
<b>Cell size(µm) SD</b>	4.09	4.19	7.27	7.73
<b>Coefficient of variation</b>	0.34	0.27	0.36	0.36
<b>Skew</b>	1.48	1.86	2.47	2.73
<b>Kurtosis</b>	0.72	2.31	5.8	7.67
<b>Confidence Level for mean (95%)</b>	0.009	0.01	0.009	0.009

\* Cell number as on day 10.

#### 4.3.8 Cell size measurements:

The cell size statistics of 3 days old cultures of 3K3D, 4K3D, clone and P5 cells are given in Table 4.3. The 3K3D and 4K3D cells showed maximum cell sizes of 33.89 and 45.17, and the mean cells sizes were 11.92 and 15.44, respectively while maintaining a uniform minimum cell size of 5.04 µm. On the other hand, the maximum cell dimensions of P5 and clone cells were higher at 51.83 and 51.91 µm with mean cell sizes of 20.48 µm



and 21.21  $\mu\text{m}$ , respectively, while the smallest cell in both the groups measured 5.45  $\mu\text{m}$ . The data from all the groups indicated highly skewed nature of cell size distribution, out of which 3K3D showed the least skewness of 1.48 compared to 1.86, 2.47 and 2.73 for 4K3D, P5 and the clone, respectively. Similarly, the MC sensitive 3K3D cells showed a tendency to a higher uniformity of cell sizes with a smaller kurtosis of 0.72 against 2.31, 5.8 and 7.67 for 4K3D, P5, and the clone, respectively. The deviation in cell size distribution of 3K3D cells compared to other tested groups is apparent from the histogram (Figure 4.11).

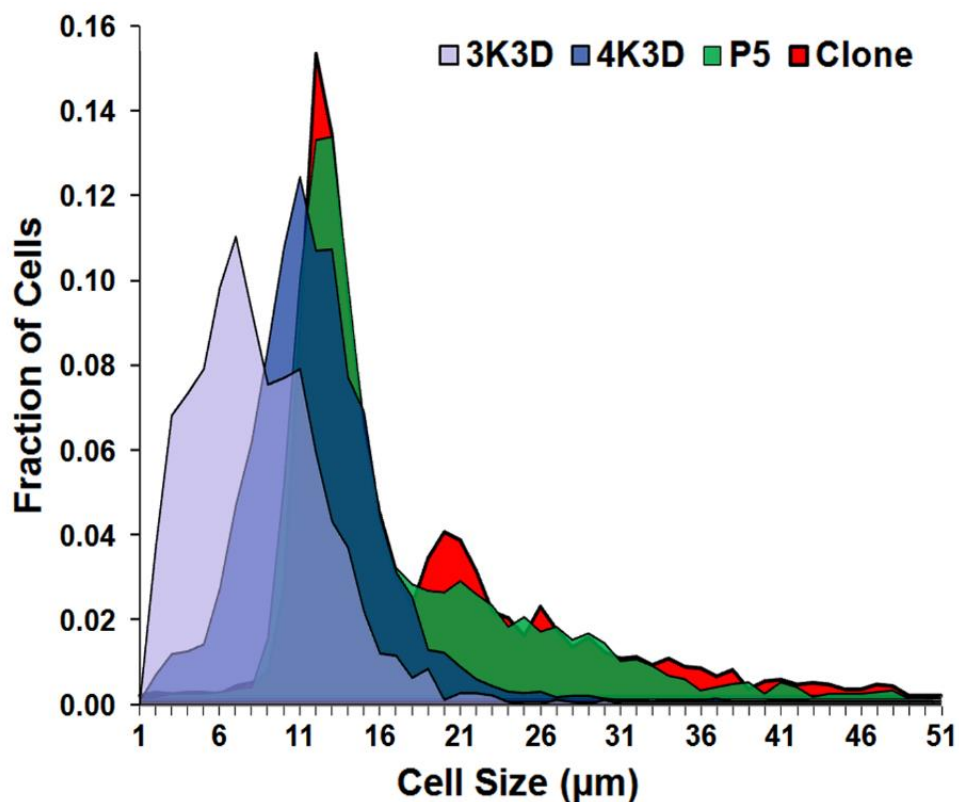


**Figure 4.11** Graphical representation of cell size distribution. Area plot showing Swiss 3T3 cells of P5, spontaneously transformed clone and the P7 cells produced by subculture schemes of 3K3D and 4K3D.

#### **4.4 Discussion:**

Murine Swiss embryonic 3T3 cells have been popularly used as feeder cells for large-scale expansion of epidermal keratinocytes for clinical exploitation in the treatment of burns (Rheinwald and Green, 1975; O'Connor et al. 1981; Atiyeh et al. 2007). The basic technique involved co-culture of epithelial cells with the 3T3 feeder cells growth arrested by Gamma-Irradiation or treatment with Mitomycin C. The epithelial cells are isolated after selectively removing the persistent feeder cells with EDTA treatment. However, the procedure always allowed a small proportion of feeder cells to remain as contaminants (Hultman et al. 1996; Alitalo et al. 1982). The problem might be aggravated further if the feeders resumed mitotic activity because foci of proliferation are known to occur in growth arrested murine embryonic fibroblasts (Connor, 2000).

We occasionally observed sporadic formation of such proliferation foci occurring more preferentially in certain feeder batches (Data not shown). We noticed that the different subculture seeding densities employed to generate these feeder batches remained well within the narrow range of supplier's recommendations. We presumed that the feeder regrowth was perhaps the reflection of subculture dependent distribution of MC resisting cells. The randomness may be due to initial low frequency of such cells which upon serial passaging might become regular. Therefore, we investigated the relationship of the growth arrest failure with the variables of seeding density, the culture duration, and the serial subculture. This study revealed that the MC resistance was specific to subculture procedure. It underlined the need to establish a safe protocol independently for each supplied culture, which possibly contained low level of such variants. The 3T3 cells, originally established by Todaro and Green (Todaro and Green, 1963), have been

extensively circulated in the world through various repositories for several decades. Each lot of cells has since been repeatedly subcultured leading to the accumulation of variants (Takeuchi et al. 2008). It is likely that the cultures resisting growth arrest facilitated a subculture dependent accumulation of specific genetic variants with innate resistance to MC.

Considering that the sensitivity to MC is specific to each feeder cell type (Ponchio et al. 2000), the presence of MC-resistant variants may necessitate the use of higher concentrations of MC to ensure irreversible growth arrest. Correspondingly, use of 4 µg/ml was tested to perform optimally in earlier studies (Watt, 1984; Hoffmann & Rheinwald, 1984), while higher concentrations of MC were reported in certain later studies (Berry et al. 1988; Pepper et al. 1995; Epstein et al. 2005; Qin & Tang, 2010; Lu et al. 2012). But the use of higher concentrations can leave harmful residues in target cells (Zhou et al. 2014). We were able to use a lower concentration yet contained the proliferation of feeder cells by identifying and validating a favorable subculture scheme that perhaps avoided the inclusion of MC-resisting variants.

The other notable point is the induction of clone by prolonged confluence state and exposure to the growth factor rich fetal bovine serum. FBS has been known to stimulate anchorage-independent growth and transformation foci in 3T3 cells (Rubin & Xu, 1989; Peehl & Stanbridge, 1981). But the use of FBS in Swiss 3T3 cell culture has been widely reported (Takeuchi et al. 2008; Hoffmann & Rheinwald, 1984, Pallen & Tong, 1991, Bray et al. 2012) despite the recommendation of the suppliers to use calf bovine serum in culture medium (ATCC, 2014). The existence of several cell lines with the same acronym 3T3 requiring FBS has further complicated the issue.

An important guidance for 3T3 cells is to subculture at 80 percent confluence or less to discourage variant selection (ATCC, 2014). We found that the cultures of all the experimental groups reached a far less confluence state than 80%, yet produced passage scheme dependent feeder regrowth. Another key directive is to limit the passages of 3T3 cells for use in bioengineering of cultured epidermis (Japan Tissue Engineering Co., Ltd. 2006) because the cultured cells respond differently to DNA damaging agents in a passage number dependent manner (Chang & Woloschak, 1997). Consistently, we found that the serial passaging even by the safer scheme of 3K3D led to MC resistance from P12 onwards, although it was intermittently absent at P13.

There is an utmost need to establish fool-proof growth arrest by observing absolute feeder disintegration because feeder regrowth occurred in P12 cells of 3K3D scheme after 11 weeks, but it took 19 weeks to the P13 cells. Therefore, the standard practice of visually assessing the regrowth of feeders under the microscope for a fixed period of 10-14 days for mitotic activity (Connor, 2000) may not be sufficient to rule out the feeder regrowth. Additionally, it is essential to validate visual observation by transferring the remaining cells for attachment and survival.

Under the normal growth conditions, the 3T3 cells do not show anchorage-independent growth in methylcellulose/soft agar (Peehl & Stanbridge, 1981). Therefore, the presentation of three-dimensional growth is indicative of selection of transformants. But this expression was apparent only during late passages as compared with the display of MC resistance at relatively earlier passages. It suggests that the variants responsible for both these presentations are probably not the same. But, on the whole, the methylcellulose assay

is of considerable value for different lots of Swiss 3T3 cells as an advance warning for a deviant culture.

The MC sensitive 3K3D cells were the smallest and showed a tendency to decrease in excess asymmetry (skew) in size distribution as compared with the 4K3D cells although both the groups presented comparable growth curves. Moreover, the presentation of the lowest skew and Kurtosis by 3K3D cells suggests phenotypic divergence. Additionally, while considering the doubling time and the saturation density of the P5 cells as near normal (Todaro & Green, 1963; ATCC, 2014), the 3K3D cells presented the highly deviated growth characteristics and the cell size distribution parameters. It suggests that the cells of 3K3D, like those of 4K3D and the clone, may not represent a truly normal population. But the presentation of absolute irreversible growth arrest qualifies them as the ideal feeders. It is possible that the 3K3D subculture might have facilitated the accumulation of variants other than those that resisted MC thereby altering the growth characteristics. Normally, the repositories perform batch-testing of cell lines for basic growth characteristics and accordingly issue guidance on subculture procedures (ATCC, 2014), but do not test for MC resistance. Therefore, several combinations of the recommended seeding densities and incubation periods need to be included during subculture and tested for MC resistance in order to identify the qualified cells. Once a validated procedure is established it is likely to work safe for the rest of the cell batches generated by a two-tiered banking system (Japan Tissue Engineering Co., Ltd. 2006).

## **Chapter 5**

# **Differential Growth Arrest by Exposure Cell Density Variation**

## **5.1 Introduction**

Ever since Puck and Marcus (1955) for the first time proposed the usefulness of confluent monolayer of feeder cells as a suitable surface for the attachment of other cells, a variety of feeder cells (Parnigotto et al., 1993, 1994; Lee et al 2004) have been used to support the growth of the otherwise difficult-to-grow cell types. The target cells that required feeder cells for their growth are epithelial cells and a variety of embryonic, adult and induced pluripotent stem cells (Rheinwald and Green, 1975, Lee et al., 2004, Chen et al., 2007, Okita et al 2007, Aasen et al 2008). The most popularly used cell lines as feeders are the murine embryonic 3T3 fibroblast cells of Swiss, NIH, Balb/C strains (Navsaria et al., 1994), fetal lung fibroblast cell line MRC-5 (Bullock et al 2006), murine STO fibroblast cells (McMahon and Bradley, 1990). It is proposed that the feeder cells stimulate the growth of target cells through cell-to-cell interactions by way of removal of toxicants from the culture medium, production of soluble growth factors and cytokines and translation of extracellular matrix–cell surface molecule interaction into intracellular signal transduction (Yaeger et al., 1991, Rajabalian et al., 2003; Fleischmann et al 2009).

An effective target cell growth support by feeders is possible only when feeders are growth arrested in a way to keep them metabolically active during their finite life time and ultimately facilitate their gradual disintegration and removal from the culture surface. Popularly, Gamma-Irradiation, sourced from either Cobalt-60 or Cesium-137, is considered rapid and accurate to achieve effective growth arrest of various feeder cells, while exposure to Mitomycin C, an anti-tumor drug and antibiotic, has also been used as an alternative, primarily due to cost factor (Navsaria, 1994; Roy, 2001, Nieto et al 2007). Mitomycin C covalently cross-links DNA with a high specificity for the sequence CpG,

## *Chapter-5 Differential Growth Arrest by Exposure Cell Density Variation*

inhibits DNA synthesis and mitosis without much affecting RNA or Protein synthesis and ultimately causing apoptosis (Verweji and Pinedo, 1990; Tomasz, 1995; Utzat et al 2005). The use of Mitomycin C gained popularity since it was recommended by several investigators as an acceptable alternative to irradiation to inhibit the feeder layer growth (Blacker et al., 1987; Ponchio et al., 2000), although there are certain inconsistencies and contradictions on comparative effectiveness of these methods (Schrader, 1999; Roy et al., 2001; Fleischmann et al 2009).

Primarily, the method of growth arrest of feeders using Mitomycin C has not been uniform among various groups for a basic reasoning that various cell populations differ in their susceptibility to Mitomycin C and Gamma-Irradiation (Webb et al., 1985; Ponchio et al 2000; Malinowaski et al., 1992). However, there have been variations on the use of Mitomycin C even with the same feeder cell type. For instance, diverse concentrations of Mitomycin C ranging from 2 to 15  $\mu\text{g/ml}$  and inconsistent exposure durations ranging from 2 to 3 hours were reportedly employed on Swiss 3T3 fibroblasts (Lechner et al 1981; Takano et al 2008; Baroffio et al 1988; Soriano et al 1995; Ramirez et al 2001; Gragnani et al 2003). Comparative analysis of various exposure concentrations of Mitomycin C ranging from 1 to 16  $\mu\text{g/ml}$  on NIH 3T3 cells (Omoto et al 2009) and exposure durations ranging from 2 to 4 hours on human foreskin fibroblasts (Nieto et al 2007) have shown diverse feeder characteristics. But the exact cell number at the time of exposure to Mitomycin C has not been taken into account by majority of the authors, while a few referred to the exposure cell density as confluent or sub confluent cultures (Fleischmann et al 2009; Zhou et al 2009).



## ***Chapter-5 Differential Growth Arrest by Exposure Cell Density Variation***

It is possible that the uneven feeder functionality could also be influenced by the exposure cell density. It is therefore, proposed that the differences in Mitomycin C induced growth arrest could perhaps be overcome, by an experimental strategy of varying cell number of feeder cells at exposure, since the action potential of a cell proliferation blocking agent has been previously shown to arithmetically depend on exposure cell density (Yerneni and Jayaraman 2003). Here in this study we adopted a similar basic strategy of treatment and analysis to test this hypothesis and investigated the influence of a range of concentrations of Mitomycin C on varied exposure cell densities of Swiss 3T3 cells.

### **5.2 Materials & Methods**

#### **5.2.1 Swiss 3T3 Cell Culture:**

The SWISS 3T3 fibroblast cells (CCL-92) were cultured and cryopreserved as described in chapter 3. In brief, frozen vial were quickly thawed and grown in 3T3 culture medium and incubated in a humidified 5% CO<sub>2</sub> atmosphere at 37°C. The cells were subcultured to establish a cryopreserved master and working banks. All the experiments in this chapter were performed using cultures initiated from the frozen working bank. The cultures were tested for Mycoplasma contamination (Kumar et al 2008) and anchorage independent growth (Jose Russo et al, 1988).

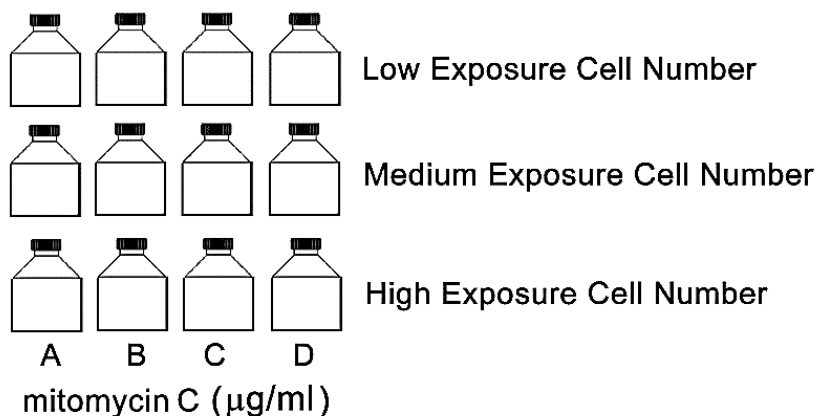
#### **5.2.2 Growth arrest Protocol:**

Swiss 3T3 cells from working bank were cultured in flasks and the output of this culture was plated into T25 flasks with seeding densities of  $4 \times 10^2$ ,  $2.5 \times 10^3$  and  $2 \times 10^4$  cells per cm<sup>2</sup> containing a fixed 10 ml of medium. The cultures were incubated for 5 days to achieve the three required Exposure Cell Numbers (ECNs) at the time of treatment to

## Chapter-5 Differential Growth Arrest by Exposure Cell Density Variation

Mitomycin C (Figure 5.1). The resultant ECNs achieved per cm<sup>2</sup> of growth area were  $0.7276 \pm 0.0844 \times 10^4$  (Low density; n=6),  $3.0711 \pm 0.3021 \times 10^4$  (Medium density; n=4) and  $6.1556 \pm 0.2309 \times 10^4$  (High density; n=4), respectively. After obtaining the required ECN, the cells were exposed to a 2 hour-pulse of Mitomycin C, which was dissolved in Hanks Balanced Earl's Salts (HBES) and diluted proportionately with 10 ml of culture medium to yield a range of Mitomycin C concentrations of 1, 3, 4, 5, and 10 µg/ml; higher than 10 µg/ml were not included because of acute toxicity across all the ECNs.

Treatment of a varied cell number with a 2-hours pulse of mitomycin C at different concentrations to derive doses



$$\Delta = \text{Dose/cell (pg/cell)} = \frac{C \cup}{\varepsilon}$$

Wherein

C = Mitomycin C concentration (µg/ml)

∪ = volume of treating solution (10 ml)

ε = Exposure cell number

**Figure 5.1** Schematic representation of experimental derivation of doses from a given concentration of Mitomycin C by cell density titration in Swiss 3T3 cells.

## *Chapter-5 Differential Growth Arrest by Exposure Cell Density Variation*

Cells exposed to the same volume of culture medium containing HBES served as control. At the end of exposure, cells were trypsinized using a solution of 0.25 % trypsin and 0.03 % EDTA in PBS, counted and replated into 24 well plates at a density of  $14 \times 10^3$  cells per well. The cells were trypsinized, stained with trypan blue and viable cells were counted in Neubauer chamber at intervals of 3 days until 12 days and a final count after 20 days. Each experiment was performed in triplicate and repeated at least twice.

### **5.2.3 Statistics:**

The data of modulation of Mitomycin C induced feeder cells; growth arrest by exposure cell number was subjected to an analytical protocol (Yerneni and Jayaraman, 2003) to verify density dependent influence of Mitomycin C on 3T3 cells. The replated control cells grew with a normal sigmoid curve as expected & reached confluence between days 6 & 9; therefore cell number comparisons between treated and control would be logically inappropriate. Therefore, independent growth curve plots were constructed for every concentration of Mitomycin C tested on the three ECNs without representing control. The cell number data at each time point was analyzed by one way ANOVA and significance was considered, if  $P < 0.05$ . Additionally, significance of variance in data resulting after the action of combinations of a given concentration with the three ECNs across Days 3 to 12 was analyzed by two-way ANOVA; day 20 data was omitted because of absence of cells in certain combinations. The dose, expressed as  $\mu\text{g}$  of Mitomycin C per million cells, which equals to  $\text{pg}$  per cell, was calculated by dividing the product of concentration in  $\mu\text{g}$  per ml and volume of treating solution in ml with exposure cell number in millions (Figure 5.1). The significance of linearity between viable cell number for each time point and Mitomycin C dose was tested by correlation coefficient. The categories of growth arrest outcome as

**Chapter-5 Differential Growth Arrest by Exposure Cell Density Variation**

defined on the basis of cell extinction trend were represented in a growth curve plot and analyzed by regression.

**5.3 Results:**

The lowest concentration of 1 µg per ml of Mitomycin C tested on feeder cells of the three exposure cell densities (ECNs) influenced significant ( $p < 0.02$ ) ECN dependent variation in cell extinction at days 6 and 9, but thereafter there was a steady increase in cell number indicating failed growth arrest (Figure 5.2 A).

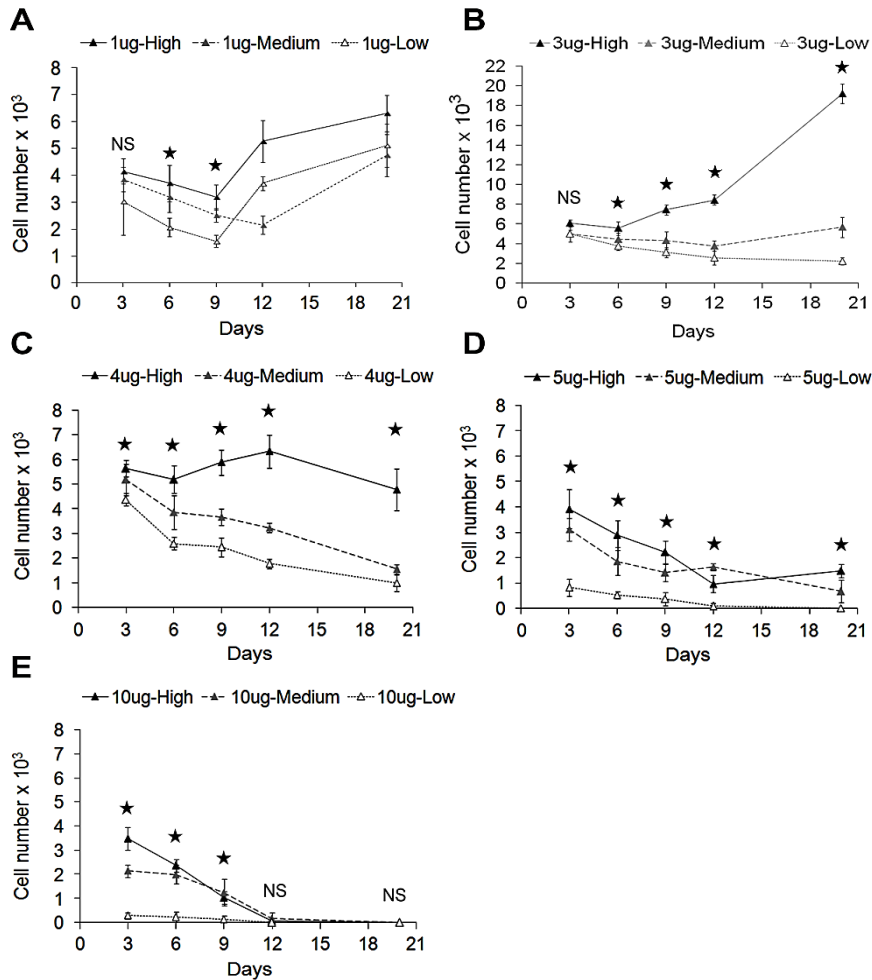


**Figure 5.2 Influence of various concentrations of Mitomycin C on cell extinction / proliferation of Swiss 3T3 fibroblast cells at various exposure cell densities. The cells at**

## ***Chapter-5 Differential Growth Arrest by Exposure Cell Density Variation***

*Low ( $0.7276 \pm 0.0844 \times 10^4$  per  $cm^2$ ), Medium ( $3.0711 \pm 0.3021 \times 10^4$  per  $cm^2$ ) and High ( $6.1556 \pm 0.2309 \times 10^4$  per  $cm^2$ ) cell densities were exposed to Mitomycin C at concentrations of 1  $\mu g/ml$  (A), 3  $\mu g/ml$  (B), 4  $\mu g/ml$  (C), 5  $\mu g/ml$  (D) & 10  $\mu g/ml$  (E) and periodical viable cell counts were performed on post exposure days of 3,6,9,12 and 20. Cell numbers are presented as the mean with standard deviation from values of triplicate cultures. Viable cell counts from the three ECNs at each time point were analysed by one way ANOVA and the significance ( $P < 0.02$  in A,  $P < 0.03$  in B & E and  $P < 0.001$  in C & D) is indicated by asterisk and insignificance ( $P > 0.05$ ) by NS.*

On the other hand, concentrations of 3 and 10  $\mu g/ml$  influenced significant ( $P < 0.03$ ) exposure cell density dependent variation in cell extinctions, which was particularly true during the period of 3 to 21 days with lower concentration, while it was only during the initial 9 days period with high concentration (Figure 5.2 B & E). In fact, the significance of variance in extinctions produced by 3  $\mu g$  was apparently influenced by the intensely opposite stimulatory influence exhibited by high cell density, because significant variance was not sustained when comparisons on extinction outcomes were made only in between low and medium density. On the other hand, extinction variation was consistently significant ( $P < 0.001$ ) at all-time points with concentrations of 4 and 5  $\mu g$  per ml (Figure 5.2 C & D). Concurrently, every Mitomycin C concentration tested across the three ECNs at all-time points brought about an overall significant ( $P < 0.04$ ) variation as revealed by 2-way ANOVA, indicating that the tested concentration alone is not the determining factor but it is rather the combination of concentration & exposure cell number which are crucial to significantly influence the periodical extinction in the current experimental design.

The ECN dependent differential cell disintegration by a given concentration could be the fallout of Mitomycin C acting in a range of different doses per cell that would result

## *Chapter-5 Differential Growth Arrest by Exposure Cell Density Variation*

from the varied exposure cell number, because notionally the total amount (weight/volume) of Mitomycin C, which is the product of concentration and volume of treating solution, is evenly shared by all exposed cells. This was tested, particularly at those effective concentrations of 3, 4, 5 & 10  $\mu\text{g/ml}$  that brought about consistent growth inhibition on at least one of the ECNs. Hence, the extinctions were correlated with a range of such doses that were arithmetically calculated by dividing the product of a given concentration, expressed in units of  $\mu\text{g}$  per ml and volume of treating solution in ml with exposure cell number in millions as depicted in Figure 5.1. The dose obtained this way was expressed as  $\mu\text{g}$  of Mitomycin C per million cells or  $\mu\text{g}$  per cell. Subsequently, the derived doses were arranged in ascending order from lower 19.5 to higher 549.7  $\mu\text{g}$  per cell showing their relationship with the respective concentration and exposure cell density (Table 5.1). Four distinct categories of action of Mitomycin C were identified amongst the total twelve tested combinations on the basis of significant linearity of post-exposure viable cell number with time as tested by correlation coefficient. These are shown to reflect the overall growth curve status and the respective curves were plotted with regression analysis (Figure 5.3).

The following four distinct categories were identified amongst the total tested combinations:

**Stimulatory:** The resultant growth curve after 3  $\mu\text{g}$  of Mitomycin C per ml were employed on high ECN which showed consistent revival with 20th day cell number higher than the seeded cell number and a significant linear positive correlation ( $P < 0.01$ ) between cell number and days of observation was assigned a final stimulatory status.

**Chapter-5 Differential Growth Arrest by Exposure Cell Density Variation**

**Stationary:** The growth curves after using 3 µg of Mitomycin C per ml to treat medium ECN and 4 and 5 µg Mitomycin C per ml to treat high ECN, showing inconsistent fall in cell number with random transient revival and insignificant linear correlation between change in Cell number and progression of culture time were together assigned a final stationary status.

<b>Table 5.1: Outcome of exposure of Swiss 3T3 cells to a 2-hour pulse of various Mitomycin C doses showing their relationship with the respective concentration, exposure cell density and correlation coefficient of cell number with time.</b>						
<b>Sl. No.</b>	<b>Concentration (µg/ml)</b>	<b>Exposure Density*</b>	<b>Dose** (µg/cell)</b>	<b>Linearity of cell number with time</b>	<b>Significance (n=5)</b>	<b>Growth curve Status</b>
<b>1</b>	3	High	19.5	0.932	P<0.01	<b>Stimulatory</b>
<b>2</b>	4	High	26.0	-0.355	P>0.05	<b>Stationary</b>
<b>3</b>	5	High	32.5	-0.805	P>0.05	
<b>4</b>	3	Medium	39.1	0.364	P>0.05	
<b>5</b>	4	Medium	52.1	-0.978	P<0.01	<b>Inhibitory</b>
<b>6</b>	10	High	65.0	-0.882	P<0.05	
<b>7</b>	5	Medium	65.1	-0.891	P<0.05	
<b>8</b>	10	Medium	130.2	-0.920	P<0.01	
<b>9</b>	3	Low	164.9	-0.900	P<0.05	
<b>10</b>	4	Low	219.9	-0.915	P<0.05	
<b>11</b>	5	Low	274.9	-0.921	P<0.01	<b>Toxic</b>
<b>12</b>	10	Low	549.7	-0.900	P<0.05	

\* Exposure cell densities employed are Low ( $0.7276 \pm 0.0844 \times 10^4$  per  $cm^2$ ), Medium ( $3.0711 \pm 0.3021 \times 10^4$  per  $cm^2$ ) and High ( $6.1556 \pm 0.2309 \times 10^4$  per  $cm^2$ ).

\*\* Doses were Arithmetically derived by dividing the actual amount of Mitomycin C present in 10 ml of medium by the cell number present at the time of exposure using the formula given in Figure 5.1 and arranged in increasing order from lower to higher.

**Chapter-5 Differential Growth Arrest by Exposure Cell Density Variation**

**Inhibitory:** The growth curves following the use of 4, 10, 5, 10, 3 and 4  $\mu\text{g}$  of Mitomycin C per ml to treat medium, high, medium, medium, low and low ECNs, respectively, indicated consistent fall in cell number with significant ( $P < 0.01$  to  $0.05$ ) negative linear correlation between change in cell number and progression of culture time and were grouped together as inhibitory.

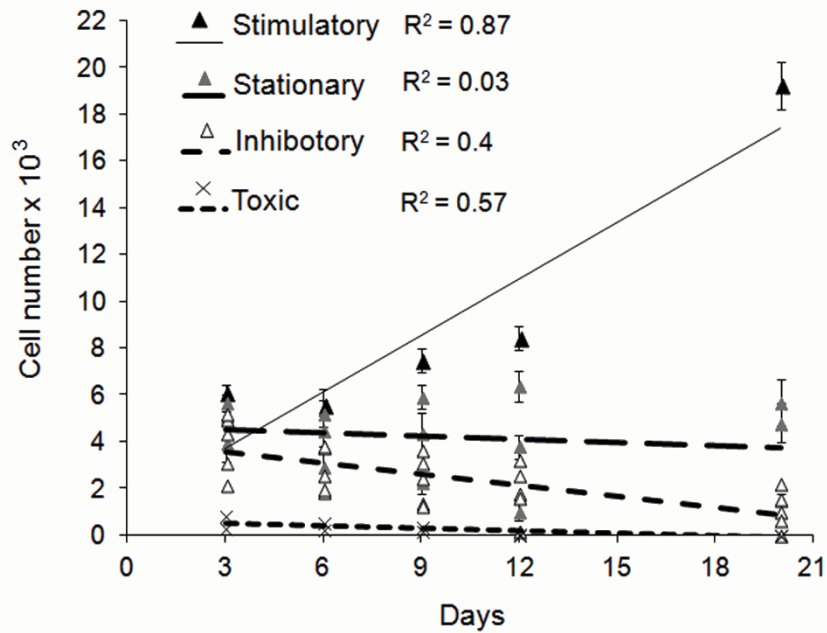


**Figure 5.3** Scatter plot showing the four categories of trends of cell extinction/proliferation of Swiss 3T3 cells over a 20 days period following a two-hour pulsed exposure to various Mitomycin C doses/cell. Stimulatory growth trend was characterized by the 20<sup>th</sup> day cell number significantly higher than seeded cells ( $P < 0.01$ ;  $R^2 = 0.87$ ;  $n = 5$ ); Stationary trend was distinguished by the inconsistent fall in cell number showing insignificant linear correlation with culture time ( $R^2 = 0.03$ ,  $n = 15$ ); Inhibitory trend was evident by consistent fall in cell number showing significant negative linear correlation with culture time ( $P < 0.01$ ;  $R^2 = 0.4$ ;  $n = 30$ ), while the trend was assigned as toxic when the fall in cell number was rapid ( $p < 0.01$ ;  $R^2 = 0.57$ ;  $n = 10$ ) with the 3rd day cell count less than 10% of seeded cells.



## ***Chapter-5 Differential Growth Arrest by Exposure Cell Density Variation***

**Toxic:** The resultant growth curves after 5 and 10  $\mu\text{g}$  of Mitomycin C per ml, employed to treat the low ECN, showed rapid fall in cell number as visualized by the very first cell count at day 3 to be less than 10% of seeded cells and significant negative linear correlation ( $P < 0.01$  to  $0.05$ ) between change in cell number and progression of culture time and were together assigned a final toxic status.

### **5.4 Discussion:**

There are certain earlier reports describing the lethal and cytokinetic effect of Mitomycin C as a function of drug concentration and exposure time while studying its anticancer action (Barlogie and Drewinko 1980), while others concluded that the concentration-response curves are specific to feeder cell type (Ponchio et al 2000), but the criticality of exposure density or dose per cell was not addressed. However, the results of density titration experiments showing differential extinction, particularly in the range of effective concentrations of 3 to 10  $\mu\text{g}$  per ml, is a clear indication of an empirical relationship between exposure cell density and the coefficient of post-exposure fall in viable cell number calculated against time. A dependable correlation between the exposure cell density and the action potential of melatonin which was used as a cell proliferation controlling agent was earlier reported from our lab to follow an arithmetic pattern (Yerneni and Jayaraman 2003). It may thus be inferred that the *in vitro* effectiveness of Mitomycin C and possibly several other chemical agents as well is a secondary but significant function of dose per cell in addition to its concentration, specifically at medially effective concentrations, while lower and higher concentrations due to their weak and intense action potential, respectively, underplay the role of dose. Such a regulatory control resulting in progressive depletion of net cumulative life-span of growth supporting feeder cells

## ***Chapter-5 Differential Growth Arrest by Exposure Cell Density Variation***

remained unreported so far. This relationship could in turn have a significant impact on proliferation of keratinocytes or any adult stem cells, because the ratio of metabolically active but growth arrested fibroblasts and the target stem cells *in vitro* is very critical for the proliferation and/or maintenance of the later (Sun et al 2009; Zhou et al 2009; Jubin et al 2011). Therefore, it may be implied that oversight of this critical consideration of dose per cell could have been one of the probable factors for the reported contradictory efficacy of Mitomycin C approach as compared to Gamma-Irradiation, because the specific exposure density of feeder cells and volume of treating solution were not compared with the resultant cell extinction rates (Ponchio et al 2000; Roy et al, 2001; Schrader, 1999; Nieto et al 2007; Fleischmann et al 2009).

It may thus be proposed that the inadequacies in Mitomycin C induced growth arrest at a certain given range of concentrations could perhaps be optimized by controlling the initial exposure cell number of feeder cells or the volumes of treating solutions. The significance of dose determination based on cell number could also be inferred from the recommended measures of controlling toxicity of chemotherapeutic agents in cancer patients by determining individualized dosing on the basis of recipient's lean body mass (Prado et al 2007) which is the difference between body mass and body fat, the former in turn is the product of cell number and average cell mass (Savage et al 2007). Further, it is proposed that if exposure cell density variation strategy was to be adopted in an *in vitro* toxicology study design, it could possibly form a basis of calculating and predicting a compound's operational *in vivo* dose from the most active concentrations studied *in vitro*.

In other equivalent terms, the range of combined factors of exposure cell density of feeders and concentration of Mitomycin C (constant volume) may be substituted with

## *Chapter-5 Differential Growth Arrest by Exposure Cell Density Variation*

corresponding permutations of volume and concentration of the later, while keeping the exposure cell density at a stably safe constant, to achieve analogous dosing and regulate live feeder cell number. There is a need to apply this alternate strategy in order to set the exposure cell number to such a constant level that the cell population does not accumulate variants through successive passaging. Because cell lines like the 3T3s are known to gradually accumulate spontaneous variants with altered characteristics in a sub-culture dependent manner (Rubin and Xu 1989; Matthews 1993; Chugh et al 2015 [chapter-4]). Connor (2000) advised the use of Mitomycin C at a high concentration of 10  $\mu\text{g/ml}$  to growth arrest mouse embryonic feeder cells, yet cautioned about feeder re-growth and offered no solution than to discard those dishes showing feeder re-growth. It is likely in the present study as well that the observed stimulatory outcome of a lower 3  $\mu\text{g}$  of Mitomycin C per ml employed on a high ECN of 60,000 cells per  $\text{cm}^2$  which is a confluent population could be perhaps the manifestation of accumulated variants with resistance to Mitomycin C. Therefore, a substitute strategy to achieve comparable differential cell extinction rates needs to be considered by employing a constant exposure cell number. This is tested by devising appropriate experiments in chapter 6.

**Chapter 6**

**Differential Growth Arrest by**

**Volumetric Titration**

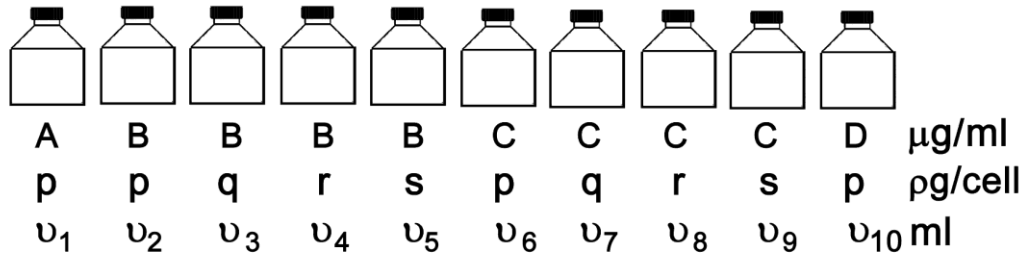
## **6.1 Introduction**

In previous chapter, it is proposed that the range of combined factors of exposure cell density of feeders and concentration of Mitomycin C in a constant volume of treating solution may be substituted with permutations of volume (which is arithmetically derived from the calculated dose) and concentration of the latter, while keeping the exposure cell density at a stably safe constant in order to regulate the cell extinction rate. The need to apply this alternate strategy is essential because the exposure cell number has to be set at such a constant level that the cell population does not accumulate variants through successive passaging. The 3T3 cell line has been shown to gradually accumulate spontaneous variants with altered characteristics in a sub-culture dependent manner (Rubin and Xu 1989; Matthews 1993; Chugh et al 2015 [chapter-4]). Therefore, a substitute strategy of employing a safe exposure cell density as shown in chapter-4 was considered to achieve comparable differential cell extinction rates.

This chapter describes a strategy of testing a range of volumes of a solution of Mitomycin C containing a concentration range of 3 to 10  $\mu\text{g}$  per ml to induce differential extinctions. These volumes would be derived by dividing the product of exposure cell number in millions and dose shown as  $\mu\text{g}$  per cell with concentration of Mitomycin C expressed as  $\mu\text{g}$  per ml of treating solution (Figure 6.1). In this way, volume titrations of a given concentration of Mitomycin C may be adopted to induce differential growth arrest through the production of varied cellular extinction rates. Eventually, a feeder cell growth arrest protocol would then consist of exposure to such derived volume-concentration permutations and generate a series of feeder cell batches from which an optimally performing batch will be identified in terms of maximal stimulation of adult stem cell

proliferation. This strategy is proposed to cut down the cost of culture as compared to Gamma-Irradiation ( $\gamma$ -Irr) technique without compromising with culture time and target cell characteristics.

**Treatment of a constant number of cells to concentration-dose combinations of Mitomycin c**



$\rho, q, r$  &  $s$  = Dose/cell ( $\rho g/cell$ ) represented by ' $\Delta$ '  
 & are derived from cell density titrations using formula

$$\Delta = \frac{C \times v}{\epsilon}$$

$C = A, B, C$  &  $D$  = Concentrations of mitomycin C ( $\mu g/ml$ )

$\epsilon$  = Exposure cell number (in millions)

$v$  = Volume (ml) of mitomycin C solution used =  $\frac{\epsilon \Delta}{C}$

Dose - Concentration combinations are obtained by varying  $v$  &  $C$ , while  $\epsilon$  is kept constant

**Figure 6.1** Schematic representation of producing differential growth arrest by titrations of Swiss 3T3 cells with permutations of concentrations and those doses that were experimentally derived by a process shown in Figure 5.1.

## **6.2 Materials & Methods**

### **6.2.1 Swiss 3T3 Cell Culture:**

The SWISS 3T3 fibroblast cells (CCL-92) were cultured and cryopreserved as described in chapter 3. In brief, frozen vial were quickly thawed and grown in 3T3 culture medium and incubated in a humidified 5% CO<sub>2</sub> atmosphere at 37°C. The cells were subcultured to establish a cryopreserved master and working banks. All the experiments in this chapter were performed using the frozen working bank cultures of 3K3D sub-culture scheme (Chapter 4). The cultures were tested for Mycoplasma contamination (Kumar et al 2008) and anchorage independent growth (Jose Russo et al, 1988).

### **6.2.2 Permutations of concentrations and doses of Mitomycin C:**

Swiss 3T3 cells from working bank were cultured in flasks and the output of this culture was plated into either in T25 or T75 flasks (Chapter 3) and then titrated with a range of dose-concentration permutations of Mitomycin C derived by including the average pre-exposure cell number which was determined from cell counts performed in randomly picked parallel flasks. The permutations were calculated by dividing the product of pre-exposure cell number in millions and the chosen dose expressed as µg per cell with the concentration in µg per ml (Figure 6.1). Further, a broader range of doses than those derived from (Chapter 5) various exposure cell density (ECNs) experiments was chosen for titrations to identifying best outcome by producing more apparent differential degrees of 3T3 cell extinction (Table 6.1).

Each permutation is depicted as a pair of whole numbers separated by a hyphen. The number on the left hand side of the hyphen stands for concentration and the one on the right

denotes the dose. E.g. 3-15 indicates concentration of 3 µg/ml and dose of 10 µg/million cells. Analogously, such permutations represent a range of volumes of treating Mitomycin C solutions in which the derived volume is directly and inversely proportional to doses and concentrations, respectively, as per the following formula.

$$V = \frac{\Sigma \Delta}{C}$$

Where

$V$  = volume of treating solution (ml)

$\Sigma$  = exposure cell number (millions) which is kept constant

$\Delta$  = dose / cell (pg/cell or µg/million cells)

$C$  = concentration of MMC (µg/ml)

Thus, the permutations of dose and concentration along with exposure cell number determine the total amount of Mitomycin C in the final treating volume. The minimum volume of treating solution to sufficiently submerge the entire cell monolayer is the lower limit, while, the maximum capacity of a chosen culture flask is the upper limits respectively. Therefore, the choice of permutations to be included in the study is restricted to only a correspondingly limited range of volumes.

In view of these considerations, several primary screening experiments were conducted by including an initial wider range of concentrations of 1, 2, 3, 4, 5 and 10 µg per ml before short-listing the effective permutations for final testing. Based on a preliminary study, 1 & 2 µg per ml were excluded from dose titrations as the growth arrest produced by them was always reversible ending in re-growth of treated cells. Permutations of 3-10 and 10-30 were included as low and high concentration controls, respectively, since none of the other volumetrically permissible higher dose permutations at these concentrations produced



significantly deviated extinction pattern. Each of the remaining intermediate concentrations of 4 and 5  $\mu\text{g}$  per ml was sub-divided into doses of 15, 75, 150, and 450  $\mu\text{g}$  per cell and the results were compared with 3-10 and 10-30.

The cells were treated with a 2 hour-pulse of Mitomycin C, after proportionately diluting it with culture medium to yield the desired dose permutation. A median volume of culture medium containing HBES was used to expose the vehicle-control flasks which were maintained under identical culture conditions. The experiments were performed to study both short-term and long term effects of Mitomycin C treatments as per the following design:

#### **6.2.2.1 Short Term Influence**

In order to study the 2-hour short term influence on cell viability following exposure of Swiss 3T3 cells to the short listed permutations, the cells in T25 flasks initiated with a fixed density of 3000 cells/cm<sup>2</sup> was pulse exposed to Mitomycin C on day 3. This protocol yielded an average exposure cell density of 490,000  $\pm$  7,775 (n=6) cells per flask and the post-exposure viability was assessed in triplicate flasks.

#### **6.2.2.2 Long Term Influence**

To study the fallout of the short-listed dose-concentration permutations on cell extinctions, the 3T3 cells in T75 flasks initiated with a fixed density of 3000 cells/cm<sup>2</sup> was pulse exposed to Mitomycin C on day 3. This protocol yielded a highly consistent reproducible exposure cell density of 1,760,247  $\pm$  42,266 (n=22) per flask throughout all the experiments and trypsinized cells from each permutation were replated into 24 well

plates at a density of  $14 \times 10^3$  cells per well to evaluate cell extinctions over a period of 12 days.

At the end of Mitomycin C exposure in short and long term influence methods, cells were trypsinized using a solution of 0.25 % trypsin and 0.03 % EDTA in PBS and counted. For long term cell extinction study the replated cells were trypsinized, stained with trypan blue and viable cells were counted in Neubauer chamber at intervals of 3 days until 12 days. Each experiment was repeated at least twice.

### **6.2.3 Statistics:**

The replated vehicle control cells grew with a normal sigmoid curve & reached confluence between 6 and 9 days; therefore comparison between treated and vehicle control was not undertaken as it would be logically inappropriate and a lower and a higher concentration control were included for appropriate comparisons. Each data point represents mean  $\pm$  standard deviation from triplicate samples. Data were subjected to analytical procedures to verify if the cell extinctions are distinct and true reflections of dose variation. For visualizing the immediate influence of 2-hour exposure to Mitomycin C on cell viability, column graphs depicting viable cell yields were constructed and each permutation was compared with 3-10 and 10-30 by Student's t test. Additionally, the 2-hour viable cell output in vehicle control was compared with pre-exposure cell number. Dose dependent fall in viability among all permutations of each concentration was tested by regression and  $R^2$  values were calculated.

For long term cell extinctions, line diagrams were constructed by plotting viable 3T3 cell number on y-axis against post-treatment time points on x-axis to show periodical cell

extinctions caused by each permutation of a given Mitomycin C concentration. Viable cell numbers at each time point was subjected to one way ANOVA to verify the significance of variance among the dose permutations of a given concentration. Additionally, the overall significance of variance across all time points among all permutations under each concentration was analyzed by two-way ANOVA; Further, linear trend lines were plotted using viable cell counts on y axis against doses on x axis by least squares fit and  $R^2$  values were calculated by regression analysis. Furthermore, column graphs were constructed in which each cluster of columns represented the specified permutation and each column represented viable cell numbers at the specified time points. Each cluster of 3-10 and 10-30 was compared with every dose permutation by Students t test after pairing the corresponding time points.

### **6.3 Results:**

#### **6.3.1 Influence on Short-term viability:**

The short-listed permutations involved a derived volume range of 1.47 to 55.12 ml (Table 6.1) wherein the minimum volume was sufficient to uniformly submerge the cell layer in T25 flask whose maximum capacity was 65 ml. Significant differences in 3T3 cell viability were observed immediately after the 2-hours pulsed exposure to Mitomycin C at various permutations of concentrations and doses (Figure 6.2). The treatment resulted in a significant ( $P < 0.05$ ) reduction of cell viability in all groups as compared to vehicle control whose viable cell fraction was similar to that of pre-exposure cell count as determined before the start of experiment demonstrating no influence of vehicle. The intergroup comparisons indicated that the viable cell outputs in 4-15 and 5-450 were comparable to

low concentration control of 3-10 and the higher 10-30, respectively, indicating that increase or decrease of action potential of Mitomycin C depended on not just concentrations but also on doses per cell. Additionally, regression analysis revealed significant dose dependent fall in viability among all the permutations of 4  $\mu\text{g}$  per ml ( $P < 0.01$ ;  $R^2 = 0.926$ ) and 5  $\mu\text{g}$  per ml ( $R^2 = 0.898$ ;  $P < 0.02$ ), further indicating the importance of dose modulation in addition to concentration.

**Table 6.1: Quantitative details of Mitomycin C employed for treating Swiss 3T3 feeder cells with a two-hour pulse.**

Concentration $\mu\text{g/ml}$	Dose $\mu\text{g/cell}$	T75 flask*		T25 flask*	
		#Total amount ( $\mu\text{g}$ )	##Derived Volumes	#Total amount ( $\mu\text{g}$ )	##Derived Volumes
3	10	17.603	5.868	4.900	1.633
4	15	26.404	6.601	7.350	1.838
4	75	132.019	33.005	36.750	9.188
4	150	264.038	66.009	73.500	18.375
4	450	792.113	198.028	220.500	55.125
5	15	26.404	5.281	7.350	1.470
5	75	132.019	26.404	36.750	7.350
5	150	264.038	52.808	73.500	14.700
5	450	792.113	158.423	220.500	44.100
10	30	52.808	5.281	14.700	1.470

\*The average Exposure cell number in T75 and T25 flasks were  $1,760,247 \pm 42,266$  ( $n=22$ ) and  $490,000 \pm 7,775$  ( $n=6$ ), respectively.

# Total amount = Exposure cell Number (millions) x Dose per cell (pg/cell)

## Volume = (Exposure cell Number x Dose per cell)/concentration

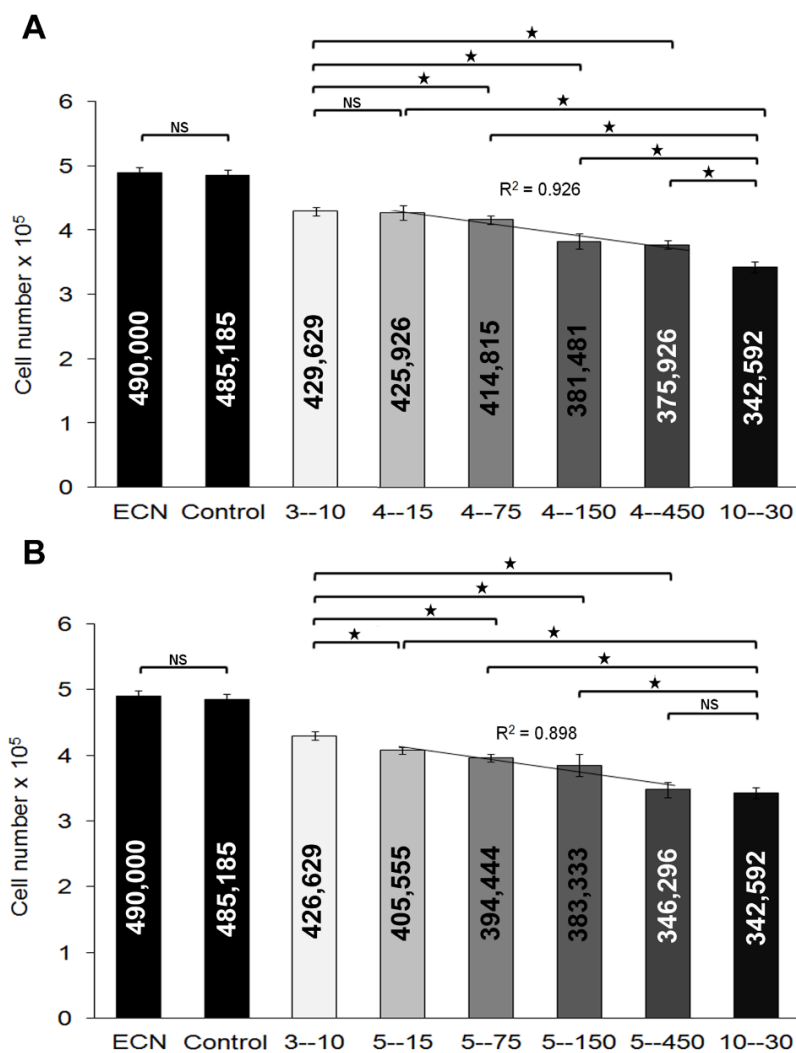


**Figure 6.2** Viable Swiss 3T3 cells from T25 flasks after 2-hour pulsed exposure to Mitomycin C solution. The concentrations of 4 µg/ml (A) and 5 µg/ml (B), each of which was formulated to give dose permutations of 15, 75, 150 or 450 µg/cell. Each permutation was compared with concentrations of 3 and 10 µg/ml, constituted at doses of 10 and 30 µg/cell, respectively, and included as the least and the most toxic permutations. Statistical comparisons performed by Student's *t* test were indicated as significant at  $p < 0.05$  (\*) or insignificant (NS). Dose dependent fall in viability among all the permutations of 4 µg/ml ( $R^2 = 0.927$ ;  $P < 0.01$ ) or 5 µg/ml ( $R^2 = 0.898$ ;  $P < 0.02$ ) was tested by regression. Pre-exposure cell number (ECN) was determined by cell counts from three random flasks before treatment. Control represents viability in flasks sham exposed to only Mitomycin C vehicle solution. Each column depicts average with standard deviation from triplicates.

### **6.3.2 Influence on long-term extinctions:**

The tested permutations involved a volume range of 5.281 to 198.028 ml while the maximum capacity of T75 flask was 265 ml. The replated Mitomycin C treated cells exhibited differential periodic cell extinction in a dose dependent manner within the tested concentrations of 4 and 5  $\mu\text{g}$  per ml (Figure 6.3).

A dose per cell dependant increase in cell extinction rate was produced by the dose permutations of 4-15, 4-75, 4-150 and 4-450 (Figure 6.3A). The variation was significant at specific time points of days 6, 9, 12, though it was insignificant ( $P < 0.09$ ) at the earliest time point of day 3. The regression analysis on the other hand (Figure 6.3B) revealed that the volume titrations brought about significant dose dependant intensification of cell extinction on day 3 ( $R^2 = 0.985$ ;  $P < 0.01$ ), day 6 ( $R^2 = 0.969$ ;  $P < 0.01$ ), day 9 ( $R^2 = 0.9$ ;  $P < 0.02$ ) and day 12 ( $R^2 = 0.888$ ;  $P < 0.02$ ). Taking into account the influence of all doses within this concentration across various time points, the dose modulation was proven to induce highly significant ( $P < 0.001$ ) variation in cell extinctions as revealed by 2-way ANOVA.

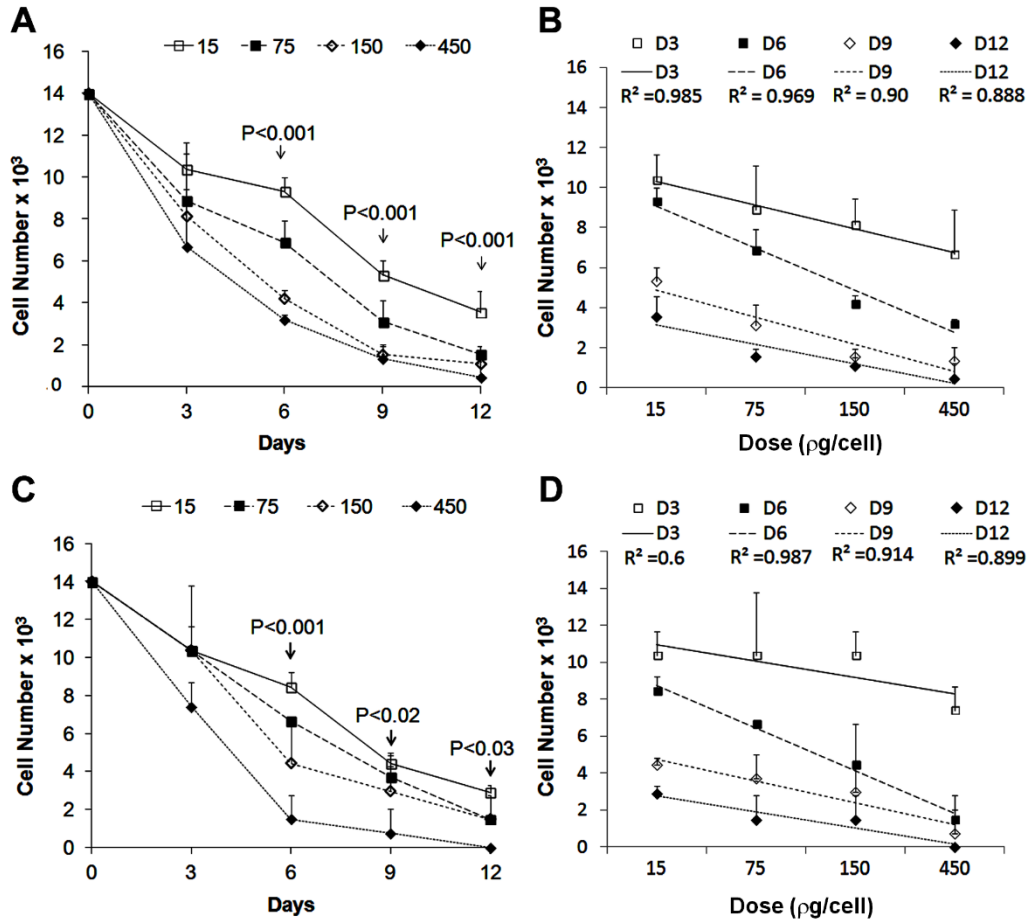


**Figure 6.3** Differential periodic cell extinctions of Swiss 3T3 cells from 24-well plates after pulsed exposure to Mitomycin C in T25 flasks. The concentrations of 4 µg/ml (A & B) and 5 µg/ml (C & D), each of which was formulated to give dose permutations of 15, 75, 150 or 450 µg/cell. Viable cell counts from all the dose permutations at each time point (A & C) were analysed by one way ANOVA and the P value was indicated if it was less than 0.05. The dose dependent variation in cell extinctions for each concentration (B & D) were represented by linear trend lines and  $R^2$  values were calculated by regression.

More or less similarly, the permutations of 5-15, 5-75, 5-150 and 5-450 also produced a dose dependant drop in cell viability pattern (Figure 6.3 C). Although, there was no early significant difference in post-exposure cell extinction on day 3, which was more obvious by the presentation of same viability with doses of 15, 75 and 150 µg per cell, but the

subsequent time points revealed significant variation by all doses. Equally, the regression analysis (Figure 6.3 D) also revealed that cell viability was not significantly ( $R^2=0.6$ ;  $P>0.05$ ) influenced by volume titrations on day 3, while they significantly modified the extinctions at day 6 ( $R^2=0.987$ ;  $P<0.01$ ), day 9 ( $R^2=0.914$ ;  $P<0.02$ ) and day 12 ( $R^2=0.899$ ;  $P<0.02$ ). But across all time points on the whole, the analysis by 2-way ANOVA clearly demonstrated a highly significant ( $P<0.001$ ) influence of dose permutations in inducing varied cell extinctions.

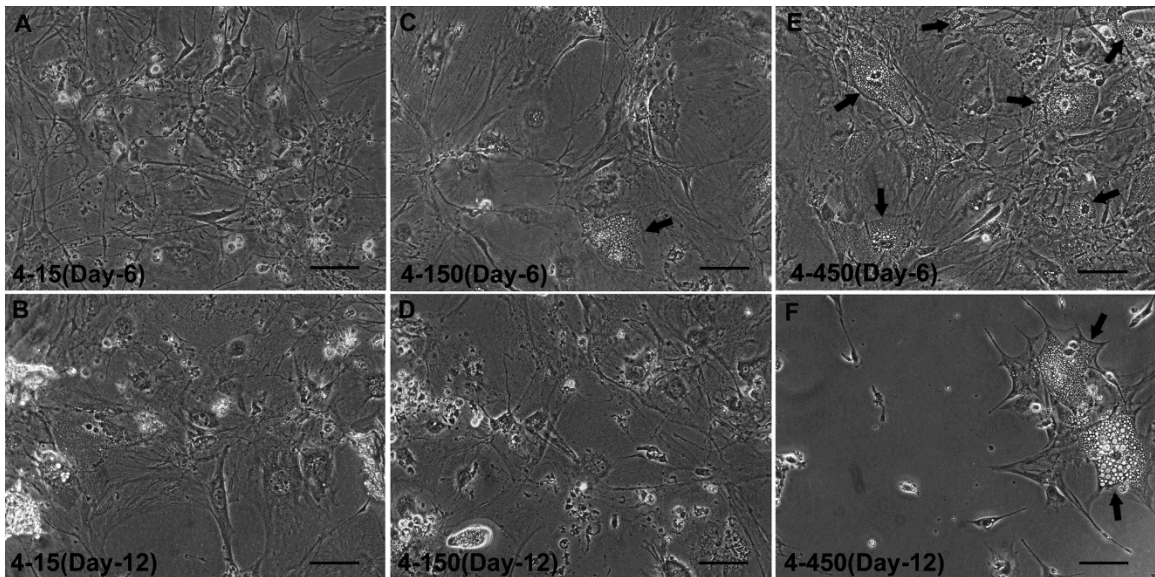


**Figure 6.4** Comparative cellularity of 3T3 cells on days 6 and 12 after they were re-plated into 24-well plates following a pulsed exposure to Mitomycin C in T25 flasks. The concentration of 4µg/ml, formulated in a way to give dose permutations of 15 (A & B), 150 (C & D) or 450 (E & F) µg/cell. Vacuolated cells (Arrows) after 6 days were rare in feeders of 4-15 (A), few in 4-150 (C) and numerous in 4-450 (E). Overall cellularity on culture surface after 12 days post-treatment was fair in 4-15 (B), moderate in 4-150 (D) and poor in 4-450 (F). Marker length is 10 µM.



The differential cell extinctions were also microscopically noticeable among permutations of 15, 150 or 450  $\mu\text{g}$  per cell (Figure 6.4). The vacuolated cells which are signs of cellular disintegration were rare in feeders of 4-15, less frequent in 4-150 (C), but become apparently numerous in 4-450 (E) after 6 days post-Mitomycin C exposure time point. This is further correspondingly reflected by loss of overall cellularity on culture surface after 12 days which ranged from fair in 4-15 (B), moderate in 4-150 (D) to very poor in 4-450 (F). Conspicuously, the cells gradually assumed broader aspect as their number depleted.

Additional time point matched comparisons undertaken to examine differential induction of cell extinction by dose titrations using either of the intermediate concentrations of 4 and 5  $\mu\text{g}$  per ml with reference to concentration controls revealed that the lower 3-10 was comparable to the dose of 15  $\mu\text{g}$  per cell, while the higher 10-30 was similar to 450 (Figure 6.5 A & B). Furthermore, the extinction produced by 4-150 was also similar to that of 10-30, though the initial cell death was significantly ( $P < 0.05$ ) slower on day 3. But, both 10-30 and dose of 450, either with 4 or 5  $\mu\text{g}$  per ml produced an almost equally acute initial cell death in contrast to comparisons with other dose permutations demonstrating the early onset of toxicity by them.

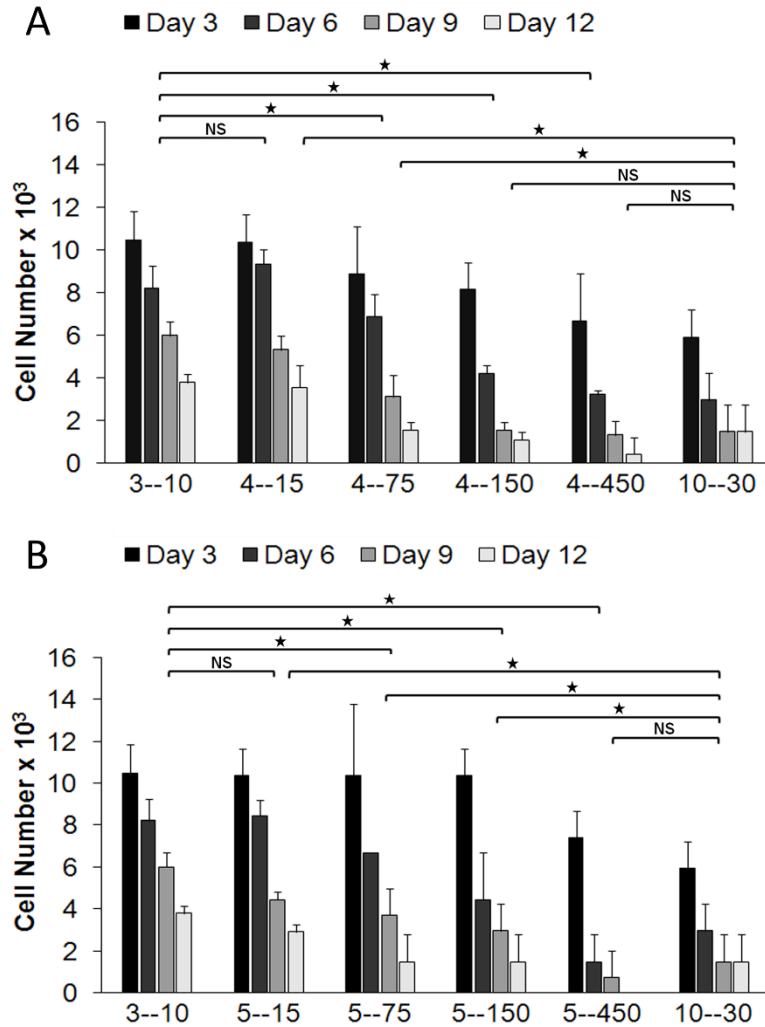


**Figure 6.5** Clustered column diagram showing differential periodic cell extinctions of 3T3 cells re-plated in 24-well plates following pulsed exposure to Mitomycin C in T25 flasks. The concentrations, 4 µg/ml (A) and 5 µg/ml (B), each of which was formulated to give dose permutations of 15, 75, 150 or 450 µg/cell. Each permutation was compared with concentrations of 3 and 10 µg/ml, used at doses of 10 and 30 µg/cell, respectively, and included as the least and the most toxic permutations. Each cluster represents viable cell number from a single dose after 3, 6, 9 and 12 post-treatment days. The clusters of 3-10 and 10-30 were compared with each of the other dose permutations by paired t test and indicated as significant at  $p < 0.05$  (\*) or insignificant (NS).

#### 6.4 Discussion:

Conventionally, *in vitro* experimental treatment protocols for effectiveness of a given drug prescribe the strength of such agents in terms of its concentration per se in treating solutions, while grossly ignoring the criticality of exposure cell density or dose per cell (Barlogie and Drewinko 1980; Connor 2000; Ponchio et al 2000). It is important to consider the exposure cell density which altered the pharmacological anti-cancer activity of a cell proliferation blocking agent in an arithmetically derived dose dependent manner (Yerneni and Jayaraman 2003; Chapter 5). In these studies, it was proposed that all the cells exposed to the drug in a culture flask would equally share the whole amount present in total volume of treating solution eventually leading to a range of doses per cell when exposure cell number was varied. Accordingly, the post exposure cell disintegration rate was proportional to the calculated dose increments, although, the phenomenon is limited to the moderately acting intermediate concentrations and is also comparable to their similar action after cell density titration in chapter 5. The exhibition of such variation at lower and higher concentrations appears to relate with their weak and intense action potential, respectively, in the very first place.

It is worth noting that while considering the same exposure cell density as employed in volumetric variation experiments, the normally recommended range of 10-15 ml of working volumes for T75 flasks, would correspond to dose ranges of 23 to 34 and 28 to 43  $\mu\text{g}/\text{cell}$ , respectively, which correspond to concentrations of 4 and 5  $\mu\text{g}/\text{ml}$ , respectively. It is important to note that these dose ranges in turn fall in between the lower tested doses of 15 and 75  $\mu\text{g}/\text{cell}$  only. At the same time, it is difficult to deduce probable working doses in several earlier reports, wherein the precise exposure cell density and volume of treating

solution were not mentioned (Schrader, 1999; Ponchio et al 2000; Nieto et al 2007; Fleischmann et al 2009). Even after presuming confluent or sub-confluent exposure densities in such studies, the dose per cell would still be limited to only a lower range and higher doses would have been certainly unexplored. Thus, the concept of attaining higher doses of Mitomycin C per cell through simpler volume titrations without raising the concentration *per se* is for the first time shown by us to produce significant alterations in post-exposure life span of feeders and is likely to influence the outcome of target cell stimulation.

Considering the sub-culture dependent occurrence of variants in 3T3 cultures (Chugh et al. 2015), the observed stimulatory outcome of 3 µg of Mitomycin C per ml which equals to a calculated dose of 19.5 µg per cell as it was employed on a confluent high ECN of 60,000 cells per cm<sup>2</sup> (Chapter 5) is perhaps the manifestation of such accumulated variants expressing resistance to low concentration of Mitomycin C. In fact, it is apparently this stimulatory influence that largely contributed to the overall reflection of significant variation in extinction profile in 3 µg group (Chapter 5) and similar outcome is expectedly prevented if the presence of variants is controlled by adopting a safe sub-culture protocol for Mitomycin C treatment. Concurrently, such an overall variation in extinction following volume titrations with any range of doses of 3 µg is abolished in volumetric titrations performed using a safe target population.

It is of particular interest to observe that the significant differences in cell extinction rates as influenced by volume titrations with intermediate concentrations of 4 or 5 µg per ml, were as consistent as with cell density titrations. It is of utmost importance to note that

the total amount of Mitomycin C at these middle order concentrations in their respective comparable doses turn out to be same, but are basically distributed at different dilutions. Concurrently, the statistical analysis between the matched volume titrations of these two concentrations (comparison not depicted in results) proved no significant deviation in cell extinctions. This again stresses the importance of considering all pertinent factors like concentration, dose per cell or exposure cell density while validating the influence of Mitomycin C on feeder cell growth arrest. Considering the broader aspect of titrations with either exposure cell densities or volumes (dose and concentration), it may be stated that the cell density variation strategy alone may not precisely project the effective combinations of concentrations, doses and exposure cell densities, but potentially provides primary estimates of probable range of such useful permutations for the subsequent testing by volume titrations. It is thus shown that the volume titrations of a range of given concentrations, but limited to a median effective range, were instrumental in either diminishing or accentuating the net cell viability and could exert objective-specific array of consequences. Particularly, in the context of proliferation and maintenance of feeder cell based keratinocyte or any adult stem cell culture, the demonstrated control of net life span of feeders, which determines the net ratio of growth arrested fibroblasts and the target cells, could be exploited to optimize such cultures, since such a ratio is a well identified key growth regulating factor *in vitro* (Sun et al 2009; Zhou et al 2009; Jubin et al 2011).

In routine toxicological evaluation studies, concentration is the term of reference for *in vitro* studies and the *in vitro* dose response curve truly represents concentration dependent evaluation, while dose is specific for *in vivo* studies (Eisenbranda et al 2002). In the current example, both concentration and dose per given cell population were

considered as discrete variables while making endpoint observation on cell death. Therefore, it is tempting to propose that if volume variation strategy was to be adopted following cell density titrations in an *in vitro* toxicology and/or pharmacological study design, it could perhaps form the basis of extrapolating a compound's operational *in vivo* dose from the most active permutation of concentration and dose studied on a fixed population of cells *in vitro*. Moreover, such an approach could further help in predicting accurate effective dosing of anti-cancer agents in a pre-clinical efficacy evaluation setting, particularly while testing moderately toxic concentrations in an attempt to simulate containment of unwanted side-effects *in vivo*. At the same time, it is suggested that further studies are necessary to explain specific mechanisms for modified biological outcome by the permutations of dose and concentration of Mitomycin C in contrast to the reported correlation of only concentration with cytotoxic effects (Barlogie and Drewinko 1980).

Considering the impact of volume titrations while using a range of less toxic intermediate concentrations of Mitomycin C in regulating the viability of feeder cells unreported so far, it may be proposed that the approach could be superior, reliable and convenient for rendering the feeder cell growth arrest than by the cell density regulation alone. Therefore, a strategy may be adopted to test the range of feeder cell batches produced by volume titrations in an epidermal keratinocyte co-culture model to verify if they influence differential stimulation of target cells and to subsequently identify the best outcome while comparing with the standard gamma-irradiation feeders. The process, if proven, will overcome the reported inadequacies of the cost-effective Mitomycin C approach as compared to Gamma-Irradiation technique.

## **Chapter 7**

# **Keratinocyte-Feeder Co-culture**

## **7.1 Introduction:-**

There are many different published methods for cultivating human epidermal keratinocytes; among the culture systems, the most efficient method is that developed by Rheinwald and Green (1975). A single suspension of disaggregated keratinocytes is seeded onto a growth arrested feeder layer of mouse 3T3 cells. The feeder layer enhances plating efficiency and stimulates growth of the keratinocytes, which gradually replace the feeder cells. Proliferation and culture lifespan can be further increased by adding various supplements to the culture medium (Green et al. 1977; Rheinwald and Green, 1977; Green, 1978; Watt and Green, 1981).

The Rheinwald-Green method allows serial passage for many generations and the method is now in widespread use both in basic research and clinical application. In spite of the fact that this culture technique does not allow the expression of the full complement of epidermal differentiation, it has had a major impact on the study of many cellular and molecular aspects of proliferation and terminal differentiation of the keratinocyte (Fuchs and Green, 1980; Green, 1980; Fuchs and Green, 1981; Watt and Green, 1981; Green et al. 1982; Watt and Green, 1982; Dover and Potten, 1988; Stoler et al. 1988; Watt, 1988b). Furthermore, it allows large-scale production of epidermal cultures suitable for the covering of skin defects such as burn wounds (Green et al. 1979; Gallico et al. 1984). Therefore, Rheinwald-Green model of human keratinocyte culture is adopted for further studies in this investigation.

So far, in chapter 6 it has been shown in a validated stock of Swiss 3T3 cells that their extinction profile following growth arrest with a pulse exposure to Mitomycin C was



regulated by a strategy of simpler volumetric titrations, in which the range of volumes is broader than the routine recommendation. It is postulated that the resultant net life span of growth-arrested feeders determines their net ratio with human epidermal keratinocytes, when both cell types are co-cultured in a medium that favors their maintenance *in vitro* and only those feeders that possess a specific extinction profile support the highest proliferation of keratinocytes in co-culture system. Therefore, this present investigation is aimed at demonstrating the experimental evidences towards the differential ability of feeder cells that are growth arrested by various concentration-dose permutations of Mitomycin C to exert varied growth stimulatory effect on the human epidermal keratinocyte cells and identifying the best outcome.

## **7.2 Materials and Methods:**

### **7.2.1 Keratinocyte and fibroblast co-culture:**

Keratinocytes used in the experiments included either the frozen 1<sup>st</sup> passage cells as received from the supplier (Genlantis) or the 3<sup>rd</sup> passage cells produced by culturing the frozen 2<sup>nd</sup> passage cells, both of which were subcultured using  $15 \times 10^3$  feeders of 4-150 group per cm<sup>2</sup>. Mitomycin C treated Swiss 3T3 cells are processed as per volume titrations (Chapter 6). Gamma-Irradiated Swiss 3T3 cells with 10,000 rads were obtained from ATCC, catalogue No.48-X IRR 3T3.

Several preliminary experiments were conducted to short-list the most effective concentration-dose permutations and identify feeder-keratinocyte cell seeding ratio for assessing the growth stimulatory influence of feeders on epidermal keratinocyte cells in a co-culture system. Initial screening indicated that the feeders of 4-150 exposure maximally

stimulated the 3<sup>rd</sup> to 5<sup>th</sup> passage keratinocytes, while feeders exposed to 75 µg Mitomycin C dose per cell produced a keratinocyte stimulation that was comparable to that of 15 µg per cell. Subsequently, out of several Keratinocyte-Feeder ratios tested using feeders of 4 µg Mitomycin C per ml concentration group, a ratio of one keratinocyte to two feeder cells (1:2) seeded at densities of 7,500 and 15,000 per cm<sup>2</sup>, respectively, was found to be optimal in which keratinocytes reached maximal growth by day 9. With the raise in feeder cell seeding density from 7,000 per cm<sup>2</sup>, whose extinctions were tested in chapter 5, to optimal 15,000 per cm<sup>2</sup>, the later were additionally evaluated alone for periodical extinctions in order to check their similarity in extinction with those of the former and Gamma Irradiated feeders (γ-Irr) were further included for comparison. Therefore, the short-listed doses included for keratinocyte growth assessment were 15, 150 & 450 µg per cell, each combined with concentrations of 4 and 5 µg per ml, respectively. Feeder groups of 3-10 and 10-30 were included along with γ- Irr feeder cells as controls for comparison.

### **7.2.2 Feeder performance on epidermal keratinocytes at clonal density:**

Colony forming Efficiency (CFE) and digital image analysis for growth area assessment were performed by plating low density of keratinocytes over various feeder groups in 6-well plates with each well containing 15,000 feeder cells per cm<sup>2</sup>.

**7.2.2.1 Colony forming Efficiency:** CFE was performed using 250 keratinocytes of 3<sup>rd</sup> passage with feeders treated with all the short-listed permutations. Subsequently, separate experiments were performed to estimate average colony size and total growth area with 170 and 340 viable 1<sup>st</sup> passage keratinocytes plated per well, respectively, and the feeders were the best performing 4-150 along with the sub-optimal 4-15 and γ-Irr. Culture plates

were incubated for 9 days, with change of culture medium every alternate day, fixed in 4% para-formaldehyde prepared in phosphate buffered (pH 7.2) saline for 45 minutes, stained with 1% Rhodamine B in distilled water for 30 minutes, washed in distilled water for color differentiation of areas of keratinocytes and feeder cells and air-dried. CFE comprised of counting of discrete keratinocyte colonies of 8 or more cells, expressed as percentage of plated cells. Estimation of average colony size was based on growth area assessment and CFE, wherein small colonies of highly irregular shape containing broad, flattened and terminally differentiated cells were considered as aborted and the rest constituted the proliferative colonies. Experiments for CFE were performed in triplicate while growth area assessment was performed in quadruplicate per feeder group.

#### **7.2.2.2 Digital Image Analysis:**

The stained plates were illuminated with constant light and photographed using Nikon field camera producing digital images having a resolution of  $9 \times 10^4$  pixels per inch<sup>2</sup>. The images were subjected to image analysis using Adobe Photoshop version 7 as per an earlier reported technique (Kumar and Yerneni 2009). The basic technique comprised of separate selection of similar color feature on digitized-images. The selection of pixels of desired colors wherein red and pale bluish pink colors representing keratinocytes and feeders, respectively, was a procedural selection using the magic wand tool. The selection process was manually controlled by the necessary corrective measures using options in Magic Wand palette and Select options in menu bar. After ensuring accurate color separation, the images were triplicated, out of which two were used for isolating the two colors, while the third un-treated one was referred for comparison. Once the respective colors were isolated, they were superimposed to verify the reproduction of an image similar to the original. This

was followed by attainment of quantification, in terms of number of pixels within the selected red area, using the Histogram command in the Image menu. The percentage of number of red pixels out of total number of pixels of the well was calculated and area of keratinocyte growth was derived from the known total area of the well. In case of wells plated with 170 keratinocytes, the calculated area in square centimeters was divided by the total number of colonies counted in the respective well to obtain average colony size.

### **7.2.2.3 BrdU labelling:**

Mitotic Index was estimated in slide flasks (Nunc) in which cultures were initiated with 70 viable 1<sup>st</sup> passage epidermal keratinocytes per flask containing the best performing feeders of 4-150 along with 4-15 and  $\gamma$ -Irr at a density of 15,000 per cm<sup>2</sup> and incubated with change of culture medium every alternate day for 10 days. Feeder cells were selectively removed with 0.02% EDTA and the keratinocyte colonies were incubated in non radio-active Bromodeoxy Uridine (BrdU) for 1 hour, fixed in Cornoy's fixative, treated with 4M HCl for antigen retrieval, neutralized with 0.1M sodium Borate, incubated in primary mouse monoclonal anti-BrdU antibody (Cat No. sc-32323, Santacruz) followed by visualization of fluorescence labelled nuclei after incubating in FITC labelled anti-mouse secondary goat polyclonal antibodies (Cat No. sc-2010, Santacruz Biotechnology Inc.). Every colony from triplicated slide flasks per feeder group was differentially counted for labelled and un-labelled nuclei. Briefly, each colony was photographed in both phase contrast and fluorescence modes on Nikon Diphot 300 microscope at 20X objective using Evolution QEI monochrome camera (Media Cybernetics); multiple images were taken if the colony was larger than the field and overlapping margins were demarcated by matching

the images before counting of nuclei was performed using manual tag tool of Image Pro-Express express software version 6.0.

### **7.2.3 Feeder performance on mass cultures of epidermal keratinocytes:**

Co-cultures were initiated in 24 well plates using 3<sup>rd</sup> passage primary epidermal keratinocytes, in the presence of short-listed feeder groups with change of culture medium every alternate day until differential cell counts performed from triplicate wells per group at days 3, 6 & 9. For differential cell collection, the cultures were first treated with 0.02% EDTA to selectively remove the feeder cells which were collected in keratinocyte medium. Subsequently, keratinocytes were collected in separate vials after detaching them using 0.08% trypsin, 0.01% EDTA and 0.008% glucose. Viable cell counts were performed in Neubauer chamber after trypan blue exclusion.

### **7.2.4 Statistics:**

For extinction of feeders plated at a density of 15,000 per cm<sup>2</sup>, column graphs were constructed in which each cluster of columns represented the specified permutation and each column represented viable cell numbers at the specified time points. Clusters of 3-10 and 10-30 or  $\gamma$ -Irr feeders were compared with other dose permutations by Students t test after pairing the corresponding time points.

Experimental groups for CFE and growth area assessment involving 4-15 and  $\gamma$ -Irr were statistically compared with 4-150 by Student's t test and considered as significant, if  $p < 0.05$ . For analysing BrdU data, separate dot plots were constructed to represent total number of cells and percent of BrdU positive cells per each colony in every feeder group.

Variance in the distribution of BrdU positive cells or total cell number per colony among the three feeder groups was analyzed by Kruskal-Wallis H test and comparisons between two feeder groups were undertaken by Mann-Whitney non-parametric U-test, while the overall BrdU positivity between any two groups of feeders was tested by Chi square.

For feeder extinctions column graphs were constructed in which each cluster of columns represented the specified permutation and each column represented viable cell numbers at the specified time points. Each cluster of 3-10 and 10-30 was compared with every dose permutation by Students t test after pairing the corresponding time points. Similarly, periodical keratinocyte cell counts were plotted in clustered column graphs with each cluster representing the specified concentration-dose permutation of Mitomycin C used for feeder cell growth arrest and each column represented mean cell number at the specified time point. Every cluster representing permutations of 3-10 and 10-30 or  $\gamma$ -Irr feeders that served as control groups was compared with tested permutations; significance of variance in their growth promoting influence was evaluated by two-way ANOVA in which the variance in between two permutations were evaluated by inputting triplicated cell counts of two independent feeder cell groups against the three time points in 2 x 3 tables. The calculated P values, when  $P < 0.05$ , are represented in the graph to denote significant variation in between two feeder groups. The calculated critical values for the Tukey HSD test were used for post-hoc analysis to estimate the real significant difference between comparable time points of two feeder groups.

### 7.3 Results:

#### 7.3.1 Colony Forming Efficiency:

Experiment involving the comprehensive screening of all short listed feeder groups for inducing CFE on 250 keratinocytes revealed that 4-150 stimulated the formation of highest number of colonies of  $67.7 \pm 0.6$  among all the tested groups which is significantly higher as compared to  $56.7 \pm 2.5$ ,  $59.7 \pm 3.2$ ,  $55 \pm 2.6$ ,  $49.7 \pm 1.5$ ,  $36 \pm 3.6$  by 3-10, 4-15, 4-450, 10-30,  $\gamma$ -Irr, respectively, while there were  $60.7 \pm 1.2$  colonies in 5-150 feeder group which is significantly higher to 3-10, 5-450 ( $53 \pm 3.6$ ), 10-30, and  $\gamma$ -IRR but insignificant compared to 5-15 which influenced formation of  $59.3 \pm 1.2$  colonies (Figure 7.1). In fact, 4-150 produced highly significant ( $P < 0.001$ ) stimulation than 5-150; hence subsequent experiments on growth area included appraisal of 4-150 in comparison with 4-15 and  $\gamma$ -Irr, which are considered as standard feeders.

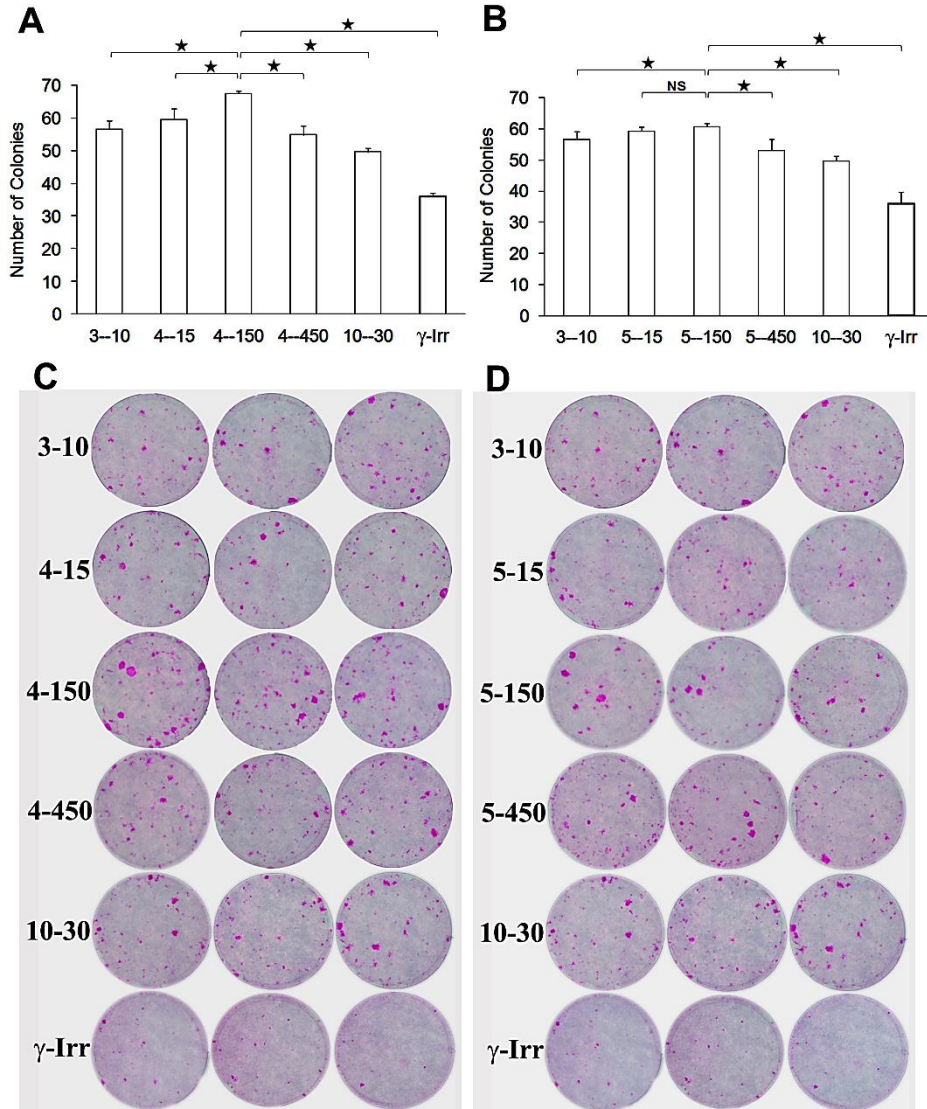


**Figure 7.1** Number of colonies and Colony Forming Efficiency of keratinocytes. 3<sup>rd</sup> passage keratinocytes co-cultured with various feeders group, growth arrested by a 2-hour pulsed exposure to Mitomycin C at a concentration of 4 μg (A & C) and 5 μg (B & D) Mitomycin C per ml, each of which was constituted to give dose permutations of 15, 150 or 450 μg/cell. Feeders exposed to 3 and 10 μg/ml at doses of 10 and 30 μg/cell, were included as least and most toxic permutations, in addition to feeders growth arrested by Gamma-Irradiation serving as standard technique. Cultures were initiated in triplicate wells of 6-well plates with keratinocytes and feeders seeded at the rates of 250 and 144,000 per well, respectively. Colonies were counted after staining the wells with Rhodamine B (C & D). All groups were statistically compared with 4-150 group by Student's *t* test and indicated as significant at  $p < 0.05$  (\*) or insignificant (NS).



### 7.3.2 Colony forming Efficiency & Digital Image analysis:

A complete color separation was possible in Rhodamine B stained preparations using Adobe Photoshop-based image analysis, since this staining resulted in two distinct shades of color, viz., red, representing keratinocyte growth and bluish grey, depicting feeder area (Figure 7.2). The color selection was found to be foolproof as the superimposed merge image of the two isolated color images revealed a near perfect match with the untreated original image in all the cases.

At first, CFE with a clonal density of 170 viable keratinocytes of frozen 1<sup>st</sup> passage supplied sample was evaluated, so as to accomplish counting of discrete colonies and image analysis to obtain average colony size in addition to total growth area. Data of pixels representing the two areas of keratinocyte growth and the back ground area of feeders and their calculated growth area are given in Table 7.1. The results showed that feeders of 4-150 facilitated growth of  $76.7 \pm 4.11$  proliferative keratinocyte colonies, which is significantly different ( $P < 0.01$ ) as compared to  $53.5 \pm 4.12$  and  $61.25 \pm 4.57$  in 4-15 and  $\gamma$ -Irr, respectively (Figure 7.3 A). It is interesting to observe that the number of colonies in  $\gamma$ -Irr was significantly higher than in 4-15. On the other hand, the occurrence of aborted colonies was more or less similar in all groups.

The image analysis of total growth area revealed that 4-150 produced largest keratinocytes growth area of  $1.109 \pm 0.1 \text{ cm}^2$  and is significantly higher than in 4-15 ( $0.613 \pm 0.05 \text{ cm}^2$ ) and  $\gamma$ -Irr ( $0.542 \pm 0.1 \text{ cm}^2$ ), but the difference in between these less performing groups was not significant (Figure 7.3 C and Table 7.1), reflecting differences in colony size. This became evident after dividing the growth area by total number of

colonies, revealing significantly higher average colony size of  $1.009 \pm 0.05$  in 4-15 than  $0.787 \pm 0.11$  mm<sup>2</sup> in  $\gamma$ -Irr, but 4-150 remained superior among all with an average colony size of  $1.335 \pm 0.18$  mm<sup>2</sup> (Figure 6.3 B and Table 7.1).

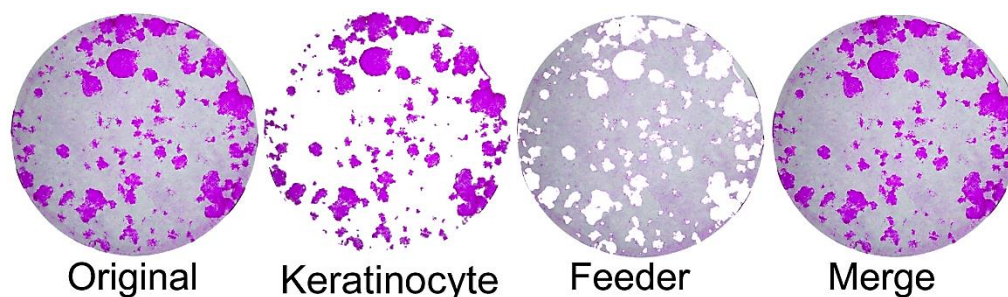


**Figure 7.2** Separation of color in a Rhodamine B stained keratinocyte colonies over a substratum of feeder cells. Complete color separation of keratinocyte colonies was done by using Adobe Photoshop that facilitated quantitative image analysis. The sub title of ‘Original’ on the extreme left represents the untreated image of a Rhodamine B stained culture plate depicting keratinocyte growth area in red and feeder substratum in bluish-gray blue. The sub-titles of ‘Keratinocytes’ and ‘Feeder’ represent the replicated samples of the original image from which the area in red representing the keratinocyte growth area and the remaining feeder substratum in bluish-grey, respectively, are isolated to facilitate quantification of both the areas in terms of pixels. The sub-title of ‘Merge’ on the right shows the reconstructed combined image produced by the superimposition of ‘Keratinocytes’ and ‘Feeder’ images, to validate color isolation.

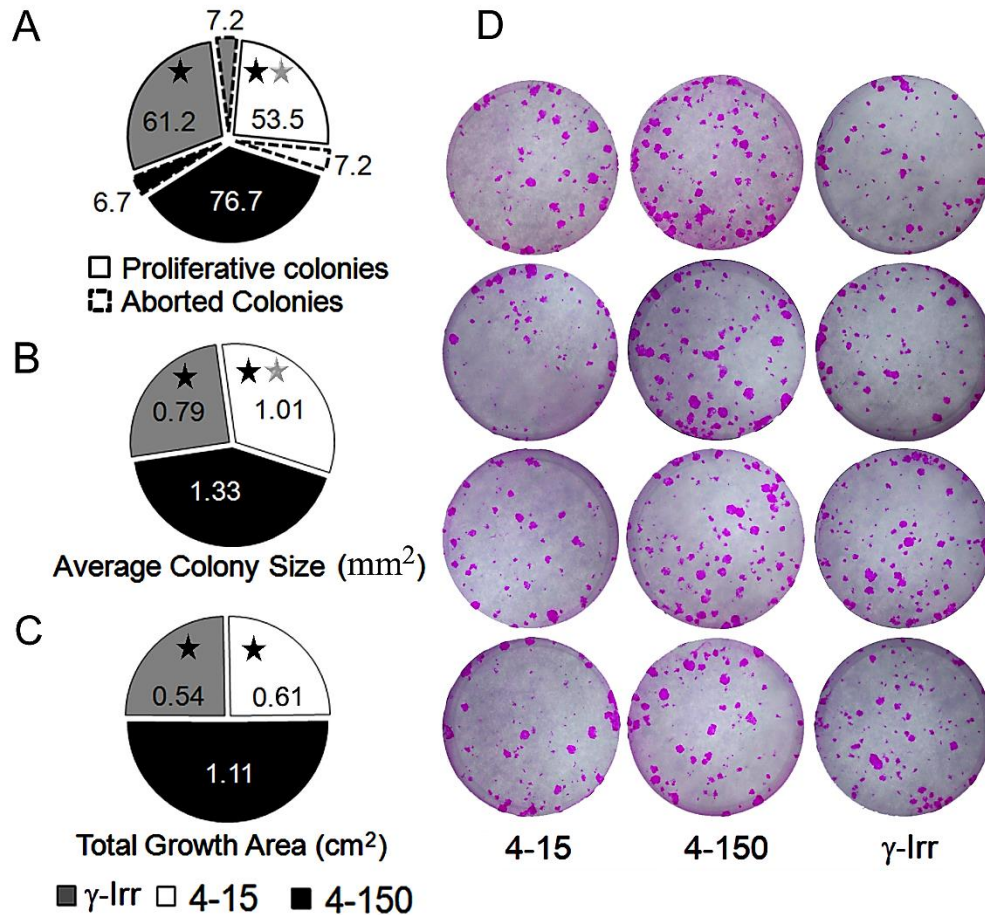


**Figure 7.3 Colony forming efficiency and Growth area analysis of Keratinocytes.** 1<sup>st</sup> passage keratinocytes co-cultured with Swiss 3T3 feeders growth arrested by a pulsed exposure to 4 $\mu$ g/ml of Mitomycin C, constituted to give a dose permutations of 15 or 150  $\mu$ g/cell. Feeder cells, growth arrested by Gamma-Irradiation ( $\gamma$ -Irr) serving as standard technique were included for comparison. Cultures were initiated in quadruplicate wells of 6-well plates and each well was seeded with 170 viable keratinocytes and 144,000 feeder cells. Colonies were counted after staining the wells with Rhodamine B (D). Average colony size (C) was derived by dividing the total growth area (B) by total number of colonies (A). Significant comparison ( $p < 0.01$ ) with 4-150 feeder group is indicated by black asterisk, while comparison between feeders of 4-15 and Gamma-Irradiation is indicated by grey asterisk.

**Table 7.1 Growth area measurements by quantitative image analysis of keratinocyte colonies grown by co-culturing 170 keratinocytes with various Swiss 3T3 feeders and colonies stained red with Rhodamine B**

Feeder Group*	Total no. of pixels of the well (A)	Keratinocyte colony pixel (B)	Percent of Growth area (C) = (B/A) x 100	Growth area <sup>#</sup> (cm <sup>2</sup> ) (9.6/100)x C	Average area ± SD (cm <sup>2</sup> )
<b>4-15 (1)</b>	1,120,088	80,886	7.22	0.693	0.613 ± 0.05
<b>4-15 (2)</b>	1,112,904	68,147	6.12	0.588	
<b>4-15 (3)</b>	1,118,724	68,426	6.12	0.587	
<b>4-15 (4)</b>	1,101,019	66,959	6.08	0.584	
<b>4-150 (1)</b>	1,041,929	135,424	13.00	1.248	1.109 ± 0.1
<b>4-150 (2)</b>	1,115,139	119,223	10.69	1.026	
<b>4-150 (3)</b>	1,130,401	129,441	11.45	1.099	
<b>4-150 (4)</b>	1,115,421	123,674	11.09	1.064	
<b>γ Irr (1)</b>	1,118,215	58,986	5.28	0.506	0.542 ± 0.1
<b>γ Irr (2)</b>	1,122,296	78,298	6.98	0.670	
<b>γ Irr (3)</b>	1,117,999	65,409	5.85	0.562	
<b>γ Irr (4)</b>	1,107,929	49,492	4.47	0.429	

# Actual total area of the well equals to 9.6 cm<sup>2</sup>

\* *Quadruplicate cultures numbered 1, 2, 3 & 4 were initiated with 1<sup>st</sup> passage keratinocytes and 144,000 feeder cells per well in 6-well plates. 4-15 and 4-150 represent feeders exposed to permutation of Mitomycin C concentration of 4 µg per ml with doses of either 15 or 150 µg per million cells, while γ Irr indicates Gamma-Irradiated feeders.*

Lastly, the experiment to assess growth stimulating potential of feeders on 340 keratinocytes plated per well which is higher than clonal density revealed a reproducibly higher keratinocyte growth area of 2.69±0.21 cm<sup>2</sup> with 4-150 feeders than 4-15 and γ-Irr feeders which yielded 1.28±0.29 cm<sup>2</sup> and 1.96±0.38 cm<sup>2</sup>, respectively(Figure 7.4). But,

growth area produced by  $\gamma$ -Irr was significantly larger than 4-15 which is in contrast to the insignificant outcome when clonal density of 170 keratinocytes were plated per well. This appears to be the consequence of cumulative growth from coalescing of high number of smaller colonies resulting from a high plating density of 340 cells per well, because, the frequency of colony formation per total plated cells is proportionately dependent on the plating density of keratinocytes, exhibiting higher the plating, higher the frequency and expectedly higher the differential because of increased resolution.

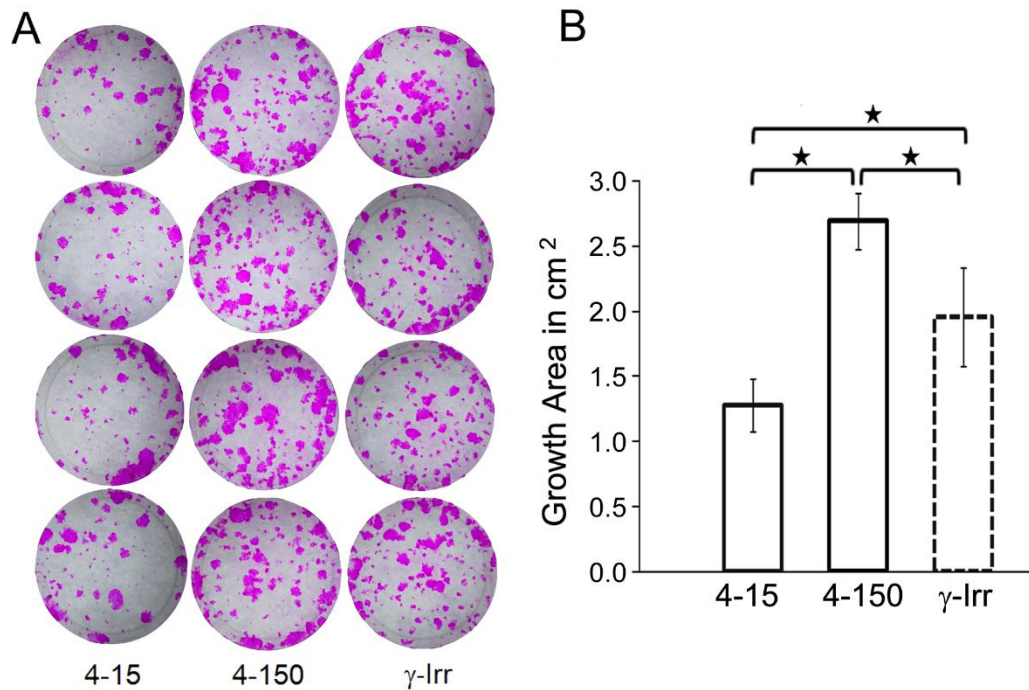


**Figure 7.4 Growth area analysis of keratinocytes.** 1<sup>st</sup> passage keratinocytes co-cultured with Swiss 3T3 feeders, growth arrested by a pulsed exposure to 4  $\mu$ g/ml of Mitomycin C, constituted to give a dose permutations of 15 or 150  $\mu$ g/cell. Feeder cells, growth arrested by Gamma-Irradiation ( $\gamma$ -Irr) served as standard control. Cultures were initiated in quadruplicate wells of 6-well plates, and each well was seeded with 340 viable keratinocytes and 144,000 feeder cells. Keratinocyte colonies were stained red with Rhodamine B (A) and subjected to image analysis to calculate per cent of keratinocyte growth area from the ratio of red pixels and total number of pixels of the well. The area of

keratinocyte growth (B) was calculated by considering actual total area of the well that equals to 9.6 cm<sup>2</sup>. 4-15 and Gamma-Irradiation were statistically compared with 4-150 group by Student's *t* test and indicated as significant at  $p < 0.01$ .

**Table 7.2: Growth area measurement by quantitative image analysis of keratinocyte colonies grown by co-culturing 340 keratinocytes with various Swiss 3T3 feeders and colonies stained red with Rhodamine B**

Feeder Group*	Total no. of pixels of the well (A)	keratinocyte colony pixel (B)	Per cent of Growth area (C) = (B/A) x 100	Growth area <sup>#</sup> (cm <sup>2</sup> ) (9.6/100)x C	Average area (cm <sup>2</sup> ) (1+2+3+4)/4
4-15 (1)	11,14,142	1,54,448	13.86	1.33	1.28
4-15 (2)	10,87,523	1,61,687	14.87	1.43	
4-15 (3)	11,13,842	1,60,927	14.35	1.38	
4-15 (4)	1113742	1,13,179	10.16	0.98	
4-150 (1)	11,18,076	3,08,456	27.59	2.65	2.69
4-150 (2)	12,49,363	3,52,535	28.22	2.71	
4-150 (3)	11,26,170	3,48,264	30.92	2.97	
4-150 (4)	11,40,765	2,90,920	25.50	2.45	
$\gamma$ -Irr (1)	11,25,776	2,82,095	25.06	2.41	1.96
$\gamma$ -Irr (2)	11,14,066	1,99,515	17.91	1.72	
$\gamma$ -Irr (3)	11,15,431	1,83,349	16.44	1.58	
$\gamma$ -Irr (4)	11,25,549	2,49,466	22.16	2.13	

# Actual total area of the well equals to 9.6 cm<sup>2</sup>

\* Quadruplicate cultures numbered 1, 2, 3 & 4 were initiated with 1<sup>st</sup> passage keratinocytes and 144,000 feeder cells per well in 6-well plates. 4-15 and 4-150 represent feeders exposed to permutation of Mitomycin C concentration of 4  $\mu$ g per ml with doses of either 15 or 150  $\mu$ g per million cells, while  $\gamma$ -Irr indicates Gamma-Irradiated feeders.

### 7.3.3 BrdU labeling studies:

The overall distribution of either cellularity or BrdU labeled keratinocytes across colonies was not significantly varied among the tested feeder groups (Figure 7.5). Nevertheless, the percent of BrdU positive keratinocytes in 4-150 feeders at 30.1% (3243/10790) from 27 colonies was significantly ( $P < 0.01$ ) higher than 4-15 which revealed 20.5% (2000/9754) positivity from 20 colonies (Figure 7.6). This elevation appears to be contributed by the additional colony formation in 4-150 resulting in significant ( $P < 0.03$ ) distribution of labeled cells per colony in this group (Figures 7.6 and 7.7). On the contrary, the percent of labeled cell number in  $\gamma$ -Irr was found to be 28.9% (3270/11321) from 21 colonies and was not significantly different from that in 4-150, but at the same time,  $\gamma$ -Irr was found to be significantly superior to 4-15.

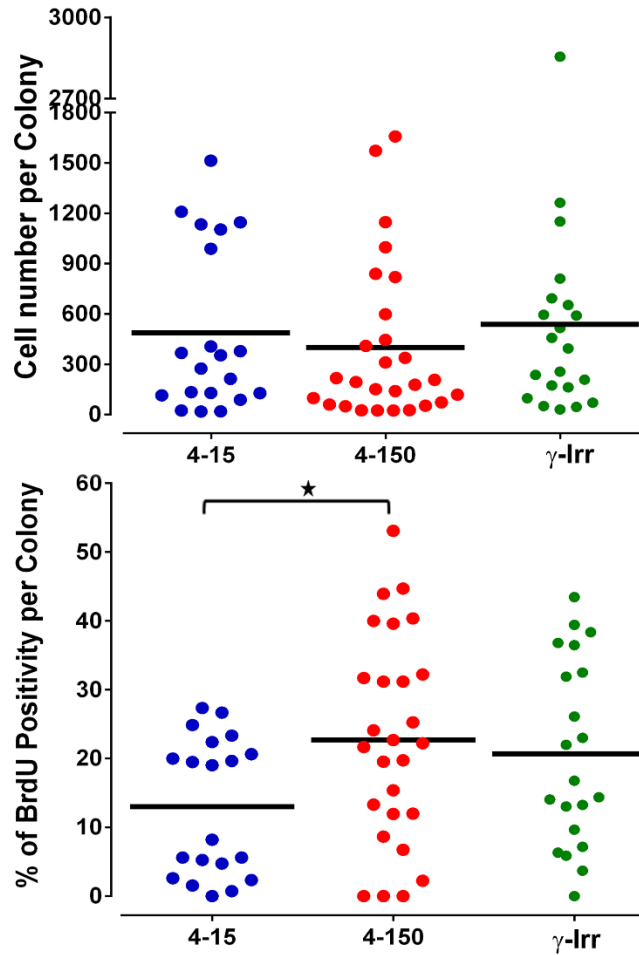


**Figure 7.5 BrdU labelling in Keratinocytes.** Dot plots depicting distribution of cellularity (Top) BrdU positive cells (Bottom) across all keratinocyte colonies produced out of 210 plated 1<sup>st</sup> passage keratinocytes per feeder group. Feeder cells included 4-150, 4-15 which were growth arrested by a pulsed exposure to 4 $\mu$ g/ml of Mitomycin C, that was constituted to give dose permutations of 15 or 150  $\mu$ g/cell and also the Gamma-Irradiated feeders ( $\gamma$ -Irr). Significance ( $P < 0.03$ ) is indicated by asterisk.



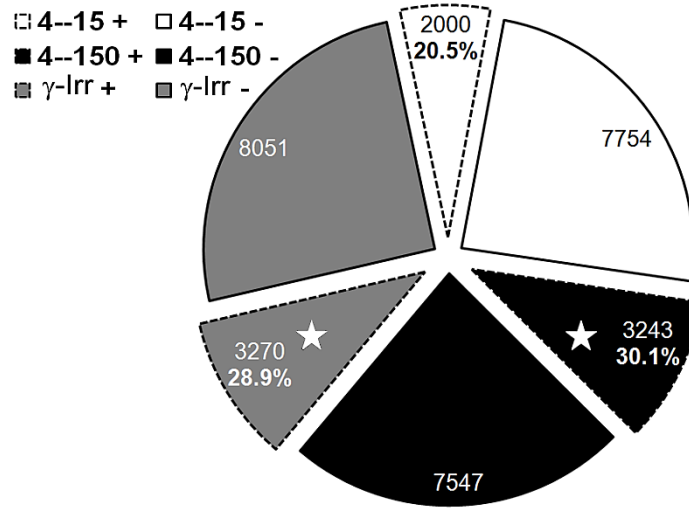


**Figure 7.6** *Number of BrdU Positive and Negative keratinocytes.* Pie diagram showing overall BrdU positive & negative keratinocytes with their corresponding percentages in cultures set up over feeder cells. Feeder cells included 4-150, 4-15 which were growth arrested by a pulsed exposure to 4µg/ml of Mitomycin C, that was constituted to give dose permutations of 15 or 150 µg/cell and also the Gamma-Irradiated feeders (γ-Irr). Significant ( $p < 0.01$ ) comparisons with 4-150 are indicated by white asterisk.

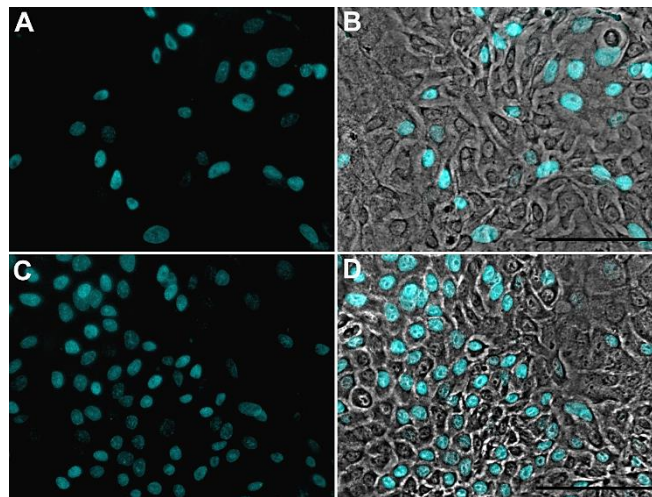


**Figure 7.7** *BrdU labelling in Keratinocytes.* Bromodeoxy Uridine (BrdU) labelling in human epidermal keratinocytes grown in the presence of Mitomycin C feeders of 4-15 (A & B) and 4-150 groups (C & D). The BrdU positive nuclei are visualized as blue-green (A & C) which are merged with corresponding phase contrast images (B & D). Magnification bar = 10 µm.

#### **7.3.4 Feeder performance on mass cultures of epidermal keratinocytes:**

Feeder cell disintegration analysis following initial plating of 15,000 cells per cm<sup>2</sup> from feeder groups of the short-listed permutations revealed differential dose dependent cell extinction patterns that were comparable to that observed after plating with 7,000 feeders per cm<sup>2</sup> (Figure 7.8). The time point matched inter group comparisons in between various Mitomycin C treated feeders under each of the concentrations of 4 µg per ml (Figure 7.8 A) and 5 µg per ml (Figure 7.8 B) showed significant differential. Furthermore, the cell death in  $\gamma$ -Irr feeders was significant and the most rapid compared to any of the Mitomycin C feeders.

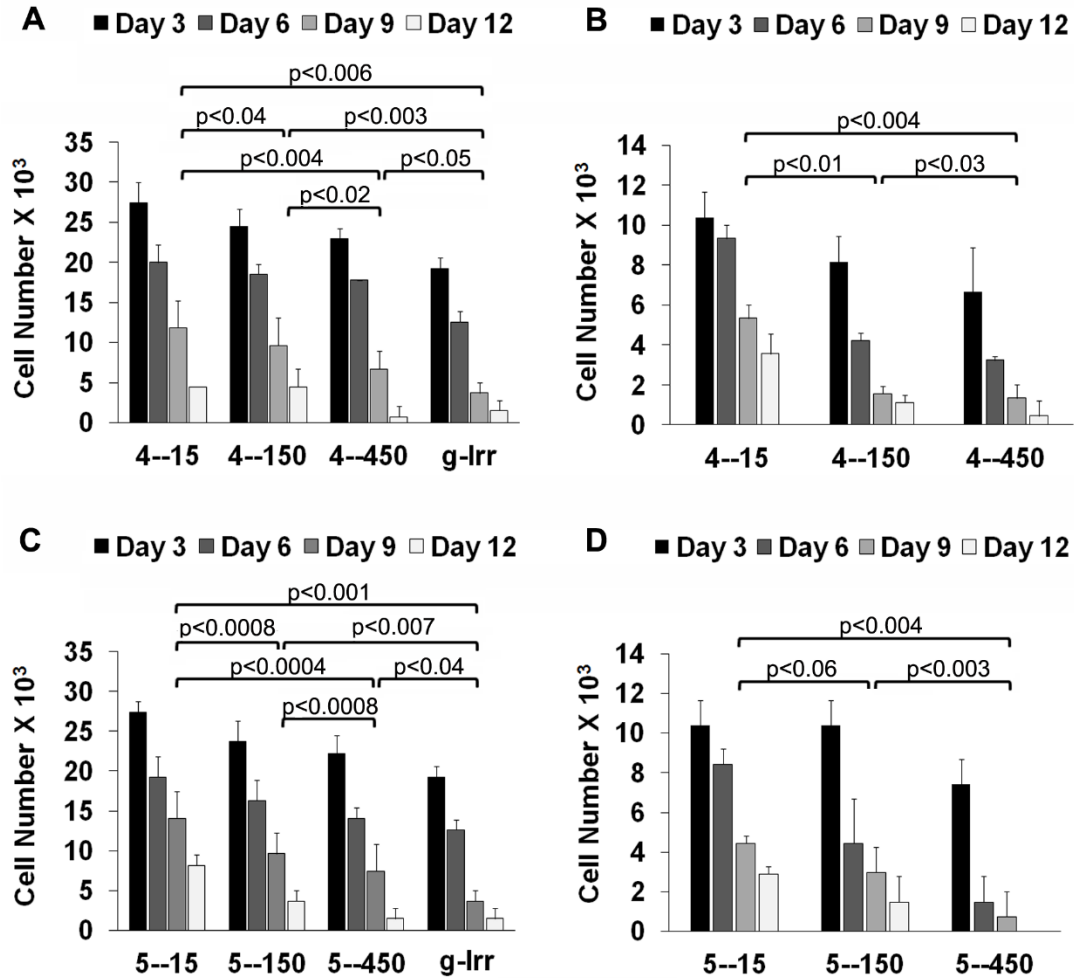


**Figure 7.8** *Differential cell extinctions of Swiss 3T3 feeder cells. Clustered column diagram showing differential periodic cell extinctions of Swiss 3T3 cells re-plated at a density of 15,000 cells per cm<sup>2</sup> into triplicate wells of 24-well plates following a 2-hour pulsed exposure to Mitomycin C in T25 flasks at concentrations, 4 μg/ml (A & C) and 5 μg/ml (B & D), each of which was formulated to give dose permutations of 15, 150 or 450 μg/cell. The Gamma-Irradiated feeders were represented by γ-Irr. Those graphs showing extinction of 7,000 plated feeders per cm<sup>2</sup> (B & D) are taken from Figure 5.8. Each cluster represents viable cell number from a single dose after 3, 6, 9 and 12 post-treatment days. The inter group comparisons between any two permutations were performed by paired *t* test and indicated as significant at *p*<0.05 (\*) or insignificant (NS).*

The keratinocyte growth experiments performed as co-cultures with the main short-listed permutations along with controls of Mitomycin C feeders proved that 4-150 was the only feeder group that produced significantly higher keratinocyte growth than the Mitomycin C control groups. The most interesting point is that the influence of controls of 3-10 and 10-30 were comparable to 4-15 and 4-450, respectively and both pairs exhibited equivalent potential, whereas none of the Mitomycin C dose permutations with 5 µg per ml produced such variation (Figure 7.9). In a more or less similar fashion, the feeders of 4-150 were significantly superior not only among the other Mitomycin C groups, but also to  $\gamma$ -Irr feeders while such a trend was not repeated with permutations of 5 µg per ml (Figure 7.10). The only similarity was that feeders of 5-15 produced a moderately higher stimulation than the  $\gamma$ -Irr feeders but this significant difference ( $P < 0.02$ ) was apparent only on the last day 9 with  $P < 0.01$ , as indicated by post-hoc analysis in contrast to significant difference on both days 6 and 9 in comparison to 4-15 ( $P < 0.001$ ). As a whole, the co-culture using 4 µg per ml Mitomycin C feeders, were superior to those of 5 µg per ml. The subsequent comparisons made among control feeders of 3-10, 10-30 and  $\gamma$ -Irr revealed insignificant differences in periodical growth output (Figure 6.11) which points out that  $\gamma$ -Irr feeders were equivalent to the sub-optimally performing feeders of 3-10 and 10-30.

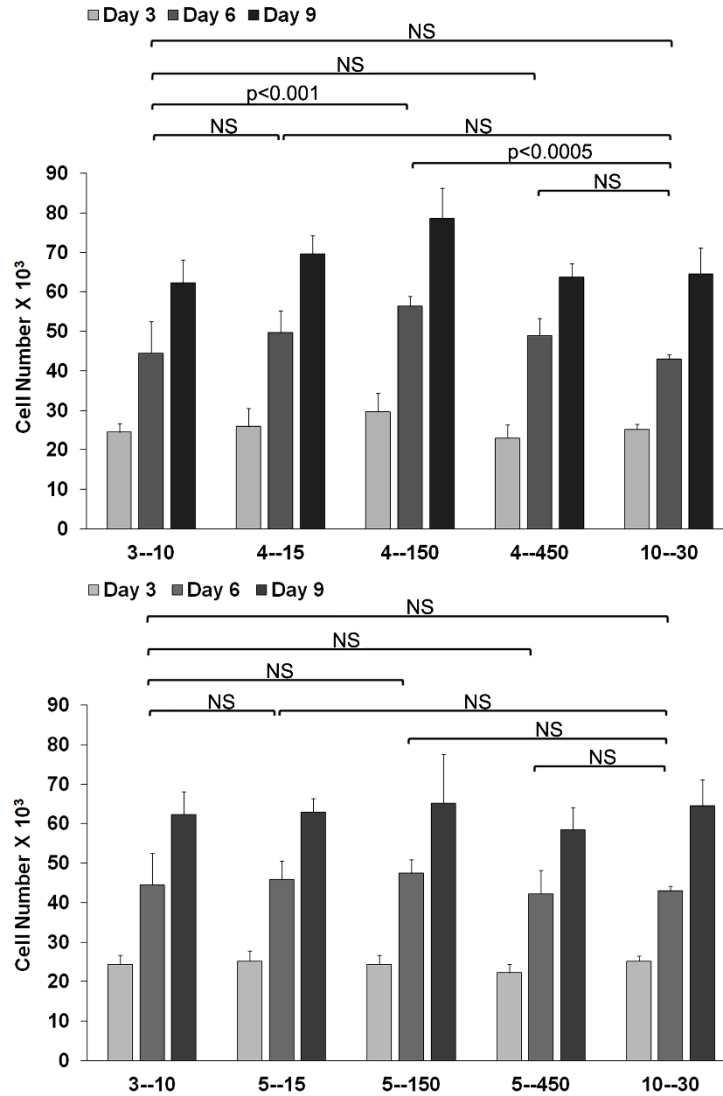


**Figure 7.9** Growth patterns of Human Epidermal Keratinocytes. Clustered column diagram showing the periodical growth patterns of human epidermal keratinocytes grown in presence of Mitomycin C feeders of 15, 150 and 450 µg per cell under concentrations of 4 (Top) and 5 (Bottom) µg per ml and compared with those of 3-10 and 10-30 feeders. The statistical comparisons between two independent feeder cell groups were performed using cell counts from all time points by two-way ANOVA with  $P < 0.05$  as insignificant (NS).

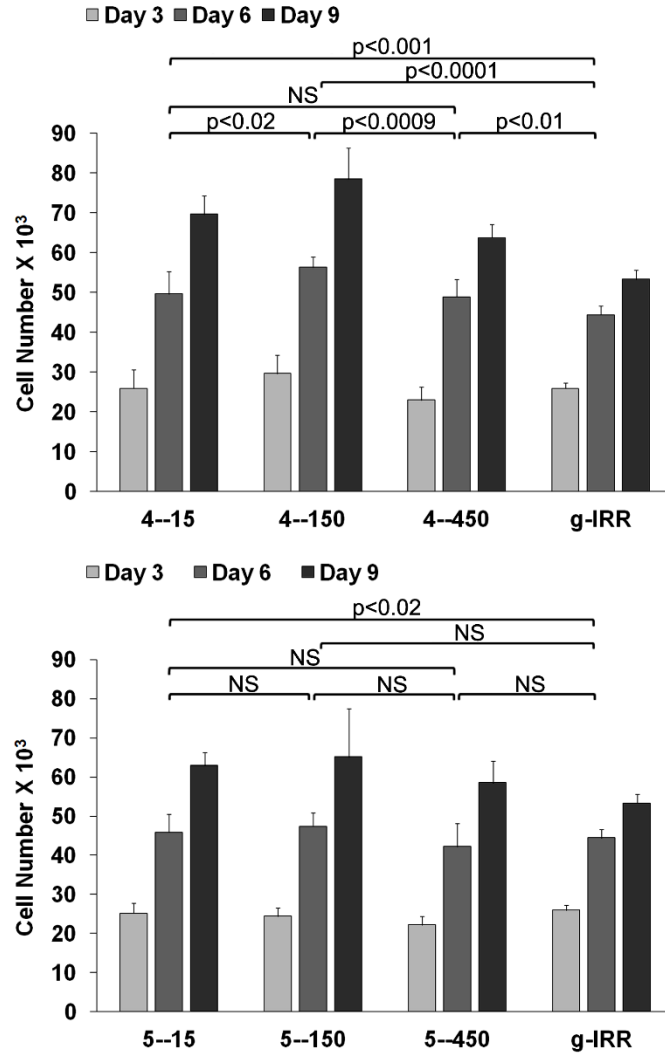


**Figure 7.10 Growth patterns of Human Epidermal Keratinocytes.** Clustered column diagram showing the periodical growth patterns of human epidermal keratinocytes grown in presence of Mitomycin C feeders of 15, 150 and 450  $\mu\text{g}$  per cell under concentrations of 4 (Top) and 5 (Bottom)  $\mu\text{g}$  per ml and compared with those of  $\gamma$ -Irr feeders. The statistical comparisons between two independent feeder cell groups were performed using cell counts from all time points by two-way ANOVA with  $P < 0.05$  as insignificant (NS).

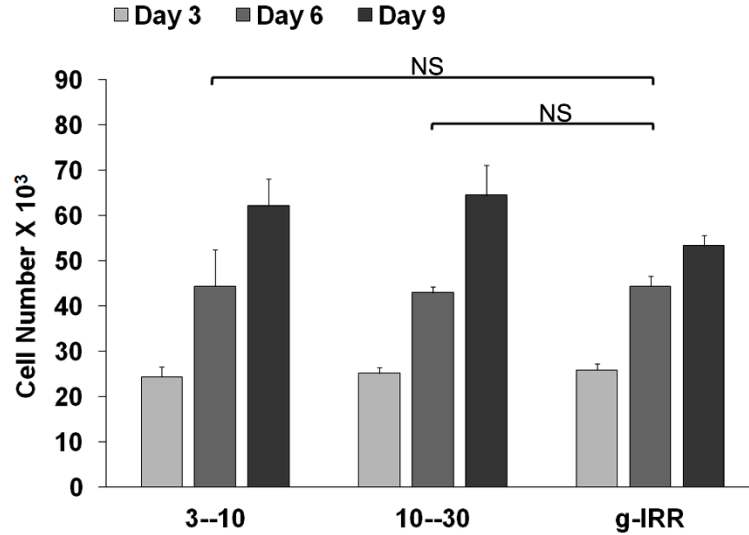


**Figure 7.11 Growth patterns of Human Epidermal Keratinocytes.** Clustered column diagram showing the periodical growth output of human epidermal keratinocytes grown in presence of controls consisting of Mitomycin C feeders of 3-10 and 10-30 and  $\gamma$ -Irr feeders. The statistical comparisons between two independent feeder cell groups were performed using cell counts from all time points by two-way ANOVA with  $P < 0.05$  as insignificant (NS).

#### 7.4 Discussion:

Zhou et al (2009) reported optimal performance of feeders exposed to intermediate durations, whereas either higher or lower exposure durations were sub-optimal. However, the influence of Mitomycin C concentrations on the ultimate performance of feeders remains unreported so far. The present study showed no significant differences in concentration-dependent feeder functionality when the concentrations were delivered in low volumes of about 5 ml as in case of 3.10, 4-15, 5-15 and 10-30. But, upon titration with arithmetically derived doses, a low concentration of 4  $\mu$ g per ml delivered at an intermediate dose of 150  $\mu$ g per cell revealed optimal influence on keratinocytes, while the

lower 15 and higher 450 were suboptimal. The results demonstrated the importance of dose derivation and its utility in optimizing the feeder efficiency. Further, the superior growth potential of 4-150 feeders on keratinocytes plated at clonal density clearly demonstrated their outperformance achieved by the dose titrations.

The most intriguing point of this investigation has been the least performing  $\gamma$ -Irr feeders, whose low mass growth support was comparable to that observed with concentrations of either 3 or 10  $\mu\text{g}$  per ml. The performance of  $\gamma$ -Irr feeders on 3<sup>rd</sup> passage keratinocytes plated at low clonal density turned out to be even worse. However, the efficiency was higher and comparable to 4-15 when the 1<sup>st</sup> passage keratinocytes were co-cultured at a low clonal density and further improved in the presence of same keratinocytes plated at a higher clonal density. But 4-150 still remained superior in stimulating the colony forming efficiency of keratinocytes. These observations suggest that the  $\gamma$ -Irr feeders perhaps perform optimally only with the early keratinocyte passages.

The BrdU studies indicated that it was the stimulation of colony initiation rather than increase in mitosis per colony that turned out to be the advantageous consequences of fine-tuning of Mitomycin C treatment by including both concentration and dose per cell. It is apparent that feeders of 4-150 were superior to 4-15 in inducing a higher BrdU label, in spite of absence of significant variation in average cellularity per colony, indicating that an overall high cell turn over would eventually set in. Thus, the importance of dose titration of feeders with Mitomycin C is further highlighted through improvement of the otherwise sub-optimal performance to match with that of  $\gamma$ -Irr feeders in achieving faster growth of keratinocytes.



The most important outcome of this whole investigation on feeder cell titrations vertically with various concentrations of Mitomycin C and also subsequent lateral titrations with arithmetically derived doses is that the degree of feeder cell extinctions proportionately rose with not just concentration but also dose, which is largely ignored so far (Schrader, 1999; Connor 2000; Ponchio et al 2000; Roy et al, 2001; Nieto et al 2007; Fleischmann et al 2009, Zhou et al 2009 & 2014). An experimental approach to derive such effective doses has also been demonstrated (Figure 5.1 Chapter 5) along with validation of such doses (Figure 6.1 Chapter 6). Further on, the results of co-culture experiments are coherent with the postulation that highest proliferation of keratinocytes which was determined by a preferred Mitomycin C dose used to growth arrest the feeder cells, would depend on the net resultant ratio between regressively depleting feeders and progressively growing human epidermal keratinocytes. Such a ratio has been a well identified key growth regulating factor *in vitro* (Sun et al 2009; Zhou et al 2009; Jubin et al 2011). Accordingly, if such a ratio was to prevail maintaining higher net feeder cell density, as in case of lower doses like 4-15 due to slower extinction, the keratinocytes would be left with less space on 2-D culture surface resulting in their hindered growth. Similar lowering of growth is also likely to occur, if feeder cell number would fall short of the minimum necessary density to support the growth of keratinocytes, due to their faster depletion as with high dosing such as 4-450. Therefore, it is more likely that 4-150 could have worked as an ideal intermediate dosing producing maximal keratinocyte proliferation through balancing of feeder extinction rate in a way to achieve optimal net ratio.

## **Chapter 8**

# **Cultured Epithelial Sheets**

## **8.1 Introduction**

Billingham and Reynolds (1953) were the first to recognize the prospective for transplantation of "Cultured Epidermis" or epidermal cell suspensions in various stages of differentiation as grafts to cover large full-thickness skin defects. A more effective method allowing for serial keratinocyte subcultivation was developed 22 years later by Rheinwald and Green (1975) who obtained the first stratified colonies of human keratinocytes from single cells. These authors used a combination of hydrocortisone, epidermal growth factor (EGF), and irradiated murine 3T3 fibroblasts to support the proliferation of keratinocytes on plastic substrates (Rheinwald and Green, 1977). The following ingredients were added to improve the culture media and to facilitate keratinocyte sheet formation: (a) insulin (to promote the uptake of glucose and amino acids), and transferrin (to detoxify iron); (b) hydrocortisone (to promote the attachment of cells and cell proliferation), (c) tri-iodothyronine (which is mitogenic for keratinocytes); and (d) cholera toxin (which upregulates cAMP). By this method, keratinocytes can undergo about 50 to 60 population doublings if cultured from neonatal foreskin. This number gradually declines with donor age (Gilchrest, 1983). "Translating" the number of doublings to area indicates that cultured keratinocytes can be expanded to form sheets up to 10,000 times larger than the original biopsy size.

Keratinocyte sheet grafting became a reality following the discovery that an enzyme, dispase, could digest adhesive molecules holding the keratinocytes to the plastic substrate without digesting the intercellular molecular links (Green et al, 1979). As a logical consequence of these preliminary experimental successes, the first cultured autologous keratinocyte sheets were used in burn patients (O'Conner et al, 1981). The epidermal

culture technique has been well-established in many western countries (Teepe et al., 1990; Daniels *et al.*, 1996; Paddle-Ledinek *et al.*, 1997; Carsin *et al.*, 2000; Elliott and Vandervord, 2002; Wood et al, 2006, Atiyeh *et al.*, 2007) and has also been standardized in India (Kumar *et al.*, 2001).

Keeping in mind the above facts, this chapter is thus aimed to generate cultured epidermal sheets using those feeders that are growth arrested with the most optimal Mitomycin C concentration-dose permutation of 4-150. As described in, the most preferred concentration-dose. This permutation was shown to produce significantly faster growth of keratinocytes in comparison to the other permutations (Chapter 6). The epidermal sheets were grown by co-culturing the primary human epidermal keratinocyte cells with feeders exposed to 4-150. The sub-optimally performing feeders of 4-15 were included in the study to compare the significance of dose titration within the same concentration. The Gamma-Irradiated ( $\gamma$ -Irr) 3T3 cells which are used as the standard feeder cells in an approved product of cultured epithelial autograft were additionally used for comparison (<http://www.accessdata.fda.gov/scripts/cdrh/cfdocs/cftopic/pma/pma.cfm?num=H990002>). The cultured epidermal sheets produced were characterized by histological evaluation and Immunohistochemistry.

## **8.2 Materials and Methods**

### **8.2.1 Establishment of Stratified Epithelial Culture**

The epithelia which are equivalent of cultured epithelial autografts were prepared using the feeder cells of 4-150, 4-15 and  $\gamma$ -Irr. Triplicate cultures were initiated in 6-well plates by seeding 400, 800 and 1700 viable 1<sup>st</sup> passage keratinocyte cells per cm<sup>2</sup> and 15,000

feeder cells per cm<sup>2</sup>. Culture medium was changed every alternate day until confluence and Epidermal growth factor (EGF) was added to the culture medium after 48 hours. Out of three confluent cultures, two wells were used for histological and immunohistochemical studies, while the third was used to generate cell suspension by trypsinization which was assessed for feeder cell contamination and growth in agar-methyl cellulose to rule out the transformation of keratinocytes.

### **8.2.2 Recovery of CEA from confluent culture of keratinocytes**

The stratified epithelium from confluent keratinocyte cultures (Figure 8.1) was recovered by incubating in solution containing 2 mg of Dispase per ml of keratinocyte culture medium without serum at 37<sup>0</sup>C for 50-70 minutes. The detached epithelial sheets were floated in excess medium transferred to a separate petridish. The cultured sheets were washed three times with PBS before used for either histological evaluation or assessing for feeder cells contamination.

### **8.2.3 Histological evaluation**

The isolated epithelia were fixed with 4% paraformaldehyde and processed for paraffin embedding by initially dehydrating through graded series of ethyl alcohol followed by clearing in xylene and embedding in paraffin. 5 µm thick sections of cultured epidermis were deparaffinized, hydrated, stained with Hematoxylin and Eosin and mounted in DPX after dehydrating.

### **8.2.4 Immunohistochemistry**

Parallel sections of cultured epithelial sheets were deparaffinized in xylene and hydrated through graded series of ethyl alcohol. Antigens of filaggrin, cytokeratin-10 (CK-10) and cytokeratin-14 (CK-14) were retrieved by immersing the slides containing sections in 10mM of sodium citrate buffer for 30 minutes at 90°C followed by cooling for 30 minutes, while involucrin was retrieved by treating for 7 min at room temperature with freshly prepared 0.1% trypsin and 0.1% CaCl<sub>2</sub> in Tris Buffered Saline (TBS). Sections were subsequently washed with TBS, blocked with 2 % of normal goat serum (Santacruz Biotech, sc-2043) for 1 hour at 37°C in a humidified chamber and incubated overnight at 4°C in mouse monoclonal primary antibodies (Santacruz Biotech) against filaggrin (sc-25896), Involucrin (sc-21748), CK-10 (sc-51581), CK-14 (sc-58724) diluted at a ratio of 1:50. Sections were then rinsed with TBS before incubating for 1 hour at 37°C in FITC-tagged goat anti-mouse IgG secondary antibody (sc-2010) diluted at 1:100 followed by mounting in DAPI containing medium (sc-24941). Negative controls were equivalently processed except for incubating in plain TBS in place of primary antibody. Normal human skin processed similarly served as positive control. The skin sample was part of the excess left out piece of unburned autograft prepared from the burn patient at the end of surgical autografting procedure and remained archived in a paraffin block. Prior ethical clearance was obtained from Safdarjung Ethical committee during a previous study on cultured epidermis in burn patients.

The third confluent keratinocyte culture was disaggregated using a solution of 0.08 % trypsin-0.01 % EDTA-0.008 % glucose and the cell suspension was used for assessing the feeder cell contamination and growth of keratinocytes in agar methyl cellulose.

### 8.2.5 Feeder contamination

The isolated keratinocyte suspension from the 3 feeder groups of 800 cell-seeding was assessed for both (a) non-proliferative and (b) proliferative feeder cell contamination by Hoechst staining.

**8.2.5.1 Non-proliferative contamination:** The cell suspension generated by the three feeder groups was plated in 60 millimeter dishes without feeders at a density of 5000 cells per dish; cells were allowed to attach overnight by incubating in KGM and number of feeder cells was counted after Hoechst staining.

**8.2.5.2 Proliferative contamination:** The trypsinized cells were plated in T25 flasks at a density of 50,000 cells per flask and incubated in KGM for a period of 3 weeks and processed for Hoechst staining.

### 8.2.6 Hoechst staining

Cultures at the end of respective incubation periods were fixed in a chilled solution of three parts of methanol and one part of glacial acetic acid, stained with Hoechst 33258 (Sigma, H-6024) at a concentration of 0.125 µg per ml of Hank's balanced salt solution, in the dark for 10 minutes. The dishes were washed with distilled water and observed in a fluorescence microscope (Nikon Diaphot 300) fitted with excitation filter of 330–380 nm and emission filter at 420 nm. 3T3 cells were distinguished from Keratinocytes on the basis of their different nuclear size, morphology and fluorescence pattern (Alitalo et al., 1982).

### **8.2.7 *In vitro* Transformation assay**

$5 \times 10^4$  isolated cells from trypsinized confluent keratinocyte cultures grown in presence of the three feeder groups were suspended in Methyl cellulose (Methocel, Sigma-Aldrich). Methyl cellulose was prepared at a final concentration of 0.8% in 3T3-CBS medium, poured over a base of 0.6% agar in 35 millimeter dish, incubated at standard culture conditions and examined under Nikon inverted phase contrast microscope after 2 weeks to look for keratinocyte growth.

### **8.2.8 Statistics**

Experimental groups for non-proliferative feeder contamination involving 4-15 and  $\gamma$ -Irr were statistically compared with 4-150 by Student's t test and considered as significant, if  $p < 0.05$ .

## **8.3 Results**

### **8.3.1 Stratified Epithelium**

Generally, Keratinocyte colonies of 2 to 5 cells appeared in the well by 2<sup>nd</sup> day in cultures. After one week, large keratinocyte colonies with specific areas of differentiation appeared. Keratinocyte colonies eventually coalesced and the confluent cultures gave rise to stratified squamous epithelium in 10-13 days depending on keratinocyte seeding density with smaller the seeding and longer the incubation time before they were isolated by dispase treatment. During incubation with dispase, the detachment of epidermal sheets from the culture surface commenced from the periphery (Figure 8.1b) and gradually progressed towards the center (Figure 8.1c).



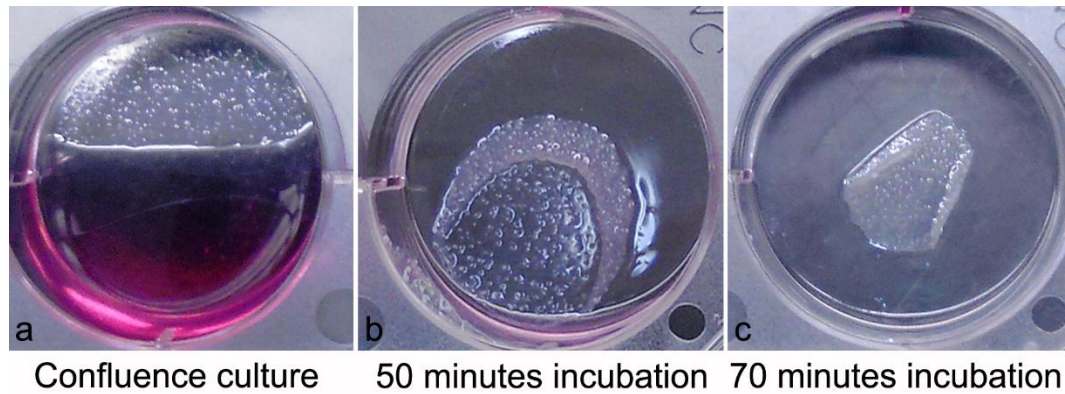


**Figure 8.1** *Recovery of culture epithelial sheet. (a) Fully confluent culture sheet, (b & c) after dispase treatment.*

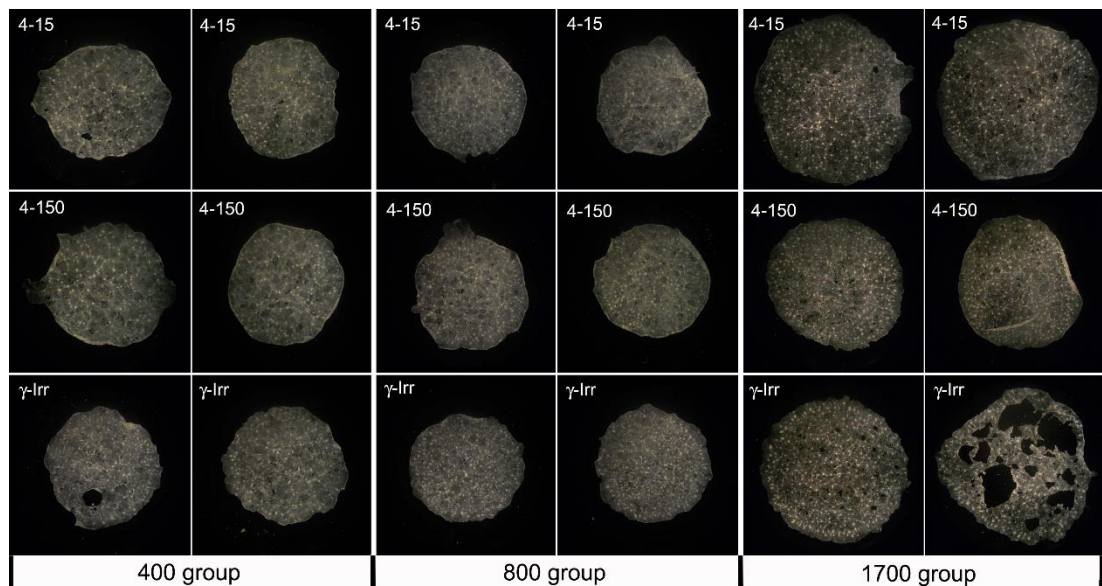


**Figure 8.2** *Cultured Epithelia from different feeder groups. Sheets of stratified epithelia in duplicate were isolated by incubating in dispase from cultures of keratinocytes cocultured with feeder groups of 4-15 (Top row), 4-150 (Middle row) and  $\gamma$ -Irr (Bottom row). The cultures were initiated by seeding the wells of 6-well plate with keratinocytes at densities of 400, 800 and 1700 cells /cm<sup>2</sup> grew to confluence at the end of 13, 12 and 10 days, respectively.. Magnification: Original.*

The isolated epithelial sheets contracted to about  $\frac{3}{4}$  the size of the well, appeared as thin, fragile, semi- translucent, free-floating tissues (Figures 8.1 & 8.2). The co-cultures initiated with a constant feeder density of 15,000 cells per  $\text{cm}^2$  and 1<sup>st</sup> passage epidermal keratinocytes at densities of 400, 800 and 1700 cells / $\text{cm}^2$  grow to confluence at the end of 13, 12 and 10 days, respectively. The shrinkage was relatively less in 1700 keratinocyte group and those from  $\gamma$ -Irr were thin and fragile.

### 8.3.2 Histological Characterization

The H & E stained paraffin sections of all the keratinocyte- feeder groups (Figures 8.3 & 8.4) revealed that the intermediate density (800 keratinocyte cells per  $\text{cm}^2$ ) produced epidermis of a more or less uniform thickness and integrity. The epithelia from other seeding groups were non-uniform with predominant basal compartment and minor suprabasal region. Hence, epithelia from 800 cell-seeding groups grown in presence of feeders of 4-15, 4-150 and  $\gamma$ -Irr were considered ideal and used for immunohistochemistry. The histological study revealed that the epidermal constructs grown over feeders of 4-150 uniformly presented the basal and the differentiated compartments with more or less even stratification, whereas the epidermal thickness resulting from its growth in presence of either  $\gamma$ -Irr or 4-15 Mitomycin C feeders was highly varied from one cell to 8 cells. Particularly, the sheets from  $\gamma$ -Irr group were very inconsistent with intermittent regions of completely differentiated segments in between zones of good thickness showing well-formed basal compartment. The inconsistent influence of  $\gamma$ -Irr feeders was more evident in 1700 feeder group which displayed a loose epidermal architecture with focused zones of terminal differentiation.

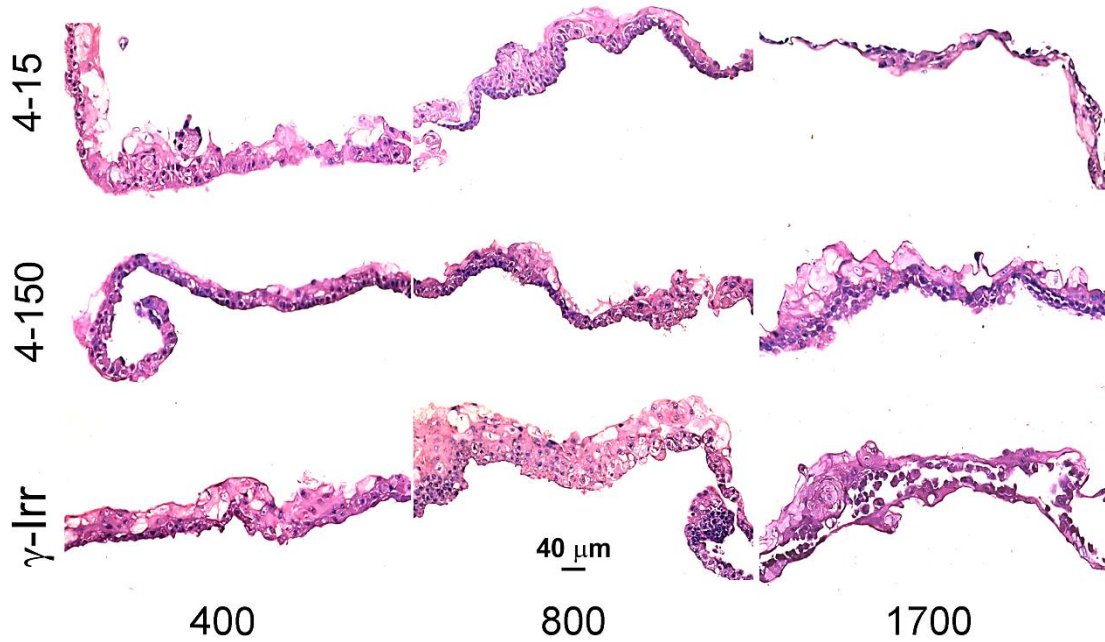


**Figure 8.3** *Hematoxylin and Eosin stained preparation of paraffin section of cultured epithelia (Low Magnification). Cultured epithelia were produced from confluent cultures of human keratinocytes grown with different seeding densities i.e. 400, 800 and 1700 per cm<sup>2</sup> of Epidermal keratinocytes over feeders of 4-15 (Top row), 4-150 (Middle row) and  $\gamma$ -Irr (Bottom row).*

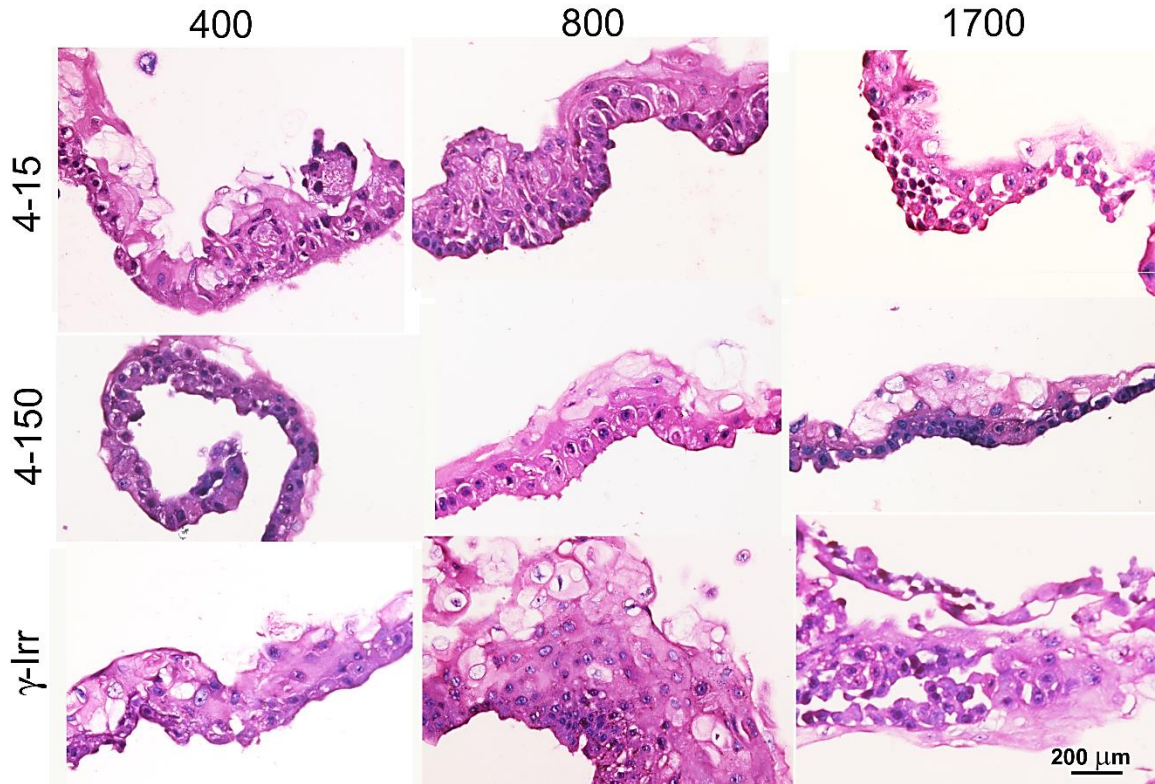


**Figure 8.4** *Hematoxylin and Eosin stained preparation of paraffin section of cultured epithelia (High Magnification). Cultured epithelia were produced from confluent cultures of human keratinocytes grown with different seeding densities i.e. 400, 800 and 1700 per  $cm^2$  over feeders of 4-15 (Top row), 4-150 (Middle row) and  $\gamma$ -Irr (Bottom row).*

### 8.3.3 Immunohistochemistry

The distribution of cytokeratin-14 was not restricted to the basal compartment as in normal human epidermis but present throughout the cultured epidermis in all the feeder groups (Figure 8.5).

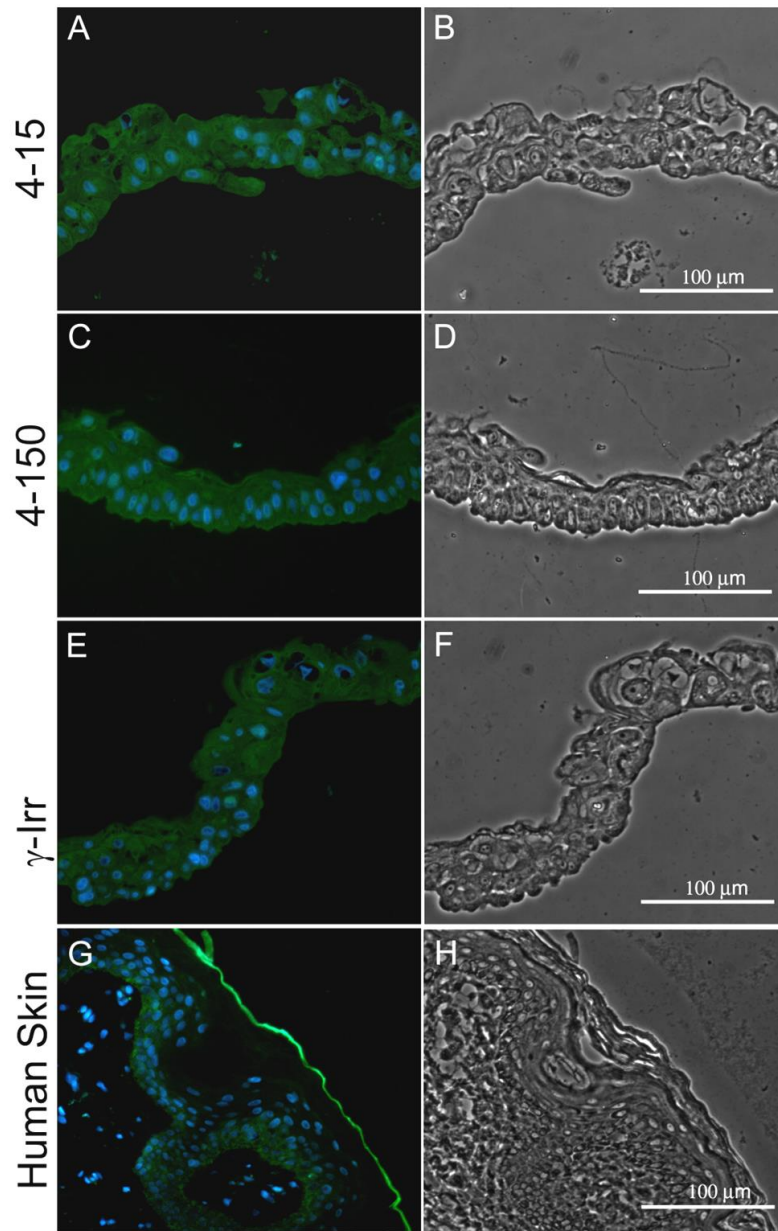


**Figure 8.5** *Expression of Cytokeratin 14 (CK-14) in cultured epidermis. Immunohistochemical localization of cytokeratin 14 in cultured epithelia of 4-15 (A & B), 4-150 (C & D),  $\gamma$ -Irr (E & F) and Normal human skin (G & H). The nuclei were stained blue with Dapi and the green deposits represent FITC tagged secondary antibody which was bound to the anti-cytokeratin 14 primary antibody. The left panel is the comparable Phase contrast image. Stratum corneum of human skin shows the usual non-specific staining (Mitchell et al 1982)*

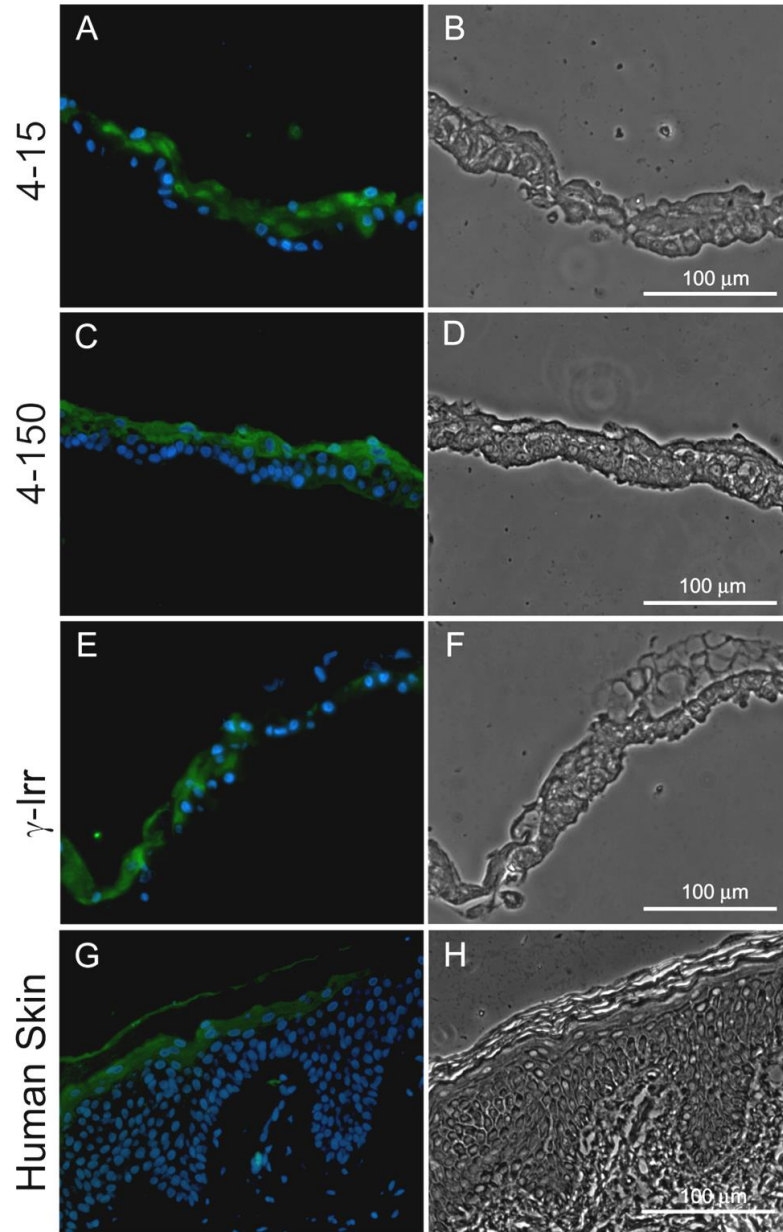


**Figure 8.6** *Expression of Involucrin in cultured epidermis. Immuno-histochemical localization of Involucrin in cultured epithelia of 4-15 (A & B), 4-150 (C & D),  $\gamma$ -Irr (E & F) and Normal human skin (G & H). The nuclei were stained blue with Dapi and the green deposits represent FITC tagged secondary antibody which was bound to the anti-cytokeratin 14 primary antibody. The left panel is the comparable Phase contrast image. Stratum corneum of human skin shows the usual non-specific staining (Mitchell et al 1982).*

On the other hand, there were feeder group dependent differences in the presentation of involucrin; those grown in presence of 4-150 Mitomycin C feeders exhibited a well demarcated and uniform distribution in the less nucleated supra-basal zone, but 4-15 and  $\gamma$ -Irr groups displayed its poorly demarcated non-uniform distribution (Figure 8.6).

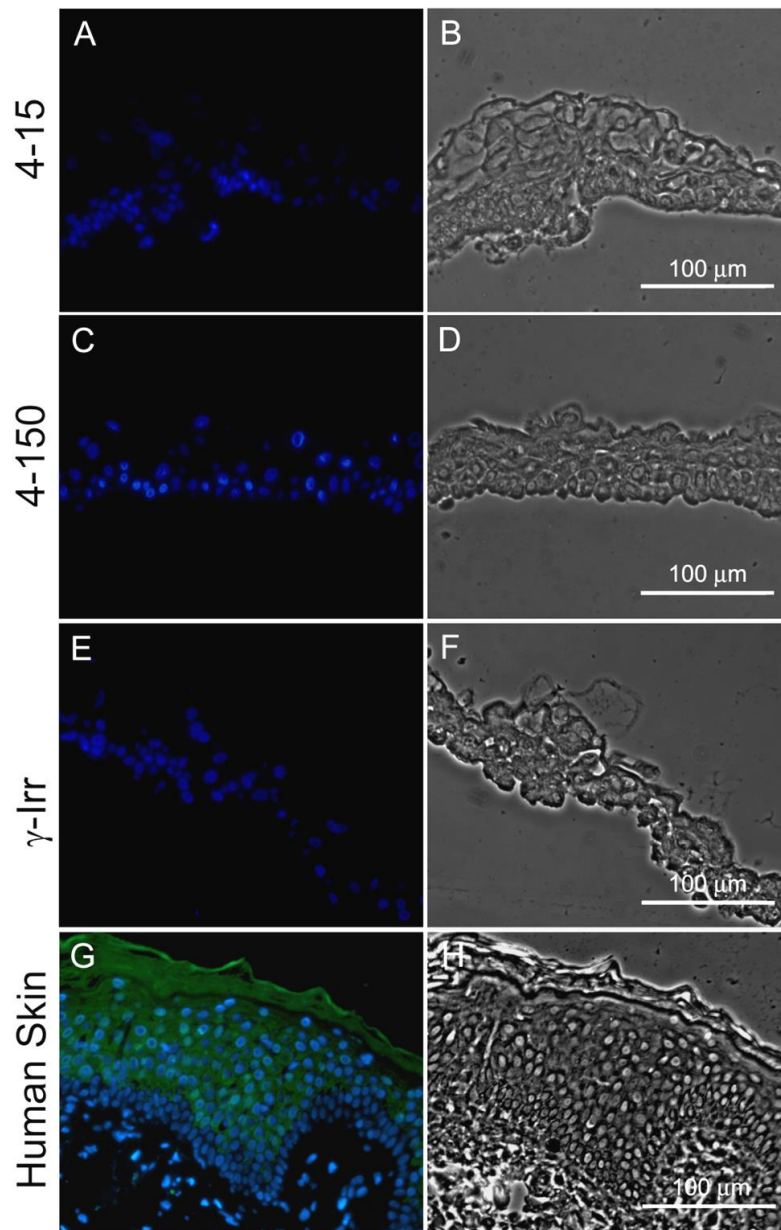


**Figure 8.7** Expression of Cytokeratin 10 (CK-10) in cultured epidermis. Immunohistochemical localization of cytokeratin 10 in cultured epithelia of 4-15 (A & B), 4-150 (C & D),  $\gamma$ -Irr (E & F) and Normal human skin (G & H). The sections show only the nuclei

were stained blue with Dapi while there were no deposits representing cytokeratin 10. The left panel is the comparable Phase contrast image. Stratum corneum of human skin shows the usual non-specific staining (Mitchell et al 1982).

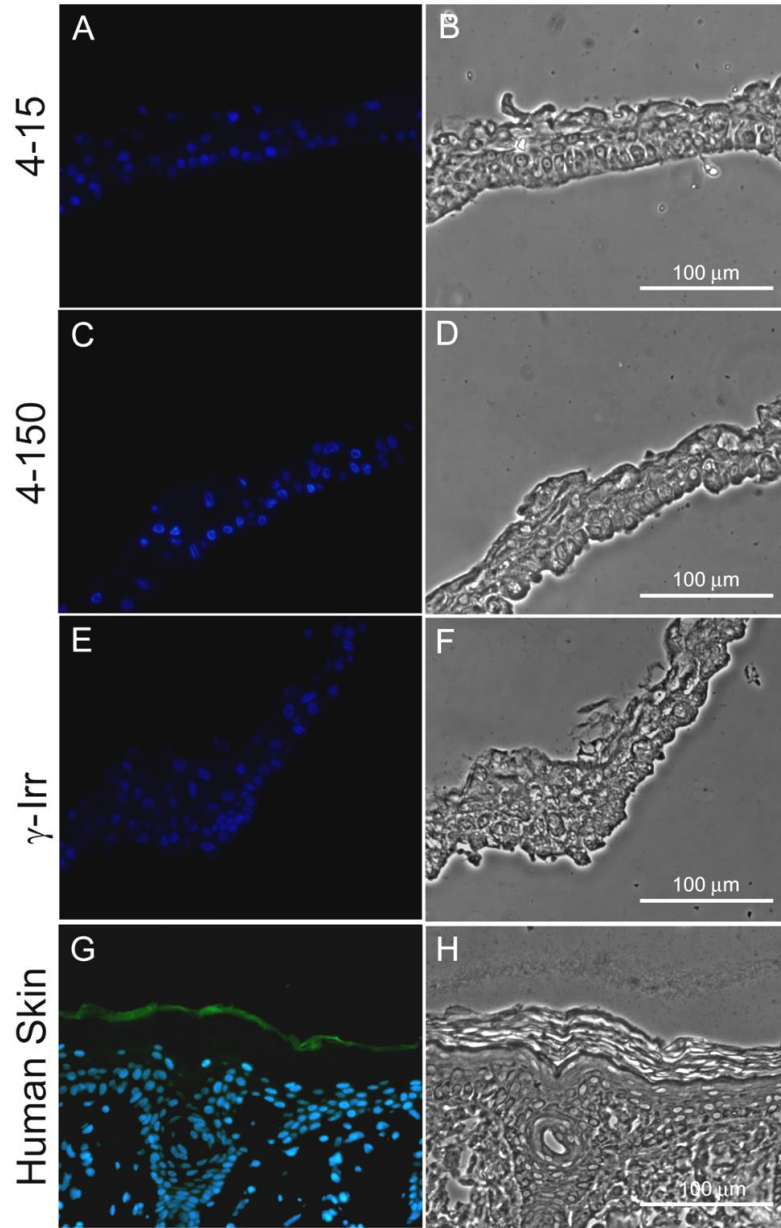


**Figure 8.8** Expression of Filaggrin in cultured epidermis. Immuno-histochemical localization of Filaggrin in cultured epithelia of 4-15 (A & B), 4-150 (C & D),  $\gamma$ -Irr (E & F) and Normal human skin (G & H). The sections show only the nuclei were stained blue with Dapi while there were no deposits representing cytokeratin 10. The left panel is the



*comparable Phase contrast image. Stratum corneum of human skin shows the usual non-specific staining (Mitchell et al 1982).*

The major deviation with normal human epidermal distribution of markers was with cytokeratin 10 (Figure 8.7) and filaggrin (Figure 8.8) which were conspicuously absent in cultured epithelia.

### **8.3.4 Feeder contamination**

**8.3.4.1 Non-proliferative contamination** The disaggregated cultured epithelia grown in presence of feeders of 4-15, 4-150 and  $\gamma$ -Irr revealed  $0.46\pm 0.03$ ,  $0.54\pm 0.04$  and  $0.56\pm 0.09$ , respectively as percentages of 3T3 cells that attached out of  $5 \times 10^3$  plated cells (Figure 8.9), which worked out to be  $3.3\pm 0.2$ ,  $3.5\pm 0.3$  and  $3.6\pm 0.6$ , respectively as percentages of feeder contaminants out of the total cells attached and the rest were keratinocytes. The data showed no significant differences.

**8.3.4.2 Proliferative contamination** The Hoechst stained preparations in T25 flasks after 3 weeks of incubating the disaggregated cell suspension containing  $5 \times 10^4$  cells from epithelial constructs showed replicated keratinocytes characterized by the presence of relatively small nuclei with smoothly diffused chromatin, but did not reveal any proliferative feeders which contained large nucleus with coarsely aggregated chromatin (Figure 8.10).

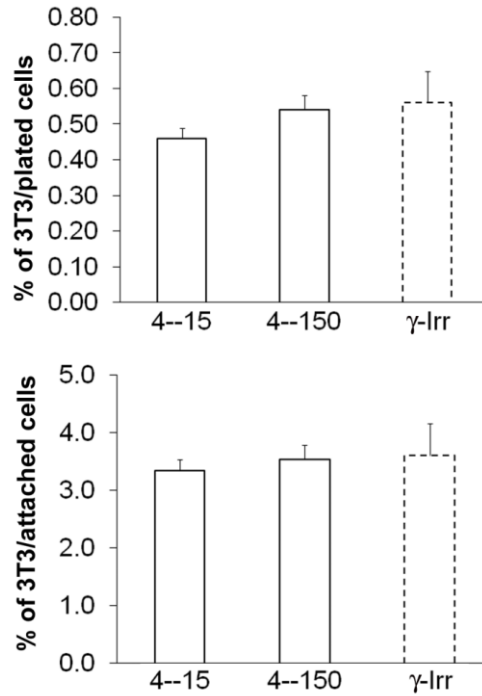


**Figure 8.9 Feeder cells contamination in Co-cultures:** consists of column charts representing non-proliferative feeder cell contamination expressed as percent of 3T3 out of total plated cells of 5000 per dish (Top) and percent of 3T3 out of total attached cells that included both 3T3 and keratinocytes (Bottom). Statistical analysis using Students 't' test revealed insignificant differences among the three groups.

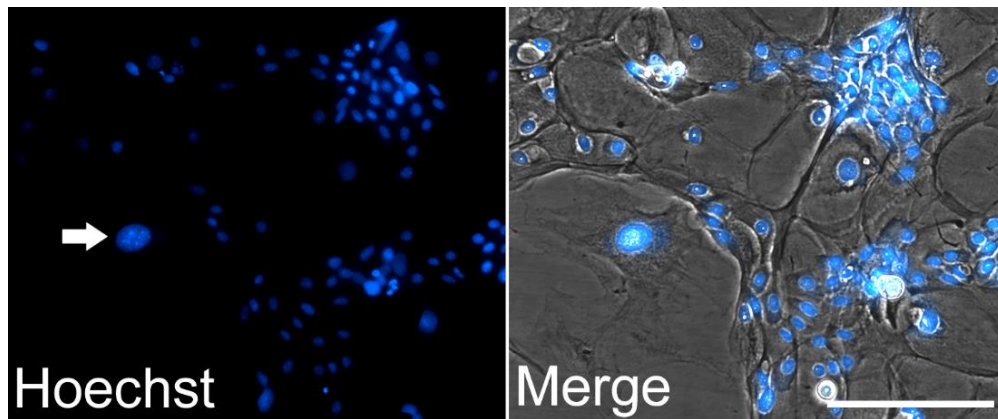


**Figure 8.10 Demonstration of Proliferative feeder cell contamination by Hoechst staining:** Hoechst stained preparation in T25 flask following 3 weeks of incubating the isolated keratinocyte suspension containing 50,000 cells. A sole broad fibroblast (arrow) is seen with large nucleus containing coarsely aggregated chromatin and bright nucleoli

as opposed to numerous keratinocytes containing relatively small nuclei with smoothly diffused chromatin and dim nucleoli. Magnification marker = 10  $\mu$ m.

### 8.3.5 Transformation Assay

None of the  $5 \times 10^4$  isolated cells from trypsinized confluent keratinocyte cultures grown in presence of the three feeder groups showed any growth in Methyl cellulose after 2 weeks of incubation.

## 8.4 Discussion

Cell based therapies in recent times have gained high importance in the treatment of various incurable diseases. Several stem-cell banking facilities have come up in recent times (<http://www.lifecellindia.com>) and involved in cell based therapies. Additionally, in these therapies there are situations wherein the human cells are manipulated ex vivo in cell culture conditions for relatively longer period of time. The *in vitro* cultivation of human corneas is a purely cell culture based technique wherein the limbal stem cells are kept in culture media for a relatively longer period of time allowing cell proliferation and constitution as transplantable cornea and several clinical studies have already been performed (Fatima *et al.*, 2006 and 2007; <http://www.lvpei.org>). The other important area of *in vitro* developed cultured cell products is the large-scale propagation of cultured epithelia sheets for burn wound coverage, was first reported in the treatment of major burn in 1981 (O'Connor *et al.*, 1981) wherein the cells are kept and handled under cell culture conditions.

This investigation comprised of a cost-effective yet efficient processing strategy for Swiss 3T3 feeder cells suitable for human epidermal keratinocyte stem cell proliferation and in vitro construction of stratified epithelium. Considering the high costs for the establishment of Gamma-Irradiation setup for generating feeder cells, Mitomycin C treatment is very cost-effective (Ponchio et al., 2000; Llames et al., 2015) and by applying our innovative strategy of volume titrations without raising the concentration *per se*, we produced significant alterations in post-exposure life span of feeders which probably was the influencing factor for the improved outcome of keratinocyte cells stimulation.

Analysis of Haematoxylin and eosin stained sections of cultured epidermis demonstrated that morphologically these experimental setup were closely similar to normal human epidermis. Earlier it was reported that cultured epithelial sheet with 5 to 8 cell layers is sufficient to provide mechanical strength and to be used as a graft material (Ueda, 1995). The cultured epidermis produced by all the three feeder groups showed that intermediate keratinocyte seeding density (800 cells/cm<sup>2</sup>) produced cultured epidermis of more or less uniform thickness and integrity. . Out of these, the 4-150 group produced epidermis with uniform basal compartment with more or less even stratification, whereas the thickness of epidermis produced by either  $\gamma$ -Irradiated or 4-15 feeders was highly varied from one cell to 8 cells. The production of better quality cultured epidermal sheets with 4-150 feeder group is in conjunction with co-culture experiments of chapter 7 in which significant increase in keratinocyte proliferation was experimentally demonstrated.. Moreover, the superior expression of normal human epidermal markers like CK14 and Involucrin in the cultured epidermis produced by 4-150 than with other feeders, qualifies it as a potential graft material for wound coverage. Additionally, the enzymatically disaggregated

epidermal sheet constructed by using feeders of 4-150 contained 0.54% of feeder contamination which is equal to what is reported in a commercially available product which is grown by Gamma-Irradiation approach ((Document entitled ‘Summary of Safety and Probable Benefit’ [www.accessdata.fda.gov/cdrh\\_docs/pdf/H990002b.pdf](http://www.accessdata.fda.gov/cdrh_docs/pdf/H990002b.pdf)).

Ebner and co-workers (1961) reported on the possibility of morphological changes in cultured cells during co-culturing of keratinocyte cells. This problem concerns the mutation potential in cultured epidermal cells that have been used for the preparation of cultured epithelium. Therefore, the safety of cells should be checked when cells or tissue prepared by using cultured cells is planned for transplantation to humans. Furthermore, it is well reported that keratinocyte cultures grown in the presence of feeder layer does not generate transformed cells and it is not associated with an increased risk of tumorigenicity (Thepot et al., 2011). In this present study, we also demonstrated in chapter 7 that the keratinocytes cultured with 4-150 did not show any anchorage-independent growth in agar-methyl cellulose assay.

Therefore, the comparative analysis among 4-15, 4-150 and Gamma-Irradiated feeders demonstrated that 4-150 group worked as an ideal intermediate dose by maintaining a balance between feeder extinction and survival rates in a way to achieve optimal proliferation of keratinocyte cells. Thus, the potential utility of novel feeder processing employing the concentration-dose permutations of Mitomycin C, is the first ever report in this study. The strategy has ultimately been identified as a faster and economical method of culturing human epidermal sheets comparable to the expensive Gamma-Irradiation approach without compromising with the quality. Therefore, it should be suitable for resurfacing the burn injuries.

## **Chapter 9**

### **Conclusion and Future Scope of work**

**Conclusion and Future Scope of work:**

This thesis work was involved with the establishment of a cost-effective yet efficient method of processing the Swiss 3T3 cells for their ultimate use as feeder cells. The research work initially addressed the sporadic failure of Mitomycin C induced growth arrest in 3T3 cells. This problem was successfully contained by adopting a safe banking protocol which was validated by specifically identified test procedures. Further, the stimulatory influence of growth arrested feeder cells on the epidermal keratinocytes was optimized by employing a permutation of concentration and volume of Mitomycin C through a novel experimental derivation. The method enabled identification of an optimal growth arrest procedure in a way to match with the functionality of gamma-irradiated feeders.

The very first critical aspect was the establishment of an ideal banking system to generate uniform cell population that excluded Mitomycin C resistant variants (Chapter 4). Because the 3T3 cells have been extensively subcultured due to wide distribution in the world, there is a strong possibility of selective inclusion of such variants in them leading to sporadic failure of growth arrest. Such a failure of growth arrest can lead to a serious risk of proliferative feeder contamination in target cell cultures. In an attempt to identify and validate the establishment of a safe banking system, Swiss 3T3 cells (CCL-92, ATCC) were passaged by three different seeding densities and incubation periods. Two of the subculture schemes denoted as 3K3D and 3K4D, represented incubation of 3000 plated cells per  $\text{cm}^2$  for 3 and 4 days, respectively. The third scheme of 4K3D involved 3 days incubation of 4000 cells plated per  $\text{cm}^2$ . The 3K3D cultures displayed unique cell size distribution and disintegrated completely in 6 weeks following Mitomycin C treatment, but

their repeated subculture resulted in feeder regrowth as late as 11 weeks after the growth arrest. In contrast, Mitomycin C failed to inhibit cell proliferation in cultures of the other subculture schemes and also in a clone that was established from a transformation focus of super-confluent culture. The resultant proliferative feeder cells contaminated the keratinocyte cultures. The anchorage-independent growth appeared in late passages as compared with the expression of Mitomycin C resistance in earlier passages. Thus, it was recommended to include the described test procedures to rule out (1) MC-resistance (2) proliferative feeder cell contamination of target cells and (3) growth in methylcellulose before qualifying the feeder batches as safe. The subculture of the already over passaged Swiss 3T3 cells should be limited. Additionally, the MC resisting clone and the late passage cultures are useful to study molecular pathways involved in chemoresistance and post-chemotherapy initiation of cell cycling in cancer cells.

Subsequently, a process of controlled growth arrest of feeder cells has been identified through a strategy of regulating their life span and their ability in supporting the proliferation of human epidermal keratinocyte stem cells.

This was achieved by the following experimental strategies:

(1) Initially it was proved that the periodical feeder cell extinctions depended on a range of Mitomycin C doses per unit cell number which were derived arithmetically by the following formula after a range of feeder cell densities were experimentally pulse exposed to various concentrations of Mitomycin C (Chapter 5).

$$\Delta = \frac{Cv}{\Sigma}$$



Where  $\Delta$  = dose / cell (pg/cell or  $\mu\text{g}/\text{million cells}$ )  
 $C$  = concentration of Mitomycin C ( $\mu\text{g}/\text{ml}$ )  
 $v$  = volume of treating solution (ml) which is kept constant  
 $\Sigma$  = exposure cell number (millions)

(2) The above formula was deciphered into the following one in order to calculate the volume of treating solution since the exposure cell density has to be fixed to a safe constant as shown by the validated sub-culture procedure.

$$v = \frac{\Sigma \Delta}{C}$$

Wherein:

$\Sigma$  = exposure cell number (in millions) which is kept to a safe constant as shown in chapter 4 to avoid inclusion of variants.

(3) A range of probable volumes of Mitomycin C solutions was then predicted based on permutations of derived doses and concentrations. Several feeder cell batches were then short-listed on the basis of inducing significant differential in cell disintegration trends following a pulse exposure to Mitomycin C (Chapter 6).

(4) An optimal feeder batch that imparted a maximal growth support to the epidermal keratinocytes in an *in vitro* co-culture system was subsequently identified and comparable with the Gamma-Irradiated feeders (Chapter 7). Out of the various permutations of concentrations and doses of Mitomycin C employed to process the feeders, we found that only the middle concentration of 4  $\mu\text{g}/\text{ml}$  with a dose of 150  $\mu\text{g}/\text{million cells}$  (4-150) performed better in both clonal and mass culture of 3<sup>rd</sup> passage keratinocytes than the

feeders exposed to other permutations and Gamma-Irradiated feeders. Additionally, studies on colony forming efficiency and growth area estimation with the 1<sup>st</sup> passage keratinocytes revealed superior influence by 4-150 feeders than the 4-15 and  $\gamma$ -Irr feeders. On the other hand, the BrdU labeling study in keratinocytes revealed that the 4-150 feeders were equivalent to  $\gamma$ -Irr feeders, but superior to 4-15. The results suggested that it was the stimulation of colony initiation rather than increase in mitosis per colony that turned out to be the advantageous consequences of fine-tuning of Mitomycin C concentration with dose per cell.

(5) The feeders of the identified batch were compared with  $\gamma$ -Irr cells in stimulating keratinocyte growth towards the formation of a stratified epithelium (Chapter 8). The histological evaluation showed that the feeders of 4-150 group produced epidermis with uniform basal compartment with more or less uniform stratification as compared with either  $\gamma$ -Irradiated or 4-15 feeders. The cultured epidermal sheets produced by all the feeders demonstrated CK14 and Involucrin by Immunohistochemistry.

Therefore, the novel experimental derivation of Mitomycin C dosing which identified the production of 4-150 feeders to be functionally comparable to Gamma-Irradiation, works out to be cost-effective and many fold efficient to the existing Mitomycin C based technique.

**Future scope of work:**

The described strategy could also be adopted to optimize the feeder functionality of human dermal fibroblasts that could serve as ideal feeders in making not just a similar product but a non-xenogeneic epidermal construct for clinical utility. The final product must, in any way, be tested for the traces of Mitomycin C in addition to fulfilling the other necessary regulatory requirements like the chromosomal stability before evaluating the clinical utility of the epidermis produced by the Mitomycin C approach.

# **Chapter 10**

## **References**

1. Aasen T, Raya A, Barrero MJ, Garreta E, Consiglio A, Gonzalez F, Vassena R, Bilic J, Pekarik V, Tiscornia G, Edel M, Boue S and Belmonte JCI (2008). Efficient and rapid generation of induced pluripotent stem cells from human Keratinocytes. *Nature Biotech* 26: 1276-1284
2. Alam H, Sehgal L, Kundu S, Dalal S, Vaidya M (2011). Novel function of keratin 5 and 14 in proliferative and differentiation of stratified epithelial cells. *Mol Biol Cell* 22: 4068–4078. doi: 10.1091/mbc.e10-08-0703.
3. Alitalo K, Kuismanen E, Myllyla R, Kiistala U, Asko-Selgavaara S, Vaheri A (1982). Extracellular matrix proteins of human epidermal keratinocytes and feeder 3T3 cells. *J Cell Biol* 94: 497–505.
4. American Type Culture Collection (ATCC) USA, CCL-92, Culture method. Available: [www.atcc.org/products/all/ccl-92.aspx#culturemethod](http://www.atcc.org/products/all/ccl-92.aspx#culturemethod). Accessed 15 September 2014.
5. Atiyeh BS, Costagliola M. Cultured epithelial autograft (CEA) in burn treatment (2007). Three decades later. *Burns* 33(4): 405-413
6. Barlogie B, and Drewinko B (1980). Lethal and Cytokinetic effects of Mitomycin C on Cultured Human Colon Cancer Cells *Cancer Res* 40: 1973-1980.
7. Baroffio A, Dupin E and Le Douarin NM (1988). Clone-forming ability and differentiation potential of migratory neural crest cells *Proc. Natl. Acad. Sci. USA* 85: 5325-5329
8. Berry RD, Powell SC, Paraskeva C (1988). In vitro culture of human foetal colonic epithelial cells and their transformation with origin minus SV40 DNA. *Br. J. Cancer* 57: 287 289.
9. Billingham RE, Reynolds 1 (1952). Transplantation studies on sheets of pure epidermal epithelium and on epidermal cell suspensions. *Br I Plast Surg* 5:25-36.
10. Bisson F, Rochefort E, Lavoie A, Larouche D, Zaniolo K, Simard-Bisson C, Damour O, Auger F, Guerin S, and Germain L (2013). Irradiated human dermal fibroblasts are as efficient as mouse fibroblasts as a feeder layer to improve human epidermal cell culture lifespan. *Int J Mol Sci* 14, 4684.

11. Blacker KI, Williams MI, Goldyne M (1987). Mitomycin C-treated 3T3 fibroblasts used as feeder layers for human keratinocyte culture retain the capacity to generate eicosanoids. *J Invest Dermatol* 89(6): 536-9.
12. Bosman FT and Stamenkovic I (2003). Functional structure and composition of the extracellular matrix. *J Pathol*, 200(4):423–428.
13. Bowen-pope DF, Vogel A, Ross R (1994). Production of platelet-derived growth factor-like molecules and reduced expression of platelet-derived growth factor receptors accompany transformation by a wide spectrum of agents. *PNAS (USA)* 81: 2396-2400.
14. Boyce ST and Ham RG (1983). Calcium-regulated differentiation of normal human epidermal keratinocytes in chemically defined clonal culture and serum-free serial culture. *J. invest. Derm.* 81, 33-40.
15. Bray LJ, Heazlewood CF, Atkinson K, Hutmacher DW, Harkin DG (2012) Evaluation of methods for cultivating limbal mesenchymal stromal cells. *Cytherapy* 14: 936-947.
16. Brown KW, Parkinson EK (1985). Alteration of the extracellular matrix of cultured human keratinocytes by transformation and during differentiation. *Int J Cancer*, 35(6): 799-807
17. Browning LM, Huang T, and Xu XH (2010). Electric pulses to prepare feeder cells for sustaining and culturing of undifferentiated embryonic stem cells. *Biotechnol J* 5, 588.
18. Bullock AJ, Higham MC, MacNeil S (2006). Use of human fibroblasts in the development of a xenobiotic-free culture and delivery system for human keratinocytes.
19. Byrne C, Tainsky M, Fuchs E (1994). Programming gene expression in developing epidermis. *Development* 120:2369–2383.
20. Carsin H, Ainaud P, Le Bever H, Rives J, Lakhel A, Stephanazzi J, Lambert F and Perrot J (2000). Cultured epithelial autografts in extensive burn coverage of severely

- traumatized patients: a five year single-center experience with 30 patients. *Burns* 26(4): 379-387.
21. Chang-Liu Chin-Mei, Woloschak Gayle E (1997). Effect of passage number on cellular response to DNA-damaging agents: cell survival and gene expression. *Cancer Letters* 113: 77-86.
  22. Chen YT, Li W, Hayashida Y, He H, Chen SY, Tseng DY, Kheirkhah A and Tseng SCG (2007). Human Amniotic Epithelial Cells as Novel Feeder Layers for Promoting Ex Vivo Expansion of Limbal Epithelial Progenitor Cells *Stem Cells* 25: 1995 – 2005.
  23. Chugh RM, Chaturvedi M, Yerneni LK (2015) Occurrence and Control of Sporadic Proliferation in Growth Arrested Swiss 3T3 Feeder Cells. *PLoS ONE* 10(3): e0122056. doi:10.1371/journal.pone.0122056
  24. Connor DA (2000). Mouse embryo fibroblast (MEF) feeder cell preparation. *Current Protocols in Molecular Biology* 51: 23.2.1 – 23.2.7.
  25. Cuono C, Langdon R, McGuire J. Use of cultured epidermal autografts and dermal allografts as skin replacement after burns injury. *Lancet* 1986; I (8490):1123–4.
  26. Daniels JT, Kearney JN and Ingham E (1996). Human keratinocyte isolation and cell culture: a survey of current practices in the UK. *Burns* 22(1): 35-39.
  27. Division of medical assistance: bioengineered skin [Internet]. Raleigh (NC): North Carolina Department of Health and Human Services; 2010 Jul. NCHC Policy No. NCHC2009.82. [cited 2010 Oct 6]. Available from: <http://www.ncdhhs.gov/dma/hcmp/NCHC-Bioengineered-Skin-Policy.pdf>
  28. Dover R and Potten CS (1988). Heterogeneity and cell cycle analyses from time-lapse studies of human keratinocytes in vitro. *J. Cell Sci.* 89, 359-364.
  29. Ebner KE, Hageman Ee and Larson BL (1961). Functional biochemical changes in bovine mammary cell cultures. *Exp. Cell Res.*, 25, 555-570.
  30. Elliott M and Vandervord J (2002). Initial experience with cultured epithelial autografts in massively burnt patients. *ANZ J Surg* 72(12): 893-895.

31. Epstein SP, Wolosin JM, Asbell PA (2005). P63 expression levels in side population and low light scattering ocular surface epithelial cells. *Trans Am Ophthalmol Soc* 103:187-199.
32. Fatima A, Sangwan VS, Iftekhhar G, Reddy P, Matalia H, Balasubramanian D and Vemuganti GK (2006). Technique of cultivating limbal derived corneal epithelium on human amniotic membrane for clinical transplantation. *J Postgrad Med*52: 257-61.
33. Fatima A, Vemuganti GK, Iftekhhar G, Rao GN and Sangwan VS (2007). In vivo survival and stratification of cultured limbal epithelium. *Clin Experiment Ophthalmol* 35: 96-98.
34. Fernandes M, Sangwan Virender S, Rao Srinivas K, Basti S, Sridhar Mittanamalli S, Bansal Aashish K, Dua Harminder S (2004). Limbal stem cell transplantation. *Current Opthmal* 52: 5-22.
35. Fleischmann G, Muller T, Blasczyk R, Sasaki E, and Horn PA (2009). Growth characteristics of the nonhuman primate embryonic stem cell line cjes001 depending on feeder cell treatment. *Cloning Stem Cells* 11: 225-233
36. Freeman AE, Igel HJ et al (1976). Growth and characterization of human skin epithelial cell cultures. *In vitro*, 12,352-362.
37. Fuchs E and Green H (1980). Changes in keratin gene expression during terminal differentiation of the keratinocyte. *Cell* 19, 1033-1042.
38. Fuchs E and Green H (1981). Regulation of terminal differentiation of cultured human keratinocytes by vitamin A. *Cell* 25, 617-625.
39. Fuchs E and Raghavan S (2002). Getting under the skin of epidermal morphogenesis. *Nat Rev Genet*, 3(3):199–209.
40. Fusenig NE (1986). Mammalian epidermal cells in culture. In *Biology of the Integument* (ed. Bereiter-Hahn, J. et al.), pp. 409-442. Berlin: Springer-Verlag.



41. Gallico GG, O'Connor NE, Compton CC, Kehinde O, Green H (1984). Permanent coverage of large burn wounds with autologous cultured human epithelium. *N Engl J Med.* 311(7): 448-451
42. Gilchrest BA (1983). In vitro assessment of keratinocyte aging. *J Invest Dermatol* 81:184-189.
43. Gagnani A, Morgan JR, Ferreira LM (2003). Experimental model of cultured keratinocytes. *Acta Cir Bras* 18 (Special Edition): 4-14.
44. Gagnani A, Sobral C and Ferreira LM (2007). Thermolysin in human cultured Keratinocyte isolation. *Braz. J. Biol.*, 67: 105-109
45. Green H (1978). Cyclic AMP in relation to proliferation of the epidermal cell: a new view. *Cell* 15, 801-811.
46. Green H (1980). The keratinocyte as differentiated cell type. *Harvey Lectures* 74, 101-139.
47. Green H, Fuschs E and Watt F (1982). Differentiated structural components of the keratinocyte. *Cold Spring Harb. Symp. quant. Biol.* 46, 293-301.
48. Green H, Kehinde O, Thomas J (1979). Growth of cultured human epidermal cells into multiple epithelia suitable for grafting *Proc Natl Acad Sci.* pp. 5665–5668
49. Green H, Rheinwald JG and Sun TT (1977). Properties of an epithelial cell type in culture: The epidermal keratinocyte and its dependence on products of the fibroblast. In *Cell Shape and Surface Architecture* (ed. Revel, J. P. et al.), pp. 493-500. New York: Alan Liss.
50. Green H, 2008. The birth of therapy with cultured cells. *BioEssays* 30, 897–903.
51. Hata K, Kagami H, Ueda M, Torii S and Matsuyama M (1995). Difference in characteristics of mucosal cells and epidermal cells as material for cultured epithelial grafting. *I. Oral Maxillofac. Surg.*, (1995 to be published).
52. Hata T, Sano Y, Sugawara R, Matsumae A, Kanamori K, Shima T & Hoshi T (1956). Mitomycin, a new antibiotic from *Streptomyces*. *J Antibiot* 9, 141-146

53. Hawleay-Nelson P and Sullivan JE (1980). Optimized conditions for the growth of human epidermal cells in culture. 1. Invest Dermatol, 75, 176-182
54. Hefton JM, Madden MR, Finkelstein JL, Shires GT (1983). Grafting of burn patients with allografts of cultured epidermal cells. Lancet 2: 428–430. doi: 10.1016/s0140-6736(83)90392-6.
55. Herndon DN, Rutan RL (1992). Comparison of cultured epidermal autograft and massive excision with serial autografting plus homograft overlay. J Burn Care Rehabil. 13(1): 154-157
56. Herzog SR, Meyer A, Woodley D, Peterson HD (1988). Wound coverage with cultured autologous keratinocytes: use after burn wound excision, including biopsy follow up. J Trauma, 1988; 28(2): 195-198
57. Hoffmann BLA, Rheinwald JG (1984). Polycyclic aromatic hydrocarbon mutagenesis of human epidermal keratinocytes in culture Proc. Natl. Acad. Sci. USA: 81: 7802-7806.
58. Hultman CS, Brinson GM, Siltharm S, deSerres S, Cairns BA, et al. (1996). Allogeneic fibroblasts used to grow cultured epidermal autografts persist in vivo and sensitize the graft recipient for accelerated second-set rejection. The Journal of Trauma 41(1): 51.
59. Hunyadi J, Simon M Jr, Dobozy A (1989). Cryopreserved 3T3 fibroblasts retain the capacity to enhance the growth of human keratinocyte cultures. Acta Derm Venereol 69(6): 509-12
60. Ishida-Yamamoto A, Kartasova T, Matsu, S, Kuroki T, and Iizuka H (1997). Involucrin and SPRR are synthesized sequentially in differentiating cultured epidermal cells. J Invest Dermatol, 108(1):12–6.
61. Jamora C and Fuchs E (2002). Intercellular adhesion, signaling and the cytoskeleton. Nat Cell Biol, 4(4):E101–E108.
62. Japan Tissue Engineering Co., Ltd. review report (August 6, 2007) Pharmaceuticals and Medical Devices Agency Available:

[http://www.pmda.go.jp/english/service/pdf/medical\\_devices/jace\\_oct2007\\_e.pdf](http://www.pmda.go.jp/english/service/pdf/medical_devices/jace_oct2007_e.pdf).  
Accessed 15 September 2014.

63. Jubin K, Martin Y, Lawrence-Watt DJ and Sharpe JR (2011). A fully autologous co-culture system utilizing non-irradiated autologous fibroblasts to support the expansion of human keratinocytes for clinical use. *Cytotechnology*, DOI 10.1007/s10616-011-9382-5
64. Kim J. et al. (2008). CD34+ Testicular Stromal Cells Support Long-Term Expansion of Embryonic and Adult Stem and Progenitor Cells. *Stem Cells* 26: 2516-2522.
65. Kumar A, Ali A, Yerneni LK (2008). Tandem use of immunofluorescent and DNA staining assays to validate nested PCR detection of mycoplasma. *In Vitro Dev Biol Anim*44: 189-192.
66. Kumar A, Bajaj SP, Mukherjee A and Yerneni LK (2001). In Vitro Cultivation of differentiated Epidermis from Human Keratinocytes Suitable for Autologous Grafting in Burns Patients. *Ind J Burns* 6: 65-68.
67. L. Sherwood (2007). *Human Physiology: From cells to systems*, 6th Edition, Thomson Brooks, Stamford
68. Lechner JF, Haugen A, Autrup H, McClendon IA, Trump BF and Harris CC (1981). Clonal Growth of Epithelial Cells from Normal Adult Human Bronchus. *Cancer Research* 41, 2294-2304
69. Lee JB, Song JM, Lee JE, Park JH, Kim SJ, Kang SM, Kwon JN, Kim MK, Roh SI and Yoon HS (2004). Available human feeder cells for the maintenance of human embryonic stem cells. *Reproduction* 128: 727-35.
70. Liu S, Li J, Wang C, Tan D and Beuerrman R (2007). Human Limbal progenitor cell characteristics are maintained in tissue culture. *Ann Acad Med Singapore* 35: 80-86.
71. Llames S G, Garcia E, Meana A, Larcher F, Del Rio M (2015). Feeder Layer Cell Actions and Applications. *Tissue Engineering: Part B*. 00: 00, DOI: 10.1089/ten.teb.2014.0547.

72. Lodish H, Berk A, Zipursky S, Matsudaira P, Baltimore D, and J D (1999a). *Molecular Cell Biology*, chapter 22, pages 979–992. W.H. Freeman and Company, New York.
73. Lu R, Bian f, Lin J, Su Z, Qu Y, et al. (2012). Identification of Human Fibroblast Cell Lines as a Feeder Layer for Human Corneal Epithelial Regeneration. *PLoS ONE* 7: e38825.
74. Macpherson I and Bryden A (1971). Mitomycin C treated cells as feeders. *Exptl Cell Res* 69: 240-241
75. Malinowaski k, Pullis C, Raisbeck AP and Rapaport FT (1992). Modulation of human lymphocyte marker expression by gamma-irradiation and mitomycin C. *Cell Immunol* 143: 368-377.
76. Matthews EJ (1993). Transformation of BALB/c-3T3 Cells: I. Investigation of Experimental Parameters that Influence Detection of Spontaneous Transformation *Environmental Health Perspectives Supplements* 101 (Suppl. 2): 277-291
77. McMahon AP and Bradley A (1990). The Wnt-1 (Int-1) Proto-Oncogene is required for development of a large region of the Mouse Brain. *Cell* 62, 1073–1085
78. McMillan J R, Akiyama M, and Shimizu H (2003). Epidermal basement membrane zone components: ultra-structural distribution and molecular interactions. *J Dermatol Sci*, 31(3):169–177.
79. Morita K and Miyachi Y (2003). Tight junctions in the skin. *J Dermatol Sci*, 31(2):81–89.
80. Munster AM. Whither (corrected) skin replacement? *Burns*, 1997; 23(1)
81. Nanchahal J, Dover R, Otto WR (2002). Allogeneic skin substitutes applied to burns patients. *Burns*,; 28(3): 254-257
82. Navasaria et al (1994). Growth of keratinocytes with a 3T3 feeder layer: basic techniques In Leigh, I.M and Watt, F.M. Eds *the Keratinocytes Hand Book*. Cambridge University Press, Cambridge, UK pp 5-12.

- 83.** Nemes Z and Steinert P (1999). Bricks and mortar of the epidermal barrier. *Exp Mol Med.*, 31(1):5–19.
- 84.** Nieto A, Cabrera CM, Catalina P, Cobo F, Barnie A, Corte´s JL, Barroso del Jesus A, Montes R, Concha A (2007). Effect of mitomycin-C on human foreskin fibroblasts used as feeders in human embryonic stem cells: Immunocytochemistry MIB1 score and DNA ploidy and apoptosis evaluated by flow cytometry *Cell Biology International* 31: 269-278
- 85.** Noble WC (1993). *The skin microflora and microbial skin disease.* University of Cambridge, Cambridge.
- 86.** O’Connor NE, Mulliken JB, Banks-Schlegel S, Kehinde O and Green H (1981). Grafting of burns with cultured epithelium prepared from autologous epidermal cells. *Lancet* 1: 75-78.
- 87.** Okita K, Ichisaka T, Yamanaka S (2007). Generation of germline-competent induced pluripotent stem cells. *Nature* 448:313–317.
- 88.** Omoto M, Miyashita H, Shimmura S , Higa K, Kawakita T, Yoshida S, McGrogan M, Shimazaki J and Tsubota1 K (2009). The Use of Human Mesenchymal Stem Cell–Derived Feeder Cells for the Cultivation of Transplantable Epithelial Sheets. *Investigative Ophthalmology & Visual Science* 50: 2109-2115.
- 89.** Paddle-Ledinek JE, Cruickshank DG and Masterton JP (1997). Skin replacement by cultured keratinocyte grafts: an Australian experience. *Burns* 23(3): 204-211.
- 90.** Pallen CJ, Tong PH (1991). Elevation of membrane tyrosine phosphatase activity in density-dependent growth-arrested fibroblasts. *Proc Natl Acad Sci USA* 88: 6996–7000.
- 91.** Parnigotto PP, Bassani V, Pastore S, Valenti F, Conconi MT (1994). Fibroblast-keratinocyte co-cultures in vitro: growth, morphometry and nutrient exchange. *Ital J Anat Embryol* 99(1): 17-30.
- 92.** Parnigotto PP, Conconi MT, Bassani V, Pastore S, Contiero E, Cortivo R (1993). Interaction between keratinocytes and fibroblasts cultured in vitro: morphology, morphometry and growth. *Ital J Anat Embryol.* 98(1): 31-9.

- 93.** Peehl DM, Stanbridge EJ (1981). Anchorage-independent growth of normal human fibroblasts. *Proc. Natl. Acad. Sci. USA* 78: 3053-3057.
- 94.** Pellegrini G, Dellambra E, Golisano E, Martinelli E, Fantozzi I, Bondanza S, Ponzin D, McKeon F, and De Luca M (2001). P63 identifies keratinocyte stem cells. *PNAS* 98: 3156-3161.
- 95.** Pellegrini G, Rama P, Di Rocco A, Panaras & De Luca M (2014) .Concise review: hurdles in a successful example of limbal stem cell-based regenerative medicine. *Stem Cells* 32, 26–34
- 96.** Pittelkow MR, Wille JJ and Scott RE (1986). Two functionally distinct classes of growth arrest states in human prokeratinocytes that regulate clonogenic potential. *J. invest. Derm.* 86, 410-417.
- 97.** Polakowska R R, Piacentini M, Bartlett R, Goldsmith LA, and Haake AR (1994). Apoptosis in human skin development: morphogenesis, periderm, and stem cells. *Dev Dyn*, 199(3):176–88.
- 98.** Ponchio L, Duma L, Oliviero B, Gibelli N, Pedrazzoli P, Robustelli della Cuna G. (2000). Mitomycin C as an alternative to irradiation to inhibit the feeder layer growth in long-term culture assays. *Cytotherapy* 2: 281-6.
- 99.** Potten CS (1974). The epidermal proliferative unit: the possible role of the central basal cell. *Cell Tissue Kinet.* 7:77–88.
- 100.** Prado CMM, Baracos VE, McCargar LJ, Mourtzakis M, Mulder KE, et al. (2007). Body Composition as an Independent Determinant of 5-Fluorouracil–Based Chemotherapy Toxicity. *Cancer Caner Res*, 13: 3264-3268.
- 101.** Puck TT, and Marcus PI (1955). A rapid method for viable cell titration and clone production with HeLa cells in tissue culture: The use of X-irradiated cells to supply conditioning factors. *Proc Natl Acad Sci USA* 41:432-437.
- 102.** Qin J, Tang DG (2010). Prostate cancer stem cells. In: Guan XY editor. *Cancer stem cells*. Transworld Research Network. pp. 37–56.

- 103.** Rajabalian S, Bahrami ZS, Farahat V and Shokri, F (2003). Supportive effects of human embryonic fibroblast cell line on growth and proliferation of EBV-transformed lymphoblastoid cells. *Iranian Biomedical Journal* 7: 147-153.
- 104.** Ramirez RD, Morales CP, Herbert BS, Rohde JM, Passons C, Shay JW and Wright WE (2001). Putative telomere-independent mechanisms of replicative aging reflect inadequate growth conditions. *Genes and Development* 15: 398-403.
- 105.** Rheinwald JG, Green H (1975). Serial cultivation of strains of human epidermal keratinocytes: the formation of keratinizing colonies from single cells. *Cell* 6:331-344.
- 106.** Rheinwald JG, Green H (1977). Epidermal growth factor and multiplication of cultured human epidermal keratinocytes. *Nature* 265:421-424.
- 107.** Rikimaru K, Todo H, Tachikawa N, Kamata N and Enomot S (1990). Growth of malignant and nonmalignant human squamous cells in a protein-free defined medium. *In Vitro Cell devl Biol.* 26, 849-856.
- 108.** Ronfard V, Rives JM, Neveux Y, Carsin H, Barrandon Y (2000). Long-term regeneration of human epidermis on third degree burns transplanted with autologous cultured epithelium grown on a fibrin matrix. *Transplantation*,; 70(11): 1588-1598
- 109.** Rongone E (1987). *Dermatotoxicology*, chapter Skin structure, function, and biochemistry, pages 1–70. Hemisphere Publishing Corp. Washington.
- 110.** Rouabhia M (1996). Permanent skin replacement using chimeric epithelial cultured sheets comprising xenogeneic and syngeneic keratinocytes. *Transplantation.* 61(9): 1290-1300
- 111.** Roy A, Krzykwa E, Lemieux R, Neron S (2001). Increased efficiency of gamma-irradiated versus mitomycin C-treated feeder cells for the expansion of normal human cells in long-term cultures. *J Hematother Stem Cell Res* 10: 873-80.
- 112.** Rubin H, Xu K (1989). Evidence for the progressive and adaptive nature of spontaneous transformation in the NIH 3T3 cell line. *Proc Nat Acad Sci USA* 86: 1860-1864.

- 113.** Rue LW, Cioffi WG, McManus WF, Pruitt BA (1993). Wound closure and outcome in extensively burned patients treated with cultured autologous keratinocytes *J Trauma*. 34: pp. 662–668
- 114.** Russo J, Reina D, Frederick J, et al (1988). Expression of Phenotypically Changes by Human Breast Epithelial Cells Treated with Carcinogens in Vitro; *Cancer Res* 1988; 48: 2837-2857.
- 115.** Salomon D, Masgrau E, Vischer S, Ullrich S, Dupont E, Sappino P, Saurat JH, and Meda P (1994). Topography of mammalian connexins in human skin. *J Invest Dermatol*, 103(2):240–247.
- 116.** Savage VM, Allen AP, Brown JH, Gillooly JF, Herman AB, et al (2007). Scaling of number, size, and metabolic rate of cells with body size in mammals. *PNAS (USA)*, 104: 4718-4723.doi: 10.1073/pnas.0611235104
- 117.** Schaeffler A and Schmidt S (1995). *Mensch Körper Krankheit*, chapter 9. Die Haut, pages 148–150. Jungjohann Verlag, Neckarsulm.
- 118.** Schoenbach KH, Joshi R, Kolb J, Buescher S, and Beebe S (2004). Subcellular effects of nanosecond electrical pulses. *ConfProc IEEE Eng Med Biol Soc* 7, 5447.
- 119.** Schrader TJ (1999). Comparison of HepG2 feeder cells generated by exposure to gamma-rays, UV-C light or Mitomycin C for ability to activate 7, 12-dimethyl-benz [a]anthracene in a cell-mediated Chinese hamster V79/HGPRT mutation assay. *Mutat Res* 423: 137-148
- 120.** Soriano JV, Pepper MS, Nakamura T, Orcil L and Montesano R (1995). Hepatocyte growth factor stimulates extensive development of branching duct-like structures by cloned mammary gland epithelial cells. *J Cell Sc* 108: 413-430
- 121.** Sorrell JM and Caplan AI (2004). Fibroblast heterogeneity: more than skin deep. *J Cell Sci*, 117(Pt 5):667–675.
- 122.** Stoler A, Kopan R, Duvic, M, Fuchs E (1988). Use of monospecific antisera and cRNA probes to localize the major changes in keratin expression during normal and abnormal epidermal differentiation. *J. Cell Biol.* 107, 427-446.



- 123.** Sun T, McMinn P, Holcombe M, Smallwood R and MacNeil S (2008). Agent Based Modelling Helps in Understanding the Rules by Which Fibroblasts Support Keratinocyte Colony Formation. *PLoS ONE* 3(5): e2129;doi: 10.1371/journal.pone.0002129.
- 124.** Szybalski W and Iyer VN (1967). Antibiotics I. In: *The Mitomycins and Porfiromycins*. Eds: Gottlieb, D. & Shaw, P.D., Springer-Verlag, New York 211.
- 125.** Takano H, Nakazawa N, Okuno Y, Shirata N, Tsuchiya S, Kainoh T, Takamatsu S, Furuta K, Taketomi Y, Naito Y, Takematsu H, Kozutsumi H, Tsujimoto G, Murakami M, Kudo I, Ichikawa A, Nakayama K, Sugimoto Y, Tanaka S (2008). Establishment of the culture model system that reflects the process of terminal differentiation of connective tissue-type mast cells. *FEBS Letters* 582: 1444–1450
- 126.** Takeuchi T, Wang L, Mori S, Nakagawa K, Hiroshi Y, Kanda T (2008). Characterization of mouse 3T3-Swiss albino cells available in Japan: Necessity of quality control when used as feeders. *Jpn J Infect Dis* 61: 9-12.
- 127.** Tan DWM, Jensen KB, Trotter MWB, Connelly JT, Broad S, Watt FM (2013). Single-cell gene expression profiling reveals functional heterogeneity of undifferentiated human epidermal cells. *Development* 140, 1433-1444 doi: 10.1242/dev.087551.
- 128.** Teepe RGC, Kreis RW and Koebrugge EJ (1990). The use of cultured autologous epidermis in the treatment of extensive burn wounds. *J Trauma* 30: 269
- 129.** Thepot A, Desanlis A, Venet E, Thivillier L Justin V, Morel AP, Defraipont F, Till M, Krutovskikh V, Tommasino M, et al. (2011). Assessment of transformed properties in vitro and of tumorigenicity in vivo in primary keratinocytes cultured for epidermal sheet transplantation. *J. Skin Cancer*. 936546.
- 130.** Todaro GJ, Green H (1963). Quantitative studies of the growth of mouse embryo cells in culture and their development in to established lines. *J. Cell Biology* 17: 299-313.
- 131.** Tomasz M (1995). Mitomycin C: small, fast and deadly (but very selective). *Chem Biol.*, 2(9): 575-9.

- 132.** Tsao MC, Walthall BJ and HAM RG (1982). Clonal growth of normal human epidermal keratinocytes in a defined medium. *J. cell. Physiol.* 110, 219-229.
- 133.** Ueda M (1995). Formation of Epithelial Sheets by serially cultivated Human Mucosal cells and their applications as a graft material. *Nagoya J. Med. Sci.* 58. 13-28
- 134.** Utzat CD, Clement CC, Ramos LA, Das A, Tomsz M and Basu AK (2005). DNA adduct of the mitomycin C metabolite 2,7-diaminomitosenone is a nontoxic and nonmutagenic DNA lesion in vitro and in vivo. *Chem Res Toxicol.* 18: 213-23.
- 135.** Verweij J and Pinedo HM (1990). Mitomycin C: Mechanism of Action, Usefulness and Limitations. *Anticancer Drugs* 1 : 5-13
- 136.** Voigt M, Schauer M, Schaefer DJ, Andree C, Horch R, Stark GB (1999). Cultured epidermal keratinocytes on a microspherical transport system are feasible to reconstitute the epidermis in full thickness wounds. *Tissue Eng.,* 5(6): 563-572
- 137.** Wakaki S, Marumo H, Tomioka K, Shimizu G, Kato E, Kamada H, Kudo S & Fujimoto Y (1958). Isolation of new fractions of antitumor mitomycins. *Antibiot Chemother* 8, 228-240
- 138.** Watt FM (1984). Selective migration of terminally differentiating cells from the basal layer of cultured human epidermis. *J Cell Biology* 98: 16-21.
- 139.** Watt FM (1987). Influence of cell shape and adhesiveness on stratification and terminal differentiation of human keratinocytes in culture. *J. Cell Sci. Suppl.* 8, 313-326.
- 140.** Watt FM (1988a). The epidermal keratinocyte. *BioEssays* 8, 163-167.
- 141.** Watt FM (1988b). Keratinocyte cultures: an experimental model for studying how proliferation and terminal differentiation are coordinated in the epidermis. *J. Cell Sci.* 90,525-529.
- 142.** Watt FM and Green H (1981). Involucrin synthesis is correlated with cell size in human epidermal cultures. *J. Cell Biol.* 90, 738-742.
- 143.** Watt FM and Green H (1982). Stratification and terminal differentiation of cultured epidermal cells. *Nature* 295,434-436.

144. Webb SR, JH Li, DB Wilson and J Sprent (1985). Capacity of small B cell-enriched populations to stimulate mixed lymphocyte reactions: marked differences between irradiated vs. mitomycin C-treated stimulators. *Eur J Immunol* 15: 92-96
145. Wilke M S, Edens M and Scott R E (1988a). Ability of normal human keratinocytes that grow in culture in serum-free medium to be derived from suprabasal cells. *J. natn. Cancer Inst.* 80, 1299-1304.
146. Wille JJ, Pittelkow MR, Shipley GD and Scott RE (1984). Integrated control of growth and differentiation of normal human prokeratinocytes cultured in serum-free medium: Clonal analyses, growth kinetics, and cell cycle studies. *J. cell. Physiol.* 121, 31-44.
147. Wokalek H (1992). *Dermatika*, chapter Die Haut. Wissenschaftliche Verlagsgesellschaft mbH Stuttgart.
148. Wood FM, Kolybaba ML, Allen P (2006). The use of cultured epithelial autograft in the treatment of major burn wounds: Eleven years of clinical experience. *Burns.* 32(5): 538-544
149. Wood FM, Kolybaba ML, Allen P (2006). The use of cultured epithelial autograft in the treatment of major burn injuries: a critical review of the literature. *Burns.* Jun; 32(4):395-401.
150. Woodcock-Mitchell, J, Eichner, R, Nelson, WG, Sun, T-T (1982): Immunolocalization of keratin polypeptides in human epidermis using monoclonal antibodies. *J Cell Biol* 95: 580–588.
151. Woodley DT, Peterson HD, Herzog SR, Stricklin GP, Burgeson RE, Briggaman RA, et al. (1988). Burn wounds resurfaced by cultured epidermal autografts show abnormal reconstitution of anchoring fibrils. *Jama.* 259(17): 2566-2571
152. Xu H, Nallathamby PD, and Xu XH (2009). Real-time imaging and tuning subcellular structures and membrane transport kinetics of single live cells at nanosecond regime. *J Phys Chem B* 113, 14393.
153. Yaeger PC, Stiles CD, Rollins BJ (1991). Human keratinocyte growth-promoting activity on the surface of fibroblasts. *J Cell Physiol* 149(1): 110-6.

- 154.** Yerneni LK and Jayaraman S (2003). Pharmacological action of high doses of melatonin on B16 murine melanoma cells depends on cell number at time of exposure. *Melanoma Res* 13: 1-5.
- 155.** Yue X-S, Fujishiro M, Nishioka C, Arai T, Takahashi E, Gong J-S, et al. (2012) Feeder Cells Support the Culture of Induced Pluripotent Stem Cells Even after Chemical Fixation. *PLoS ONE* 7(3): e32707. doi:10.1371/journal.pone.0032707
- 156.** Zhou D, Lin G, Zeng SC, Xiong B, Xie PY et al. (2014). Trace levels of mitomycin C disrupt genomic integrity and lead to DNA damage response defect in long-term-cultured human embryonic stem cells. *Arch Toxicol* DOI 10.1007/s00204-014-1250-6.
- 157.** Zhou D, Liu T, Zhou X and Lu G (2009). Three key variables involved in feeder preparation for the maintenance of human embryonic stem cells. *Cell Biol Int*: 33, 796-800.

# **List of Publications-Patents**

## List of Publications/Patents

---

### Publication:

1. **Chugh RM**, Chaturvedi M, Yerneni LK (2015). Occurrence and Control of Sporadic Proliferation in Growth Arrested Swiss 3T3 Feeder Cells. PLoS ONE 10(3): e0122056. doi:10.1371/journal.pone.0122056
2. **Chugh RM**, Chaturvedi M, Yerneni LK (2015). An evaluation of the choice of feeder cell growth arrest for the production of cultured epidermis. (Burns- Article in Press, Accepted on 10 August 2015, <http://dx.doi.org/10.1016/j.burns.2015.08.011>)
3. Rishi Man Chugh, Madhusudan Chaturvedi, Lakshmana Kumar Yerneni. Growth Arrest of feeder cells by Exposure Cell Density Variation (under preparation)
4. Rishi Man Chugh, Madhusudan Chaturvedi, Lakshmana Kumar Yerneni. Growth Arrest of feeder cells by Volume Variation (under preparation)

### Patent:

1. A Method for Processing Of Feeder Cells Suitable For Adult Stem Cell Proliferation. 3115/DEL/2014. CBR No. 21862. L. K. Yerneni and Rishi Man Chugh. (Filed, Date: 30.10.2014)

# **Brief Biography of the Candidate**

## Brief Biography of the Candidate

---

### Personal Particular

- < Name: Rishi Man Chugh
- < Date of Birth: 09<sup>th</sup> August 1982
- < Present Address: E-57, Second Floor Tagore Garden Extention,  
New Delhi-110027
- < E-mail: rishimanugh@gmail.com
- < Contact No. +91-9868356888, +91-9716481897
- < Area of Interest: Tissue engineering and Animal Cell Culture

### Educational Qualification

- < **Master of Science (M. Sc.):** Biotechnology, 76.70%, 1st Division (2006), School of Life Science, Khandari Campus, Dr. B. R. Ambedkar University, Agra. India.
- < **Bachelor of Science (B. Sc.):** Biology, 63.33%, 1st Division (2004), S. M. College, Chandausi, M. J. P. Rohilkhand University, Bareilly. India

### Position Held

- 24.04.2014 - Till Date: ICMR Independent Senior Research Fellowship  
Cell Biology Lab, National Institute of Pathology (ICMR).
- 22.04.2013 - 23-04-2014: Institutional Senior Research Fellow
- 22.04.2010 - 21.04.2013: Senior Research Fellow, in ICMR funded project.
- 01.05.2008 - 21.06.2005: Junior Research Fellow, in ICMR funded project.
- 01.09.2007 – 31.03.2008: Research Assistant, in DBT funded project, National Institute of Immunology.

### Extra Curriculum Activities

- Hands on training Experience Metafer Slide Scanning Platform, an automatic dedicated workstation for scanning, capturing and analysis of karyotype.
- Training course in Fundamentals of HPLC with Lab Solution workstation at Shimadzu Analytical (India) Pvt. Ltd. New Delhi.
- Pursuing Distance learning Post graduate diploma in Intellectual Property Rights (PGDIPR) from IGNOU, New Delhi.



- Appreciable understanding of the concepts related to Intellectual Property Management and Regulatory. Passed DL-101 certificate course conducted by World Intellectual Property Rights Organization (WIPO), Geneva, Switzerland.
- Awarded ICMR independent Senior Research Fellowship in 2014 to conduct research at National Institute of Pathology, New Delhi.
- Certificate course in Bioinformatics from Ramjas College.(Delhi University)
- ‘O’ level diploma in computer application.
- Got merit certificate in various competition such as drawing competition and writing competition.
- During my college days I have also participated in various “Bharat Scout and Guide” programmes.

**Publication:**

1. **Chugh RM**, Chaturvedi M, Yerneni LK (2015) Occurrence and Control of Sporadic Proliferation in Growth Arrested Swiss 3T3 Feeder Cells. PLoS ONE 10(3): e0122056. doi:10.1371/journal.pone.0122056
2. **Chugh RM**, Chaturvedi M, Yerneni LK (2015). An evaluation of the choice of feeder cell growth arrest for the production of cultured epidermis. (Burns- Article in Press, Accepted on 10 August 2015, <http://dx.doi.org/10.1016/j.burns.2015.08.011>)
3. Rishi Man Chugh, Madhusudan Chaturvedi, Lakshmana Kumar Yerneni. Growth Arrest of feeder cells by Exposure Cell Density Variation (under preparation)
4. Rishi Man Chugh, Madhusudan Chaturvedi, Lakshmana Kumar Yerneni. Growth Arrest of feeder cells by Volume Variation (under preparation)

**Patent:**

1. A Method for Processing Of Feeder Cells Suitable For Adult Stem Cell Proliferation. 3115/DEL/2014. CBR No. 21862. L. K. Yerneni and Rishi Man Chugh. (Filed, Date: 30.10.2014)

## **Brief Biography of the Supervisor**

## Brief Biography of the Supervisor

---

Name Lakshmana Kumar Yerneni

Designation: Scientist “E”

Discipline: CELL BIOLOGY

Address (Off): Cell Biology Lab,  
National Institute Of Pathology  
Safdarjang Hospital Campus,  
P O Box. 4909, New Delhi –  
110029.  
Tel (Lab) 2618 1261; FAX 2619  
8401

Email : [lkyerneni@yahoo.com](mailto:lkyerneni@yahoo.com); [yernenilk@icmr.org.in](mailto:yernenilk@icmr.org.in)

Education: 1. Masters in Cell Biology 1983  
2. Ph.D Pharmaceutical Toxicology 1988

Positions held: **AIIMS, New Delhi:**  
Research Associate– Biochemistry 1990-92  
**National Institute of Pathology, New Delhi**  
1. Research Associate – 1992-96  
2. Research Officer – 1996-2001  
3. Scientist C – 2001-07  
4. Scientist D – 2007-12  
5. Scientist E- 2012—Till Date

Awards: 1. WHO In-country Fellowship, 2004  
2. Shri Shyam Lal Saksena Memorial Award of National Academy of Medical Sciences (**NAMS, India**) in **Bio-Medical Engineering** for developing technique for ex-vivo growth of human epidermis, 2006.

Patent:

1. Indian Patent entitled “A culture system for the growth of stem cells” 2009 (Yerneni & Kumar)
2. A Method for Processing Of Feeder Cells Suitable For Adult Stem Cell Proliferation (Filed 3115/DEL/2014. CBR No. 21862. L. K. Yerneni and Rishi Man Chugh)

Research Experience:

1. **Bio-Engineering of Skin:**
  - Culture technique for human Keratinocyte stem cells.
  - Clinical application of autologous cultured epidermis in burns.
  - Bio Engineering of skin using biopolymers as scaffolds
2. **Pigment Cell Biology:** In vivo model for screening the therapeutic regimen in vitiligo.
3. **Mycoplasma surveillance in Cell Culture:** identification of mycoplasma contamination in cell culture & Development of methods for identification of mycoplasma infections.
4. **Melanoma:** Murine melanoma model in C57 mice and anti-melanoma activity of melatonin.

Publications & Patents:

Publications in indexed foreign journals 13

Publications in Proceedings 12

Patents 2

RESEARCH ARTICLE


# Occurrence and Control of Sporadic Proliferation in Growth Arrested Swiss 3T3 Feeder Cells

Rishi Man Chugh, Madhusudan Chaturvedi, Lakshmana Kumar Yemeli\*

Cell Biology Laboratory, National Institute of Pathology (ICMR), New Delhi, India

\* [yemelik@icmr.org.in](mailto:yemelik@icmr.org.in)



 OPEN ACCESS

**Citation:** Chugh RM, Chaturvedi M, Yemeli LK (2015) Occurrence and Control of Sporadic Proliferation in Growth Arrested Swiss 3T3 Feeder Cells. *PLoS ONE* 10(3): e0122056. doi:10.1371/journal.pone.0122056

**Academic Editor:** Mauro Picardo, San Galliciano Dermatologic Institute, ITALY

**Received:** November 7, 2014

**Accepted:** February 6, 2015

**Published:** March 23, 2015

**Copyright:** © 2015 Chugh et al. This is an open access article distributed under the terms of the [Creative Commons Attribution License](https://creativecommons.org/licenses/by/4.0/), which permits unrestricted use, distribution, and reproduction in any medium, provided the original author and source are credited.

**Data Availability Statement:** All relevant data are within the paper and its Supporting Information files.

**Funding:** The study was supported by extra mural Research grant 2009-02800 to LKY by the Indian Council of Medical Research, (<http://www.icmr.in>) New Delhi, India. The funders had no role in study design, data collection and analysis, decision to publish, or preparation of the manuscript.

**Competing Interests:** The authors have declared that no competing interests exist.

## Abstract

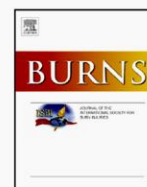
Growth arrested Swiss mouse embryonic 3T3 cells are used as feeders to support the growth of epidermal keratinocytes and several other target cells. The 3T3 cells have been extensively subcultured owing to their popularity and wide distribution in the world and, as a consequence selective inclusion of variants is a strong possibility in them. Inadvertently selected variants expressing innate resistance to mitomycin C may continue to proliferate even after treatment with such growth arresting agents. The failure of growth arrest can lead to a serious risk of proliferative feeder contamination in target cell cultures. In this study, we passaged Swiss 3T3 cells (CCL-92, ATCC) by different seeding densities and incubation periods. We tested the resultant cultures for differences in anchorage-independent growth, resumption of proliferation after mitomycin C treatment and occurrence of proliferative feeder contaminants in an epidermal keratinocyte co-culture system. The study revealed subculture dependent differential responses. The cultures of a particular subculture procedure displayed unique cell size distribution and disintegrated completely in 6 weeks following mitomycin C treatment, but their repeated subculture resulted in feeder regrowth as late as 11 weeks after the growth arrest. In contrast, mitomycin C failed to inhibit cell proliferation in cultures of the other subculture schemes and also in a clone that was established from a transformation focus of super-confluent culture. The resultant proliferative feeder cells contaminated the keratinocyte cultures. The anchorage-independent growth appeared in late passages as compared with the expression of mitomycin C resistance in earlier passages. The feeder regrowth was prevented by identifying a safe subculture protocol that discouraged the inclusion of resistant variants. We advocate routine anchorage-independent growth assay and absolute confirmation of feeder disintegration to qualify feeder batches and caution on the use of fetal bovine serum.

## Introduction

Large quantities of cultured epithelial autografts (CEA) for clinical use in the treatment of extensively burned patients are speedily grown from the adult epidermal keratinocytes over the

Available online at [www.sciencedirect.com](http://www.sciencedirect.com)

ScienceDirect

journal homepage: [www.elsevier.com/locate/burns](http://www.elsevier.com/locate/burns)

## An evaluation of the choice of feeder cell growth arrest for the production of cultured epidermis

Rishi Man Chugh<sup>a</sup>, Madhusudan Chaturvedi<sup>a,b</sup>,  
Lakshmana Kumar Yerneni<sup>a,\*</sup>

<sup>a</sup> Cell Biology Laboratory, National Institute of Pathology (ICMR), New Delhi, India

<sup>b</sup> Department of Medical Elementology and Toxicology, Jamia Hamdard, New Delhi, India

### ARTICLE INFO

#### Article history:

Accepted 10 August 2015

#### Keywords:

Cultured epidermis  
Gamma irradiation  
Mitomycin C  
Keratinocyte colony formation assay  
Growth area quantification  
BrdU labeling

### ABSTRACT

Growth arrested 3T3 cells have been used as feeder cells in human epidermal keratinocyte cultures to produce cultured epidermal autografts for the treatment of burns. The feeder cells were ideally growth-arrested by gamma-irradiation. Alternatively, growth arrest by mitomycin C treatment is a cost effective option. We compared the functional efficacy of these two approaches in keratinocyte cultures by colony forming efficiency, the net growth area of colonies, BrdU labeling and histological features of cultured epidermal sheets. The growth area estimation involved a semi-automated digital technique using the Adobe Photoshop and comprised of isolation and enumeration of red pixels in Rhodamine B-stained keratinocyte colonies. A further refinement of the technique led to the identification of critical steps to increasing the degree of accuracy and enabling its application as an extension of colony formation assay. The results on feeder cell functionality revealed that the gamma irradiated feeders influenced significantly higher colony forming efficiency and larger growth area than the mitomycin C treated feeders. The BrdU labeling study indicated significant stimulation of the overall keratinocyte proliferation by the gamma irradiated feeders. The cultured epidermal sheets produced by gamma feeders were relatively thicker than those produced by mitomycin C feeders. We discussed the clinical utility of mitomycin C feeders from the viewpoint of cost-effective burn care in developing countries.

© 2015 Elsevier Ltd and ISBI. All rights reserved.

### 1. Introduction

Rapid ex-vivo turnover of epidermal keratinocytes was achieved by employing the growth-arrested 3T3 feeder cells leading to large-scale production of epidermal sheets for autologous application in burns [1–4]. The choice of feeder cell growth arrest in epithelial and stem cell culture has been a subject of debate. Popularly, the gamma-irradiation ( $\gamma$ -Irr) performed at a dose of 6000 rads sourced from Co-60, has been considered ideal for growth arresting the 3T3 cells [5].

Alternatively, feeder cell growth arrest has also been attained by treating with Mitomycin C (MC) primarily due to the cost factor [5–9]. Some investigators concluded that the Mitomycin C treatment of feeder cells was adequate but not as efficient as gamma irradiation to stimulate proliferation of co-cultured target cells maximally [10–12]. On the other hand, both the approaches were considered equivalent in long-term culture conditions [13,14]. In fact, it is important to consider that the susceptibility to such agents is specific to the concerned feeder cell type [15,16]. As no comparative studies were reported pertaining to these growth arresting methods in 3T3 feeder

\* Corresponding author. Tel.: +91 9312904126; fax: +91 11 26198401.

E-mail address: [yernenik@icmr.org.in](mailto:yernenik@icmr.org.in) (L.K. Yerneni).

<http://dx.doi.org/10.1016/j.burns.2015.08.011>

0305-4179/© 2015 Elsevier Ltd and ISBI. All rights reserved.

**PATENT OFFICE**  
**INTELLECTUAL PROPERTY BUILDING**  
 Plot No. 32, Sector 14, Dwarka, New Delhi-110075  
 Tel No. (091)(011) 28034304-06 Fax No. 011  
 28034301,02  
 E-mail: delhi-patent@nic.in  
 Web Site: www.ipindia.gov.in



सत्यमेव जयते



Docket No 29359

Date/Time 30/10/2014

To  
 Indira Banerjee

User Code: Isdavar1

32 Radha Madhav Dutta Garden  
 Lane

Sr. No.	Ref. No./Application No	App. Number	Amount Paid	C.B.R. No.	Form Name	Remarks
1	3115/DEL/2014		40800	21862	FORM 1	A METHOD FOR PROCESSING OF FEEDER CELLS SUITABLE FOR ADULT STEM CELL PROLIFERATION

Total Amount : ₹ 40800

Amount in Words: Rupees Forty Thousand Eight Hundred Only

Print